SANDIA REPORT
SAND2012-0181
Unlimited Release
Printed January 2012

Linking Ceragenins to Water-Treatment Membranes to Minimize Biofouling

Susan J. Altman, Michael Hibbs, Paul B. Savage, Howland D. T. Jones, Steven Branda, Lucas K, McGrath, Yanshu Feng, Matthew F. Kirk, Jacob Pollard, Alyssa Lichtenberger, Christopher Marry, Shane Stafslien, Darla Goeres and Kelli Buckingham-Meyer

Prepared by
Sandia National Laboratories
Albuquerque, New Mexico 87185 and Livermore, California 94550

Sandia National Laboratories is a multi-program laboratory managed and operated by Sandia Corporation, a wholly owned subsidiary of Lockheed Martin Corporation, for the U.S. Department of Energy's National Nuclear Security Administration under contract DE-AC04-94AL85000.

Issued by Sandia National Laboratories, operated for the United States Department of Energy by Sandia Corporation.

Available to DOE and DOE contractors from
U.S. Department of Energy
Office of Scientific and Technical Information
P.O. Box 62
Oak Ridge, TN 37831

Telephone: (865)576–8401
Facsimile: (865)576–5728
E–Mail: reports@adonis.osti.gov
Online ordering: http://www.doe.gov/bridge

Available to the public from
U.S. Department of Commerce
National Technical Information Service
5285 Port Royal Rd
Springfield, VA 22161

Telephone: (800)553–6847
Facsimile: (703)605–6900
E–Mail: orders@ntis.fedworld.gov
Online order: http://www.ntis.gov/ordering.htm

SAND2012-0181
Unlimited Release
Printed January 2012

Linking Ceragenins to Water-Treatment Membranes to Minimize Biofouling

Susan J. Altman[1], Michael Hibbs[2], Paul B. Savage[3], Howland D. T. Jones[4], Steven Branda[5], Lucas K. McGrath[6], Yanshu Feng[3], Matthew F. Kirk[1], Jacob Pollard[3], Alyssa Lichtenberger[5], Christopher Marry[1], Shane Stafslien[7], Darla Goeres[8] and Kelli Buckingham-Meyer[8]

[1]Geochemistry Department
[2]Materials, Devices, And Energy Technologies Department
[4]Bioenergy and Defense Technology Department
[5]Biotechnology & Bioengineering Department
Sandia National Laboratories
P.O. Box 5800
Albuquerque, NM 87185–0735

[3]Department of Chemistry and Biochemistry
Brigham Young University
Provo, Utah 84602-5700

[6]LMATA
P.O. Box 5800, MS0754
Albuquerque, NM 87185

[7]Center for Nanoscale Science and Engineering
North Dakota State University
Fargo, ND 58102

[8]Center for Biofilm Engineering
Montana State University
Bozeman, MT 59717

Abstract

Ceragenins were used to create biofouling resistant water-treatment membranes. Ceragenins are synthetically produced antimicrobial peptide mimics that display broad-spectrum bactericidal activity. While ceragenins have been used on bio-medical devices, use of ceragenins on water-treatment membranes is novel. Biofouling impacts membrane separation processes for many industrial applications such as desalination, waste-water treatment, oil and gas extraction, and

power generation. Biofouling results in a loss of permeate flux and increase in energy use. Creation of biofouling resistant membranes will assist in creation of clean water with lower energy usage and energy with lower water usage.

Five methods of attaching three different ceragenin molecules were conducted and tested. Biofouling reduction was observed in the majority of the tests, indicating the ceragenins are a viable solution to biofouling on water treatment membranes. Silane direct attachment appears to be the most promising attachment method if a high concentration of CSA-121a is used. Additional refinement of the attachment methods are needed in order to achieve our goal of several log-reduction in biofilm cell density without impacting the membrane flux.

Concurrently, biofilm forming bacteria were isolated from source waters relevant for water treatment: wastewater, agricultural drainage, river water, seawater, and brackish groundwater. These isolates can be used for future testing of methods to control biofouling. Once isolated, the ability of the isolates to grow biofilms was tested with high-throughput multiwell methods. Based on these tests, the following species were selected for further testing in tube reactors and CDC reactors: *Pseudomonas* ssp. (wastewater, agricultural drainage, and Colorado River water), *Nocardia coeliaca* or *Rhodococcus* spp. (wastewater), *Pseudomonas fluorescens* and *Hydrogenophaga palleronii* (agricultural drainage), *Sulfitobacter donghicola*, *Rhodococcus fascians*, *Rhodobacter katedanii*, and *Paracoccus marcusii* (seawater), and *Sphingopyxis* spp. (groundwater). The testing demonstrated the ability of these isolates to be used for biofouling control testing under laboratory conditions. Biofilm forming bacteria were obtained from all the source water samples.

ACKNOWLEDGEMENTS

This research was funded by the Sandia National Laboratories Laboratory Directed Research and Development (LDRD) program, Energy, Climate, and Infrastructure (ECIS) Investment Area.

Angela Adams, Joey Nogales, Bill Varnava, and John Walp are greatly appreciated for their time and effort in helping us to obtain our source waters for bacteria isolation. Jerilyn Timlin is thanked for the maintenance and alignment of the hyperspectral microscope. Michelle Raymer and Omar Garcia helped collect the hyperspectral images. We thank Kathy Alam and Laura Martin for the infrared and Raman microspectroscopy data collection.

CONTENTS

LIST OF TABLES

LIST OF FIGURES

1 INTRODUCTION

With the growing scarcity of fresh water, treatment of impaired waters will become increasingly important for creation of new water supplies. These supplies are and will be needed for drinking as well as in the energy sector, as described below. Membrane treatment is a likely method for creating clean water. The National Academies lists "develop high-permeability, fouling-resistant, high rejection, oxidation-resistant membranes" as one of their goals [NRC and Academies, 2008]. Hightower and Pierce [2008] state that "Membrane fouling is one of the most problematic issues facing seawater desalination."

Biofouling impacts membrane separation processes for many industrial applications such as desalination [*Watson et al.*, 2003], waste-water treatment [*Ridgway et al.*, 1983], oil and gas extraction, and power generation. Biofouling results in a loss of permeate flux and an increase in energy use. Biofouling becomes an issue in the energy sector as water recycling becomes more and more prevalent. Examples include re-use of cooling water and water used for steam injection for heavy oil extraction. Other sectors that need ultrapure water, such as pharmaceuticals and the microchips and electronics industries, can also benefit from biofouling resistant membranes.

Ceragenins are synthetically constructed molecules that mimic antimicrobial peptides produced by the innate immune system [*Savage,* 2002]. The peptides kill bacteria by interfering with their cell membranes; consequently, they show broad-spectrum activity and high selectivity of prokaryotic cells over eukaryotic cells (e.g., bacteria over human cells). Moreover, anitmicrobial peptides are thought to be less likely to develop resistance because their mechanism of action does not depend upon the metabolic state of the bacteria. Like the natural peptides they mimic, ceragenins show broad-spectrum antimicrobial activity and high selectivity, and they can efficiently kill multiple drug resistant bacteria [*Chin et al.*, 2007; *Chin et al.*, 2008]. In contrast to the natural peptides, however, ceragenins are simple to prepare and purify on a large scale, and they are not subject to inactivation by host proteases. Thus far, ceragenins have been incorporated into catheter segments to prevent adhesion of organisms, and polymeric forms of ceragenins have been incorporated into medical devices for sustained release, for prevention of infection.

In this study we linked ceragenins to water-treatment membranes to create biofouling-resistant membranes. Creation of biofouling resistant membranes will assist in creation of clean water and energy with lower energy usage. We examined different methods of linking different ceregenin molecules to water-treatment membranes without compromising the permeate flux. This work is discussed in Section 2.

In parallel, we isolated biofilm forming bacteria from source waters relevant for water treatment. These isolates can be used for future testing of methods to control biofouling. Microbes were isolated and cultured from the samples using state-of-the art protocols and their biofilm growing capabilities were tested in several laboratories. This work is discussed in Section 3.

2 ATTACHMENT OF CERAGENINS TO MEMBRANES AND BIOFOULING TESTING

2.1 Background

2.1.1 Reverse osmosis membrane chemistry

Commercial reverse osmosis (RO) membranes differ from other water treatment membranes (e.g., micro- or nanofiltration membranes) because the active layer of RO membranes is not porous. Instead, water must diffuse through a thin, dense polymer layer which is supported on a porous substrate. The polymer layer is composed of a highly crosslinked poly(amide) which is typically formed by the interfacial polymerization of trimesoylchloride and meta-phenylene diamine (Figure1). Interfacial polymerizations typically have low conversions and this means that the active surface of an RO membrane will have some free amine and carboxylic acid (after hydrolysis of the acid chloride) groups. Some of the attachment methods described below are intended to use the free amines as points for chemical attachment of ceragenins to the membrane surface. In a patent issued to the Dow Chemical Company, Mickols [2001] has demonstrated the attachment of organic compounds to amines on RO membranes to form coatings with thicknesses up to 1 micron.

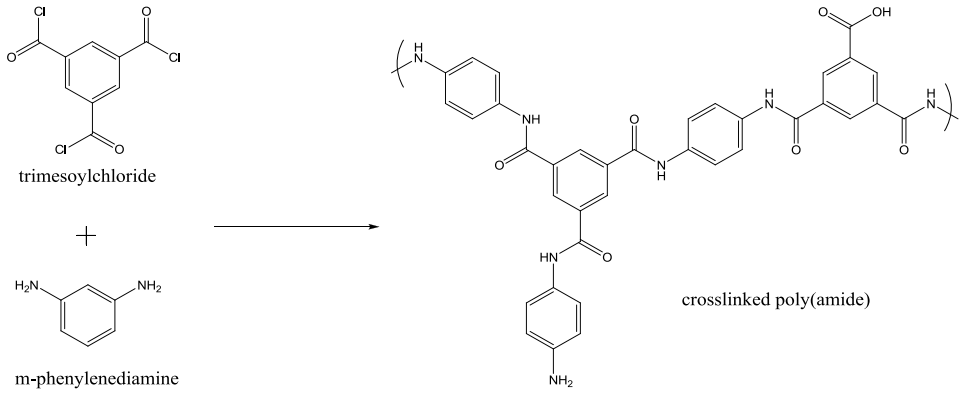

Figure 1: Interfacial polymerization to form the active layer of an RO membrane.

Commercial RO membranes are commonly prepared with a hydrophilic protective coating on top of the poly(amide) layer. This protective coating is typically composed of poly(vinylalcohol) (PVA) and it can block access to the free amines in the poly(amide). To circumvent this issue, RO membranes without PVA coatings were prepared by Separation Systems Technology, Inc. for use as substrates with the attachment methods that required access to the amines. By contrast, the attachment methods that are based on silane chemistry required the use of substrates with PVA coatings. In these cases, the free alcohols in the PVA were used as points of attachment for trialkoxysilane moieties in the ceragenin coatings.

Separation Systems Technology, Inc. created two membranes for this project, referred to as SST1 and SST2, where SST2 has more free amines on the surface than SST1, which in turn should have more free amines than the commercial membrane used for this project. The commercial membranes used for testing were purchased from GE Osmonics and are brackish

water reverse osmosis (BWRO) membranes (GE Sepa™ CF Polyamide RO AG Membrane, part number 1206368). These membranes are referred to as GE BWRO in this report.

2.1.2 Ceragenins

Ceragenins are mimics of naturally occurring antimicrobial peptides and they were invented by team member Paul Savage (BYU). Antimicrobial peptides are ubiquitous in nature and constitute a primary means by which higher organisms control microbial growth. Extensive comparisons of ceragenins and endogenous antimicrobial peptides have revealed that they share a common mechanism. This type of antimicrobial agent selectively attacks microbial membranes and rapidly causes cell death. For large-scale and wide-spread use, antimicrobial peptides present difficulties due to the cost of synthesis and susceptibilities of peptides to enzymatic degradation by proteases. The ceragenins, however, are amenable to large-scale synthesis and because they are not peptide based, they are not substrates for proteases. Ceragenins are broad-spectrum antimicrobial agents with activity against Gram-positive and negative bacteria, lipid-enveloped viruses, and fungi, and, like antimicrobial peptides, ceragenins are highly selective for microbial membranes over eukaryotic membranes. Primary colonization by microorganisms such as bacteria, algae, and fungi is a critical step in the biofouling process. Thus, the uniqueness of this project is derived from the use of peptide mimics to prevent bacterial colonization and thus disrupt the fouling process.

The structure of a typical ceragenin, CSA-13, and the starting material, cholic acid, are shown in Figure 2. Ceragenins are based on a steroid core (the system of four fused saturated rings) with several substituents arranged in such a way that one face of the molecule is hydrophilic while the other face is hydrophobic. In the case of CSA-13, it is the three primary amines (which become ammonium salts when protonated) that cause the near face of the molecule to be hydrophilic. It is this arrangement of hydrophilic and hydrophobic regions that enables ceragenins to mimic antimicrobial peptides. The substituent on the upper right corner of a ceragenin (when drawn as CSA-13 is arranged in Figure 2) could be varied without having a large impact on the biocidal activity of the ceragenin. So that region of the molecule was used as a "handle" for attaching the specific functionalities desired for the various attachment methods described below.

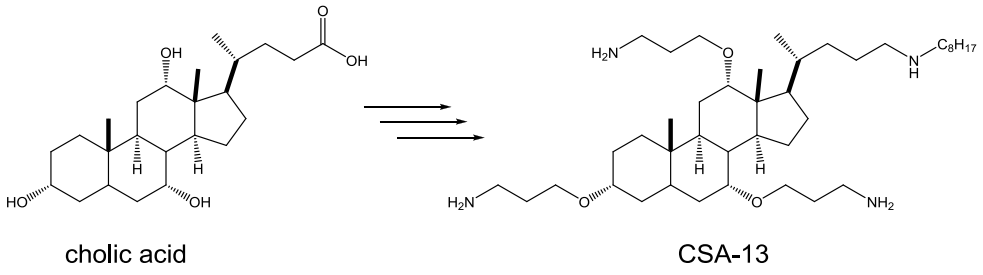

Figure 2: A typical ceragenin, CSA-13, and its precursor, cholic acid.

2.1.3 Surface Characterization

2.1.3.1 Ninhydrin staining

Ninhydrin is a compound commonly used by forensic scientists to develop images of fingerprints. By itself, ninhydrin is colorless but it reacts with primary amines (such as those found on amino acids and thus, in the oils on human skin) to form a dye with a dark purple color [*Meyer*, 1957]. Since ceragenins have several primary amines and one of the surface-modifying agents used in the attachment methods below has a primary amine, many of the membrane samples were exposed to heated solutions of ninhydrin as a qualitative test for the presence of the desired coatings.

2.1.3.2 Hyperspectral Imaging

Hyperspectral imaging was employed to visualize and quantify the various ceragenin attachment procedures. The ceragenin attached samples were stained using ninhydrin as described in Section 2.1.3.1 prior to measuring the samples with hyperspectral imaging. Because the RO membranes we are investigating have a large amount of autofluorescence emission that overlaps the ninhydrine fluorescence emission, it was important to use a technique that could separate and quantify the different emission sources. Hyperspectral imaging combined with multivariate analysis techniques, such as multivariate curve resolution (MCR), allows for the separation of many overlapping fluorescence species and creates interpretable quantitative images from biological samples with both known and unknown fluorescence species. We used a fluorescence line scanning imager developed at Sandia originally designed and built to scan and quantify multiple fluorophores on DNA microarray slides [*Sinclair et al.*, 2004]; however this imager also has been useful for many applications in which large areas need to be scanned and imaged, e.g., biofilms on water-treatment membranes [*Altman et al.*, 2010]. After the membrane was stained with ninhydrine and completely dried, the membrane was taped onto a microscope slide using double-sided tape in preparation for imaging. A 1 cm^2 region of the membrane was imaged using the line scanning hyperspectral microscope [*Sinclair et al.*, 2004] by imaging ten 1mm by 1cm sections at a time using a 532 nm Nd:YVO4 laser. An infinity-corrected 10x apochromatic objective (NA 0.45) was used to achieve a final spatial resolution being 30 μm. These images were preprocessed to remove spectral artifacts associated with the imager (cosmic spikes, offset, curvature and keystome), then the ten sections were concatenated together to create a 1 cm^2 hyperspectral image of the membrane. These images consisted of approximately 110,000 spectra, with each spectrum consisting of 458 wavelengths (550-900 nm). The acquired spectral images were analyzed using Sandia's proprietary multivariate curve resolution (MCR) analysis software [*Haaland et al.*, 2009; *Jones et al.*, 2008; *Kotula et al.*, 2003; *Ohlhausen et al.*, 2004; *Van Benthem and Keenan*, 2004; *Van Benthem et al.*, 2002] to obtain the pure spectral components and their associated intensities from each hyperspectral image. Infrared Attenuated Total Reflectance (ATR)

A Varian 7000 Fourier Transform Infrared (FTIR) microscope with a Germanium ATR microscope objective was used to acquire infrared spectra from ceragenin attached RO membranes (courtesy of Laura Martin, Sandia Organization 02555). Ten different locations were measured with this ATR objective for each membrane investigated, producing 10 spectra per membrane. Each spectrum consisted of 8 cm^{-1} resolution and 64 scans co-added together to improve the signal-to-noise of the spectra collected. The spectra were ratioed to an air

background and converted to absorbance. These spectra then were analyzed with MCR to determine whether there was a pure spectral component that could be associated with the attached ceragenin and whether that spectral feature could be used to evaluate future ceragenin attachment procedures.

2.1.4 Biofouling Testing

2.1.4.1 Method Description

The method used to quantify biofouling on the membrane surface is based on a standard method [*ASTM*, E 2562-07]. Experiments were carried out using Centers for Disease Control and Prevention (CDC) biofilm reactors (BioSurface Technologies, Corporation). Prior to running each experiment, the reactor and carboys were autoclaved at 121°C for 30 minutes. Experiments are summarized in Table 1. For the experiments run using the amine-linked polymer brush method and the UV-grafted polymer brush method drinking water (DW) supplied by Kirtland Air Force Base tap water was used as the source of bacteria. Organic carbon and chlorine were removed from the tap water by sequentially passing it through columns containing granular activated carbon and biologically activated carbon. Nutrients consisted of a solution with 1.84 mg/L glutamic acid, 1.88 mg/L glucose, 1.88 mg/L galactose, 1.88 mg/L arabicose, 2.52 mg/L KNO_3, and 0.22 mg/L K_2HPO_4. These concentrations have a consistent Carbon: Nitrogen: Phosphorous ratio to what is found in drinking water. Solutions from the separate containers of the DW and nutrient solution flowed into the reactor at equal flow rates of 0.95 mL/min each for a total flow rate of 1.9 mL/min into the reactor (residence time ≈ 3.5 hours). Reactors were continually mixed. All experiments were incubated at room temperature.

Artificial seawater with Trypticase™ soy broth (TSB) nutrients were used as the aqueous medium for the experiments run using the silane direct attachment method. The reactor was inoculated with 1 mL mid-log phase *Pseudomonas fluorescens* (ATCC 700830) cell solution (*Pseudomonas* species are ubiquitous in aqueous environments [*Moore et al.*, 2006], making the use of this organism in our experiments appropriate) and variable concentrations of TSB (see Table 1). For 24 h following incubation, flow to the reactor was held stagnant (batch phase) and the reactor was stirred at 150 rpm. The batch phase allows for the microbial community to become established and to initiate attachment of cells to reactor surfaces. Afterward, a 100 mg/L solution of TSB was pumped through the reactor at 11.8 mL/min (residence time 0.5 h) and the reactor was stirred at 150 rpm (continuous flow phase). During this portion of the experiment, aqueous medium is pumped through the reactor at a rate rapid enough to flush many of the suspended cells from the reactor. Cell accumulation in the reactor is then largely limited to reactor surfaces.

The reactor used for the experiments has eight rods each having three polycarbonate coupons that can be removed for biofilm sampling. For the experiments run on membranes using the amine-linked polymer brush method and the UV-grafted polymer brush method, samples were collected at two different times after flow was initiated. For the experiments run using the silane direct attachment method, samples were collected 1 day after flow was initiated (Table 1).

Biofilm was scraped from reactor coupons with a polypropylene cell lifter (Corning) and placed into 10 mL of DI. The solution was then sonicated for 5 to 10 minutes to reduce cell clumping

Table 1: Summary of biofouling testing experiment conditions

Date Flow Initiated	Attachment Method	Membrane	Medium	Sampling Times (days after flow initiation)	# Ceragenin Coupons¥	# control Coupons¥
10/26/2009	Amine	GE BWRO	Drinking water with C:N:P nutrients	14, 28	9	9
12/23/2009	Amine	SST1	Drinking water with C:N:P nutrients	14, 28	9	9
03/17/2010	Amine	SST2	Drinking water with C:N:P nutrients	7, 14	9	9
03/01/2010	UV	GE BWRO	Drinking water with C:N:P nutrients	7, 14	9	9
02/04/2010	UV	SST1	Drinking water with C:N:P nutrients	14, 28	9	9
03/22/2010	UV	SST2	Drinking water with C:N:P nutrients	7,14	9	9
05/05/2011	Silane (2.6% & 5.2%)	GE BWRO	Artificial seawater with 300 mg/L of TSB in batch phase and 100 mg/L TSB in flow phase	1	3	3§
08/10/2011	Silane (15% & 20%)	GE BWRO	Artificial seawater with 100 mg/L of TSB in batch phase and 100 mg/L TSB in flow phase	1	3	3
09/15/2011	Silane (15%)	GE BWRO	Artificial seawater with 300 mg/L of TSB in batch phase and 100 mg/L TSB in flow phase	1		3

¥ - Number of coupons per sampling period

§ - Note that one coupon was contaminated for the 5.2% so there were only 2 coupons used.

[*Heersink*, 2003] vortexed, and serially diluted. Cell concentrations in the diluted samples were quantified using pour plating. Diluted samples of DW biofilm were plated onto R2A agar (Difco™) and were incubated at room temperature for 7 days. Samples of *P. fluorescens* were plated onto Trypticase™ soy agar (TSA). Plates were incubated at 30°C for approximately 48 h prior to counting. Three plates were counted for each sample.

Statistical comparisons of results from ceragenin-membranes and results from corresponding control coupons were performed using a paired Student's t test. Differences between the results of each were interpreted to be significant at probability values less than 0.05.

Membranes created using both the UV-grafted polymer brush method and the silane direct attachment method were also tested using the cross-flow testing system [*Altman et al.*, 2010; *Ho et al.*, 2008]. Methods used for the silane direct attachment method is the same as described in Altman et al. [2010].

2.1.4.2 Method Evaluation

In general, the availability of nutrients and number of cells used to inoculate bioreactor experiments tends to be high compared to natural environments. This characteristic reflects the need to produce growth within a reasonable length of time. To evaluate how this practice could affect the results of antifoulant testing, experiments were performed to evaluate the impact that nutrient and inoculation levels have on growth and the antifouling properties of a commercial test coating.

The results show that (1) the inoculum levels tested do not influence the final density of cells on test materials in the reactor, and (2) cell growth begins to occur at nutrient levels greater than 10 mg L^{-1} (Figure 3).

2.2 The Direct Attachment Method

2.2.1 CSA-111 Attachment

The idea behind this method is to attach a single ceragenin (CSA-111) directly to free amines on the RO membrane surface. CSA-111 has an amine-reactive *N*-hydroxysuccinimide group that reacts with a free amine on the surface of the RO membrane to form an amide linkage (Figure 4). The amines on CSA-111 are protected with 9-fluorenylmethyl carbamate (Fmoc) groups to prevent the CSA-111 from reacting with itself. Thus, after the attachment, the Fmoc groups need to be removed by treatment with a base such as piperidine. This method is the simplest, most direct way of attaching ceragenins to membranes but it only allows for one ceragenin to attach per free amine on the surface. Ninhydrin staining of these membranes did not yield any color visible to the naked eye, indicating that the concentration of ceragenin was probably not high enough to prevent biofouling. Also the mobilities of the ceragenins attached this way are very limited, possibly compromising the anti-bacterial activity of the ceragenins.

2.2.2 Experimental Sample

A 1" x 3" piece of RO membrane was pretreated by soaking in a 5% solution of sodium bicarbonate (aqueous) for 1-2 hours. Then it was rinsed with water, dipped briefly into ethanol

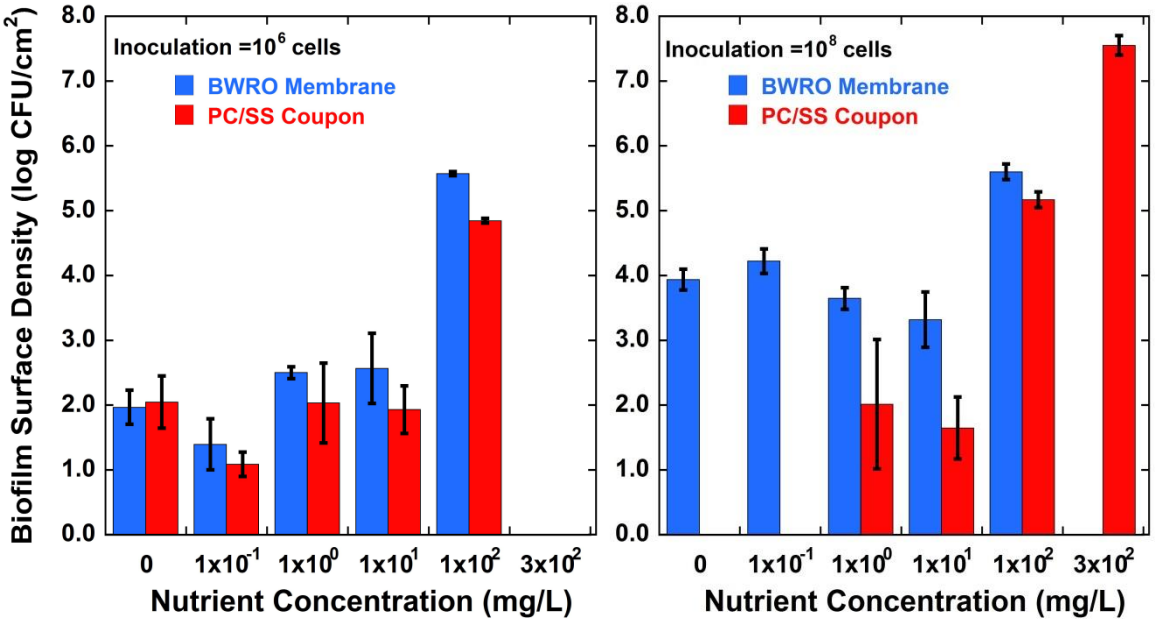

Figure 3: Results of the method evaluation experiments. The chart on the left shows the results of experiments inoculated with 10^6 cells. The chart on the right shows results of experiments inoculated with 10^8 cells. Nutrient concentrations are for both batch and flow phase, except for the 300 mg/L case, where flow nutrient concentrations were 100 mg/L. The nutrient was TSB. Two groups of coupons were evaluated, those with BWRO membranes on them and a second set of either polycarbonate (PC) Or stainless steel (SS) coupons. The stainless steel coupons were those in the test with 10^6 cell inculum and 10 and 100 mg/L TSB concentration and the test with 10^8 cell inculum and 10 mg/L TSB concentration. Note that only cell attachment was observed when nutrient concentrations were 10 mg/L or below. At 100 and 300 mg/L nutrient concentrations, biofilm growth was observed.

and then the surface was treated with a solution of CSA-111 (30 mg) and triethylamine (5 drops) in 9 mL of ethanol. The reaction was covered and heated to 45 ^{o}C for 22 hours. The membrane was rinsed with ethanol and then soaked in a 3:1 v/v solution of ethanol/piperidine for 6 hours. Finally the membrane was rinsed thoroughly with ethanol and then water.

2.2.3 Biofouling Testing

Biofouling testing was not conducted using samples created with the direct attachment method.

2.3 The Amine-Linked Polymer Brush Method

2.3.1 CSA-113 Attachment

In the amine-linking method of attachment, free amines on the RO membrane are first treated with an epoxy alkene (3,4-epoxy-1-butene) in order to attach an alkene to each free amine (Figure 5). Then the membrane surface is treated with an aqueous solution of CSA-113, acrylamide, and a radical initiator. This kind of aqueous radical polymerization of acrylate-type monomers on an RO membrane surface was originally reported by Belfer et al. [1998]. Within

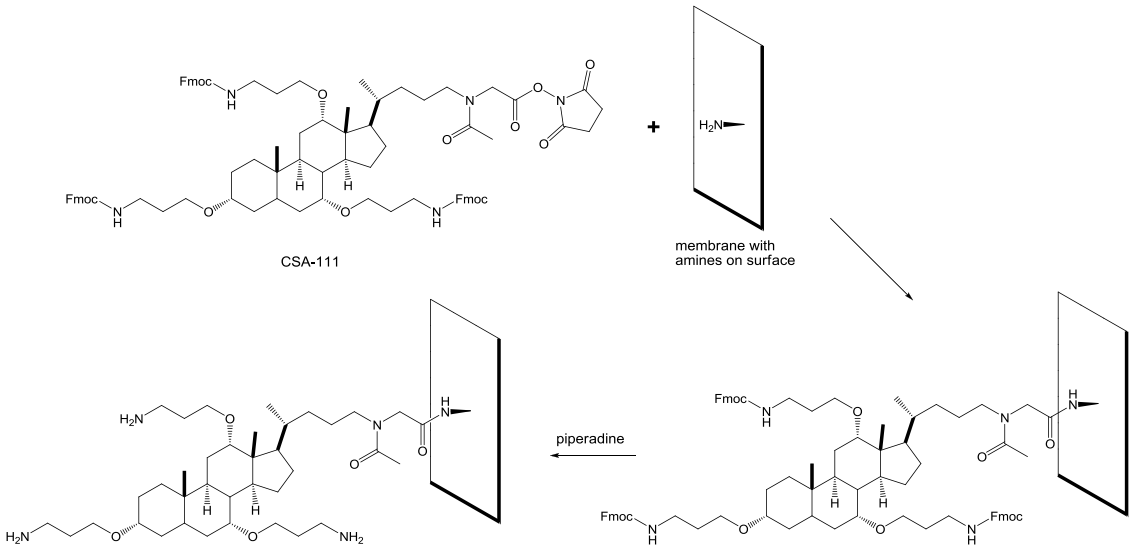

Figure 4: Scheme for direct attachment of CSA-111.

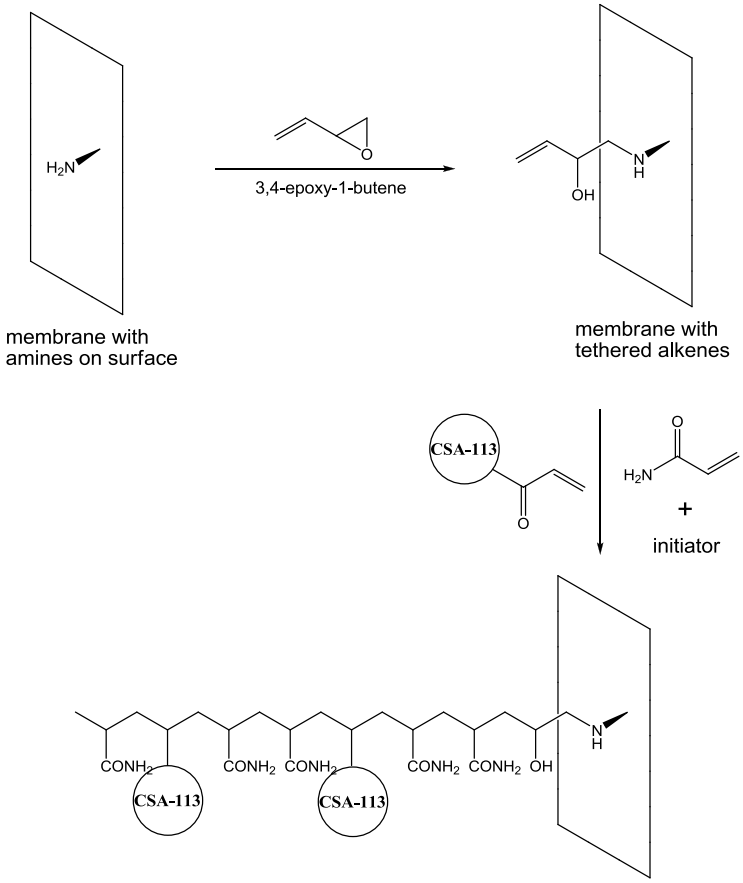

Figure 5: Scheme for amine-linked polymer brush method.

the solution, a chain growth polymerization occurs and some of these polymer chains react with and attach to the alkenes bound to the membrane surface. The result is a membrane surface with covalently attached copolymer chains which extend off of the surface and into the water. Each one of these copolymer chains can contain many ceragenin molecules. Figure 6 shows the synthetic scheme for making CSA-113. The acrylamide moiety on CSA-113 serves as the point of attachment during the polymerization reaction. Another ceragenin, CSA-109 (not pictured), with a pendant allyl group instead of an acrylamide group was also prepared. The amine linking method was also tried with CSA-109 and acrylic acid, but the CSA-113 + acrylamide combination was found to polymerize more easily.

Ninhydrin staining of these samples gave inconsistent results. In the best cases, a light purple color was clearly visible although its shading was usually uneven across the sample surface. In a few cases, no color at all was visible, indicating either a failure of the polymerization to initiate properly or a lack of incorporation of the tethered alkenes into the polymers. Hyperspectral imaging was used to improve the sensitivity for visualizing the ninhydrine stain on the membrane surface.

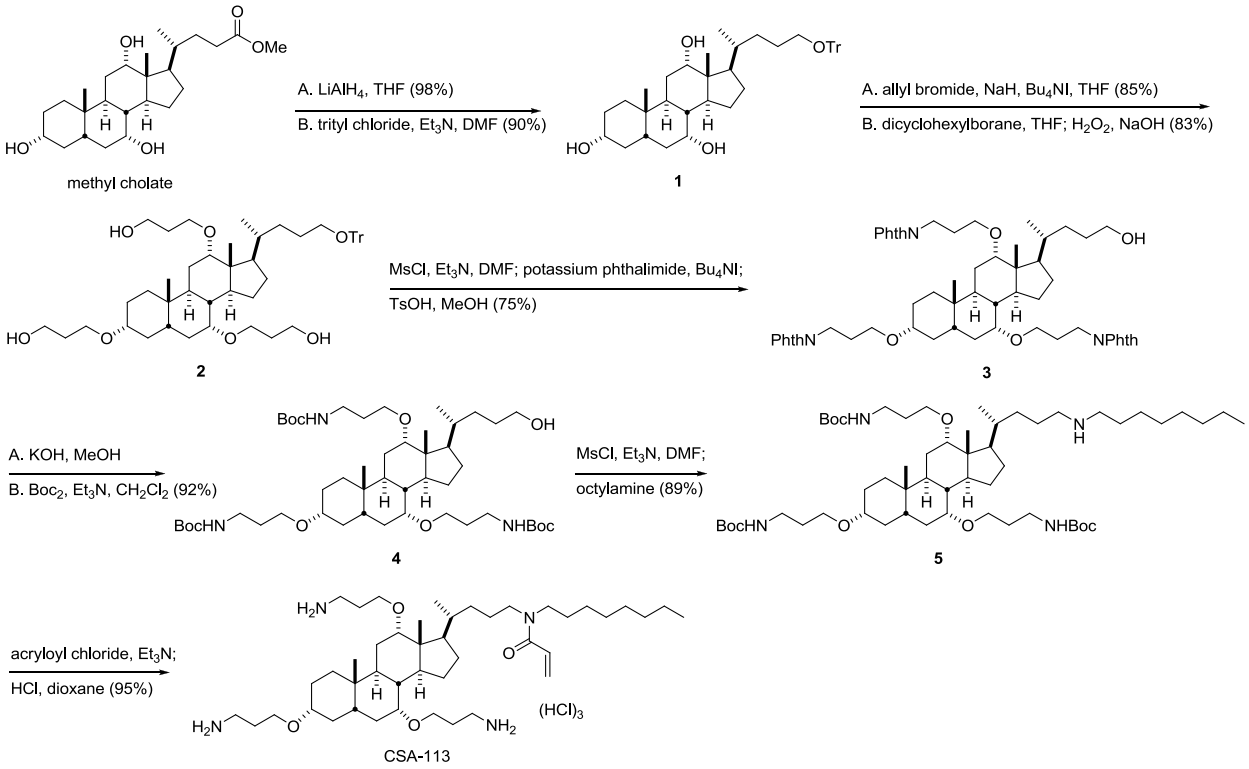

Figure 6: Synthetic scheme for CSA-113.

Figure 7 shows the hyperspectral imaging results for the attachment of CSA-113 to RO membranes and stained with ninhydrin. Four spectral images were collected from four different formulations consisting of different ratios of CSA-113 to acrylamide (only 3 are shown in Figure 7). Shown are 3 pure spectral components: 1) The fluorescence emission of the ninhydrin stain present in an ethanol solution of a primary amine(n-propylamine) (Ninhydrin – Solution) which was used as a spectral reference, 2) The MCR derived spectral component for ninhydrin bound to the ceragenin (Ninhydrin - Membrane), and 3) The MCR derived spectral component representing the fluorescence emission emanating from the membrane itself (Membrane Autofluorescence). The MCR derived ninhydrin pure spectral component from the membrane matches quite well with the spectral reference for ninhydrin (Ninhydrin – Solution), suggesting that we can detect ninhydrin in the presence of the membrane autofluorescence. Figure 7 also shows three intensity or concentration image maps for 3 different formulations. Notice that the intensity of the concentration images increase with an increase in the ratio of CSA-113 to acrylamide. An increase in the amount of acrylamide did not change the results, confirming the ninhydrin intensity is solely dependent on the amount of ceragenin present on the surface of the membrane. The fourth membrane (not shown) was a membrane without CSA-113 and acrylamide. This membrane had increased membrane autofluorescence (possibly due to the lack of a membrane coating) and with no indication of the ninhydrin stain. When coating methodologies increased the amount of ceragenin on the surface of the membranes, this hyperspectral imaging technique was no longer required because visual inspection of purple ninhydrin stain could be accomplished with the human eye.

Figure 8 shows the results obtained from the infrared ATR measurement of several formulations of CSA-113. The MCR derived spectral component #4 (Figure 8A) correlates with those membranes that should contain CSA-113 in the membrane coating. The largest spectral signature in the spectral component in Figure 8A can be seen in the sp3 C-H stretching region (2800-3000 cm^{-1}), because of the increased amount of hydrocarbons on the surface of the membrane due to the ceragenin. The concentrations or intensities for six different membranes with different CSA-113 formulations are shown in Figure 8B. The first three formulations contain no CSA-113, only the chemical precursors prior to the attachment of the CSA-113 (blank membrane, alcohol and alkene pretreatment, or Poly(acrylamide)). The last three membranes contain formulations that all have CSA-113. The red center line in each box plot represents the

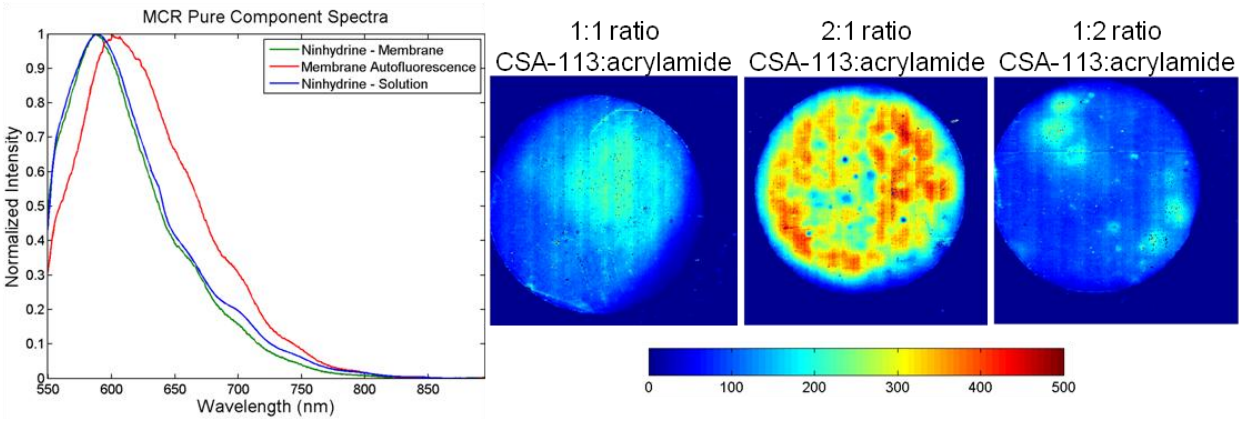

Figure 7: Hyperspectral imaging results for CSA-113 attached to membranes.

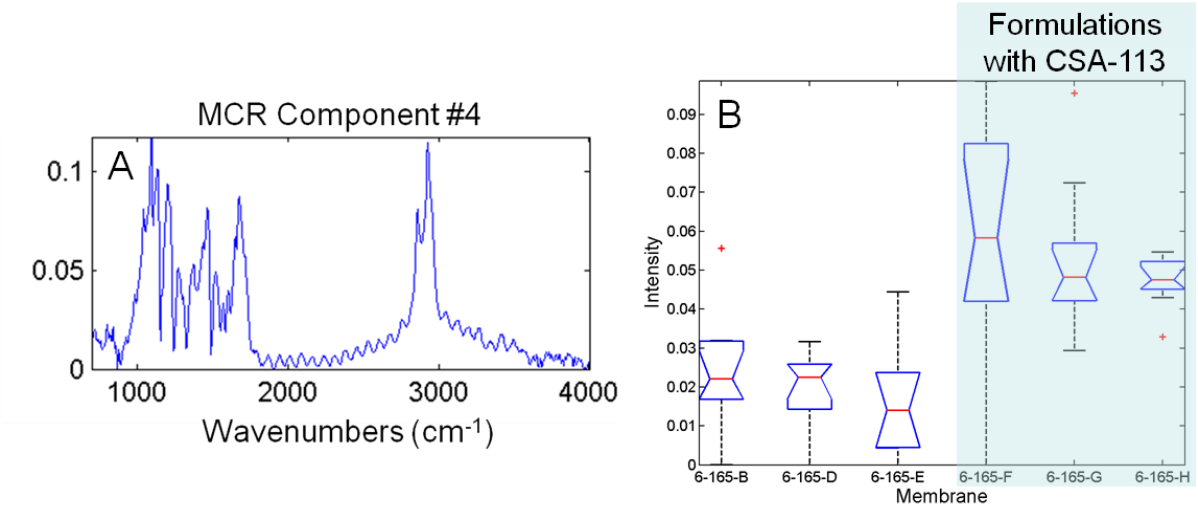

Figure 8: MCR results of the Infrared ATR spectral data.

median intensity of component #4. If the notches in the box plots do not overlap then the medians are different at greater than the 95% confidence interval. The bottom and top of the box represents the 25th and 75th percentiles. The whiskers extend to approximately +/– 2.7σ, which is ~ 99.3% coverage of the data. The red + symbols represent outliers, which represent data that lie outside the whisker range. It is clear from these plots that spectral component #4 is clearly associated with membrane bound CSA-113. The advantage of using this infrared technique was that it didn't require any exogenous stains, however it was more laborious than the visual inspection of the purple ninhydine with the human eye, therefore this technique was not used routinely. Instead this technique was used to confirm formulations in which the purple ninhydrin could not be seen with the naked eye.

2.3.2 Experimental Sample

A 2" x 4" piece of RO membrane was pretreated by soaking in a 5% solution of sodium bicarbonate (aqueous) for 1-2 hours. Then it was rinsed with water, dipped briefly into isopropyl alcohol (IPA) and then the surface was treated with 800 mg of 3,4-epoxy-1-butene dissolved in 32 mL of IPA. During this treatment, the membrane and solution were heated to 45 ^{o}C for 15 minutes. The membrane was rinsed with IPA and then water. The surface of the membrane was then treated with a solution of CSA-113 (224 mg), acrylamide (19 mg) in 26.67 mL water. The initiator (0.83 mg potassium persulfate + 0.28 mg sodium metabisulfite) was added and the reaction was allowed to take place at room temperature for 24 hours. Finally, the membrane was rinsed with water.

2.3.3 Biofouling Testing

With only a few exceptions, the biofilm cell density on the ceragenin-linked membranes was lower than that of the control membranes (Table 2). The largest reduction observed was 79% or a 0.68 log reduction on the SST1 membrane run with a 1:2 CSA-13:acrylamide ratio for 14 days. Student's t-tests showed significant differences between the controls and the ceragenin-linked membranes for the GE BWRO and SST1 membranes for all membranes with ceragenins compared to all of the controls.

There is clearly a lot of noise in the data (Figure 9). Trends in biofouling reduction as a function of CSA-13:acrylamide ratio was not observed. Trends in in biofouling reduction as a function of time were also not observed.

Table 2: Summary of Biofouling Testing Results for Membrane Created Using Amine-Linked Polymer Brush Method (shading indicates biofouling reduction).

Membrane	CSA-113:acrylamide Ratio	Biofouling Reduction					
		Log 7 days	Log 14 days	Log 28 days	% 7 days	% 14 days	% 28 days
GE BWRO	1:1	---	0.08	0.01	---	16.8%	2.6%
GE BWRO	1:2	---	0.42	0.02	---	61.9%	5.2%
GE BWRO	2:1	---	0.39	0.03	---	59.3%	7.6%
SST1	1:1	---	0.40	0.28	---	60.6%	47.7%
SST1	1:2	---	0.68	0.37	---	79.0%	57.5%
SST1	2:1	---	0.52	0.40	---	69.9%	59.8%
SST2	1:1	0.04	0.24	---	9.6%	42.2%	---
SST2	1:2	-0.01	0.28	---	-2.0%	47.7%	---
SST2	2:1	0.13	0.25	---	26.5%	43.2%	---

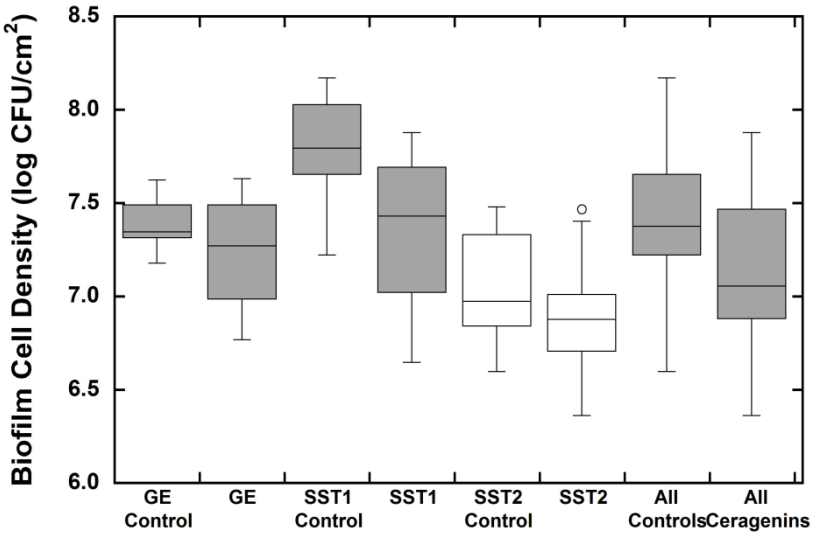

Figure 9: Comparison of biofouling testing results between controls and ceragenin-linked membranes created using the amine-linked polymer brush method as a function of membrane type. Note that the data collected on membranes generated with different CSA-13:acrylamide ratios are pooled. Statistically different data are shaded in gray.

2.4 The UV-Grafted Polymer Brush Method

2.4.1 CSA-113 Attachment

In the UV grafting method of attachment, copolymers similar to those described in Section 2.3 are grown off of the surface, but the number of polymers chains is not limited by the number of free amines on the surface. Figure 10 shows the scheme for the UV-grafted polymer brush method of attachment. The process begins with the deposition of benzophenone, a UV-absorbing photoinitiator, on the RO membrane. The surface is then covered with an aqueous solution of CSA-113 and acrylamide and a UV lamp is placed above the solution. When the benzophenone molecules absorb the UV light, radicals are formed and the polymerization reaction begins at the membrane surface. As with the amine-linking method, each one of the copolymer chains can contain many ceragenin molecules. The UV grafting method has the potential to result in the attachment of more ceragenin molecules, although there is also the potential problem that UV exposure could damage the RO membrane.

Ninhydrin staining of these membranes tended to give more consistent results than those described in Section 2.3 although the color was still only a light purple. Cross-flow testing of these membranes as well as control membranes that were exposed to UV but no monomers showed significant decreases in the flux of water through the membranes, indicating damage to the polyamide layer of the RO membrane.

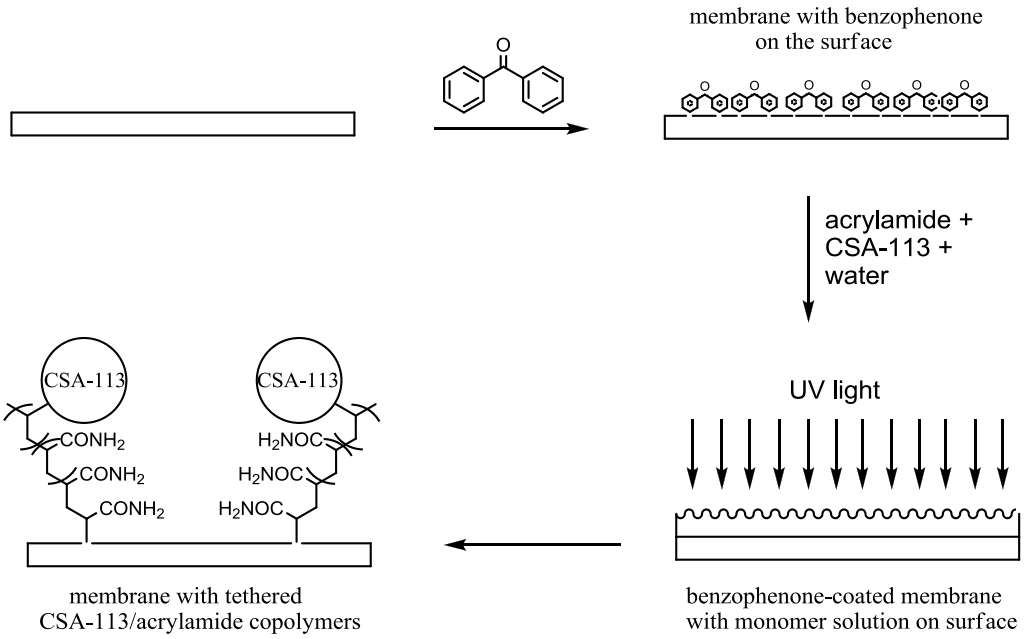

Figure 10: Scheme for UV-grafted polymer brush method.

2.4.2 Experimental Sample

A 1" x 3" piece of RO membrane was pretreated by soaking in deionized water for 24 hours and then in ethanol for 5-10 minutes. Then it was soaked in a 10 mM solution of benzophenonoe in ethanol at room temperature for 1 hour, after which it was removed and dried under vacuum. Next the surface of the membrane was covered with a solution of CSA-113 (337 mg) and acrylamide (28 mg) in 8 mL water. The membrane and solution were covered with a quartz plate and UV radiation (365 nm) was directed through the quartz plate for 30 minutes. Finally, the membrane was rinsed with water.

2.4.3 Biofouling Testing

With 14 days of biofouling, biofouling reduction was observed on the GE BWRO and SST1 membranes with ceragenins (Table 3). In contrast the SST2 membranes with ceragenins had greater biofilm surface densities than the controls. With 7 days of biofouling, a biofouling reduction was observed on the GE BWRO membranes but an increase in biofouling was observed in the SST2 membranes. A biofouling reduction was observed with 28 days of growth on the SST1 membrane. The largest reduction observed was 78% (or a log reduction of 0.67) on the GE BWRO membrane with a 1:3 CSA-113:acrylamide ratio and 14 days of biofouling. In cases where a biofouling reduction was observed on a specific membrane, biofouling reduction increases with increasing CSA-113:acrylamide ratio. Student's t-tests only show significant differences between the controls and the ceragenin-membranes for the SST1 membranes (Figure 11). There is a large variation in measured biofilm surface densities.

Membranes with CSA-113 linked to them were also tested on the cross-flow system to determine whether the UV-grafted polymer brush method damaged the membrane. Flux through these membranes was greatly reduced. Therefore, this attachment method is not a viable option.

Table 3: Summary of Biofouling Testing Results for Membrane Created Using UV-Grafted Polymer Brush Method (shading indicates biofouling reduction).

Membrane	CSA-113:acrylamide Ratio	Biofouling Reduction					
		Log 7 days	Log 14 days	Log 28 days	% 7 days	% 14 days	% 28 days
GE BWRO	1:1	-0.33	0.13	---	-113%	26%	---
GE BWRO	1:2	-0.25	0.17	---	-79%	33%	---
GE BWRO	1:3	-0.12	0.67	---	-32%	78%	---
SST1	1:1	---	0.23	0.27	---	42%	46%
SST1	1:2	---	0.20	0.36	---	37%	57%
SST1	1:3	---	0.25	0.38	---	44%	58%
SST2	1:1	0.46	-0.15	---	65%	-40%	---
SST2	1:2	0.35	-0.29	---	55%	-94%	---
SST2	1:3	0.19	-0.26	---	35%	-81%	---

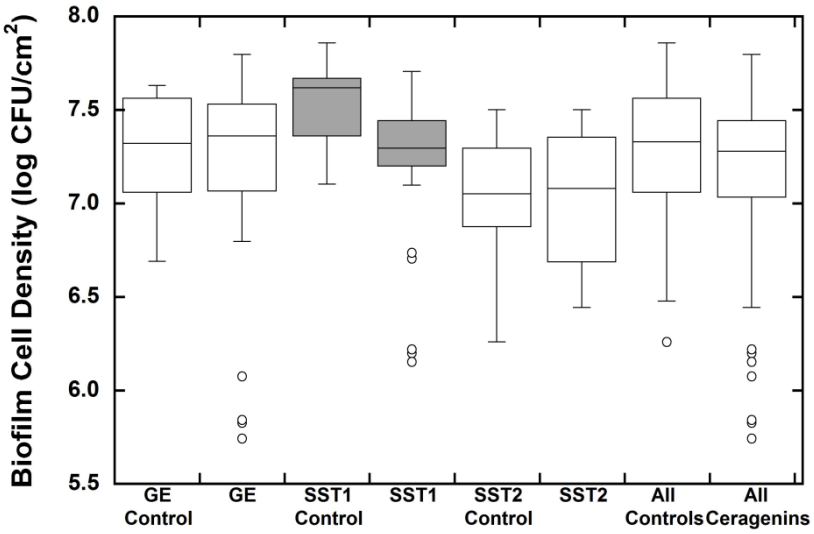

Figure 11: Comparison of biofouling testing results between controls and ceragenin-linked membranes created using the UV-grafted polymer brush method as a function of membrane type. Note that the data collected on membranes generated with different CSA-13:acrylamide ratios are pooled. Statistically different data are shaded in gray.

2.5 The Silane-Linked Polymer Brush Method

2.5.1 CSA-113 Attachment

In the silane-linked polymer brush method of attachment, a very thin silane coating is initially attached to the surface. The silane coating contains free amine groups that can then be used to create points of attachment for subsequent steps (Figure 12). The silane coating material is 3-aminopropyl trimethoxysilane (APTMOS) which can bind to free alcohols on the surface as well as to other APTMOS molecules. Initially there was some concern that the silane coating might block the passage of water through the RO membranes but cross flow tests of membranes treated with APTMOS showed no significant changes in the water flux.

The cross-linked silane network has many primary amine groups attached to it and these can be used for two different attachment techniques. In one embodiment, the aminosilane surface was treated with acryloyl chloride or with 4-(chloromethyl)benzoyl chloride (CMBC) to form acrylamide or chlorobenzyl moieties on the surface, respectively. These acrylamide and chlorobenzyl groups could then participate in a UV-initiated grafting reaction similar to that described in Section 0, although the UV treatment was found to damage the polyamide layer, thus making this method ineffective. In a second embodiment, the aminosilane surface was treated with 4-chloromethyl benzoylchloride (CMBC) and the chlorobenzyl groups functioned as atom-transfer radical polymerization (ATRP) initiators which were attached to the surface. Ceragenin-containing polymers were then grown off of the surface by an ATRP reaction which did not require UV light. As with the amine-linking and UV-grafting methods, each one of the copolymer chains can contain many ceragenin molecules. The silane-linked polymer brush

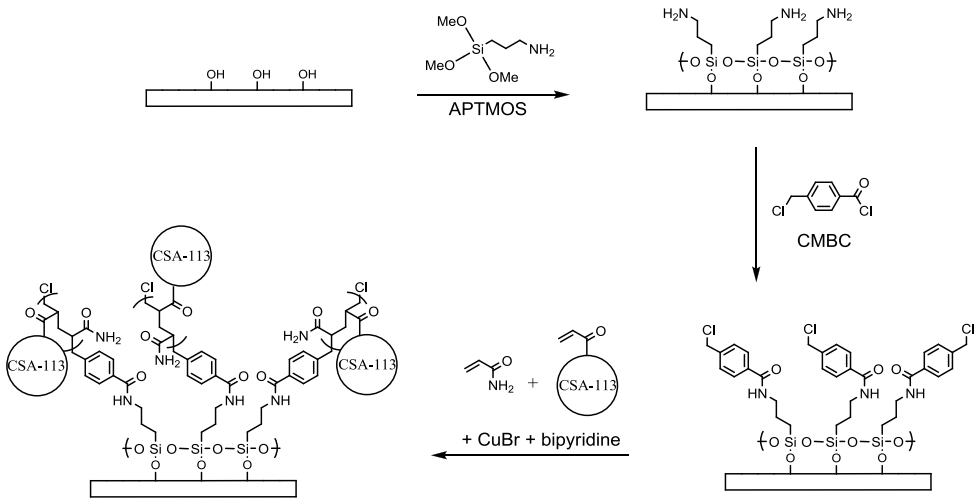

Figure 12: Scheme for silane-linked polymer brush method utilizing ATRP to form tethered acrylamide/CSA-113 copolymers.

method has the potential to result is the attachment of more ceragenin molecules without the problem of damage to the membrane by UV exposure.

Ninhydrin staining yielded more useful information with this method than with any other. Staining tests were performed after each of the reaction steps shown in Figure 12 to track the progress of the synthesis. After treatment with APTMOS, the membranes showed an even purple color of medium intensity. This color was completely absent from the same membranes after treatment with CMBC, indicating that the amines had all been converted to amides. After the ATRP reaction, the membranes showed inconsistent staining results similar to those discussed in Section 2.3.1. In some cases, the polymerizations appeared to fail to initiate, possibly due to oxidation of the copper(I) catalyst. In most cases the color was slight or uneven, indicating low amounts of attached ceragenins.

2.5.2 Experimental Samples

2.5.2.1 UV-initiated polymerization

The surface of a 1" x 3" piece of RO membrane was covered with a 2% solution of 3-aminopropyltrimethoxysilane (APTMOS) in ethanol for 90 minutes at room temperature. After rinsing with ethanol, the surface of the membrane was covered with a 1.5 wt. % solution of CMBC (or alternatively, acryloyl chloride) in ethanol at room temperature for 20 minutes. The membrane was then washed with ethanol and dried in air at room temperature.

The membrane was dipped into a solution of CSA-113 (1.22 g) and acrylamide (0.094 g) in a water: methanol (1:1, 20 mL, degassed) mixture. After removing it from the monomer solution (without rinsing or washing), the membrane was placed under a UV lamp (365 nm) for 15 minutes. Finally, the membrane was rinsed thoroughly with ethanol.

2.5.1.2 ATRP procedure

The surface of a 1" x 3" piece of RO membrane was exposed to a 2 wt. % solution of APTMOS in isopropanol for 90 minutes at room temperature. After rinsing with ethanol, the surface of the membrane was exposed to a solution of HCl (0.01M) for 1 hour, followed by a solution of Na_2CO_3 (1 wt. % in water) for 18 hours, followed by water for at least 1 h, followed by ethanol for at least 1 hour. Next, the surface of the membrane was exposed to a 1.5 wt. % solution of CMBC in ethanol for 4.5 hours. The membrane was then immersed in ethanol briefly, then in a solution of Na_2CO_3 (1 wt. % in water) for 18 hours, followed by water for at least 1 h, followed by ethanol for at least 1 hour. Next, the surface of the membrane was exposed to a 1.5 wt. % solution of CMBC in ethanol for 4.5 hours. The membrane was then immersed in ethanol briefly, followed by water for at least 1 hour.

The surface of the membrane was exposed to a solution of CSA-113 (1.22 g) and acrylamide (0.094 g) in a water: methanol (1:1, 20 mL, degassed). Copper(I) bromide (100 mg) and bipyridine (109 mg) were added and the reaction was covered and allowed to proceed at room temperature for 5 hours. Finally, the membrane was rinsed thoroughly with ethanol and water.

2.5.3 Biofouling Testing

Biofouling testing was not conducted using samples created with the direct attachment method.

2.6 The Silane Direct Attachment Method

2.6.1 CSA-121a Attachment

In the silane direct attachment method, the ceragenin (CSA-121a) is designed with a short tether with a terminal trimethoxysilane (TMS) group. Upon exposure to a membrane surface with alcohol functional groups (such as the PVA coating described in Section 2.1.1) the TMS groups will react to form covalent bonds with the surface and with each other (Figure 13). This should result in a high density of ceragenin molecules attached to the surface without any brush-like result in a high density of ceragenin molecules attached to the surface without any brush-like result in a high density of ceragenin molecules attached to the surface without any brush-like

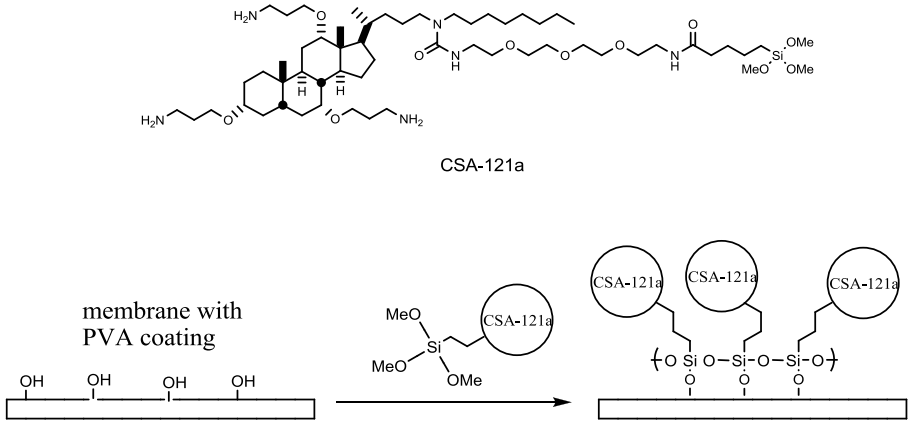

Figure 13: Structure of CSA-121a and scheme for silane direct attachment method.

result in a high density of ceragenin molecules attached to the surface without any brush-like polymers extending off of the surface and without relying on the free amines on the RO membrane. The tether on CSA-121a is designed to give the ceragenin molecule a limited range of motion in order to allow it to remain toxic to nearby organisms.

Samples that were prepared with low concentration solutions of CSA-121a (≤15 wt. %) gave a faint purple color upon ninhydrin staining. In some cases, this color faded away within 4 hours. Samples prepared with higher concentrations of CSA-121a showed dark, even coloring without a tendency to fade. Figure 14 staining with ninhydrin. Based on these results, the membranes that were treated with CSA-121a solutions with concentrations ≥20 wt. % were clearly the membranes with the highest concentration of attached ceragenins prepared in this project.

2.6.2 Experimental Sample

The surface of a 1" x 3" piece of RO membrane was exposed to a 20 wt. % solution of CSA-121a in isopropanol for 24 hours at room temperature. After rinsing with isopropanol, the membrane placed in a vacuum oven at 35 ^{o}C for 1 hour. Finally, the membrane was soaked in isopropanol for 24 hours.

2.6.3 Biofouling Testing

Three experiments were run testing on the membranes using the silane-linked polymer brush method, the first tested the membranes created using a solution with 2.6% and 5.2% of CSA-121a. The second tested membranes created with 15% and 20% solutions. Finally, the last experiment was run with membranes created with a 50% solution of CSA-121a. Because the three experiments were run using the same membranes for controls, comparisons were made between the ceragenin membranes and the controls run in the same experiment as the specific membranes and also between the controls for all three experiments.

The only case where a significant difference between the controls and the ceragenins was calculated using at Student's t-test, was for the membranes created with a 50% CSA-121a concentration (in comparison to the controls in the same experiment) (Figure 15). Biofouling reduction was observed for the membranes created with the 2.6%, 5.2%, and 50% CSA-121a solutions (Table 4). It should be noted that there was a large variation (over an order of magnitude) in biofilm surface densities for the controls. The largest biofouling reduction observed was 64% (or a log reduction of 0.45).

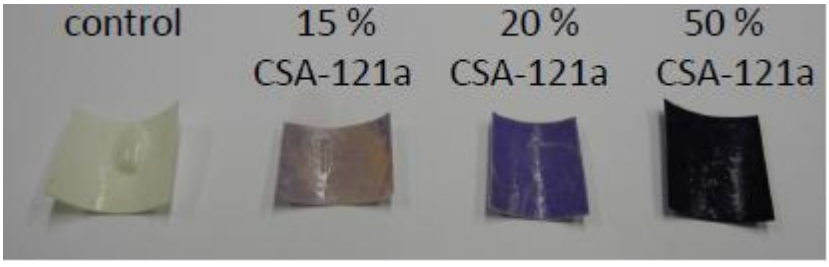

Figure 14: RO membrane samples treated with varying concentrations of CSA-121a, stained with ninhydrin.

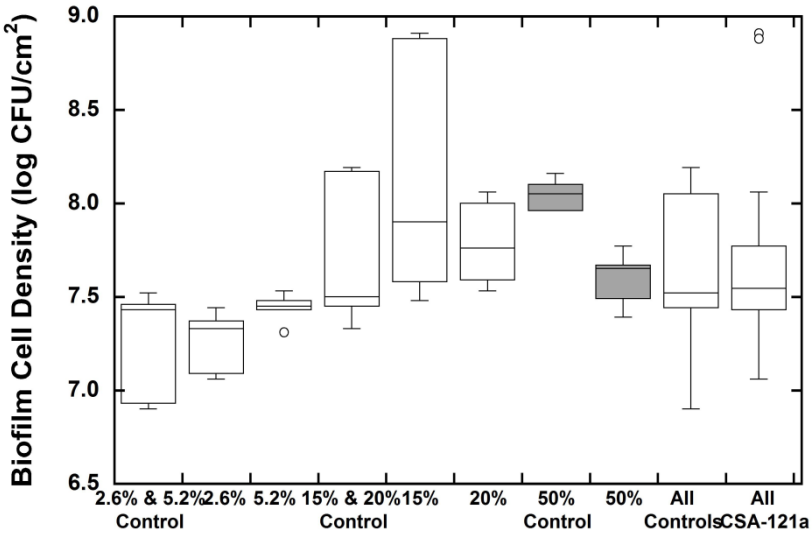

Figure 15: Comparison of biofouling testing results between controls and ceragenin-linked membranes created using the silane direct attachment method as a function of CSA-121a concentration. Statistically different data are shaded in gray.

Table 4: Summary of Biofouling Testing Results for Membrane Created Using the Silane Direct Attachment Method .(shading indicates biofouling reduction)

% CSA-121a	n (ceragenin membranes)	% Biofouling Reduction		Log Biofouling Reduction	
		Exp. Control	All Controls	Exp. Control	All Controls
2.6%	9	0.4%	59%	0.00	0.39
5.2%	6	-48%	41%	-0.17	0.23
15%	9	-164%	-175%	-0.42	-0.44
20%	9	-25%	-31%	-0.10	-0.12
50%	9	64%	15%	0.45	0.07

An accelerated biofouling test was also run on the cross-flow membrane system. The goal of this experiment was to test the membrane created with the 50% CSA-121a solution under more the more realistic flow conditions of the cross-flow system. This is a high-pressure system with flux through the membrane, much like a water treatment system. This test used an accelerated biofouling protocol [*Altman et al.*, 2010], thus the membrane was exposed to extreme biofouling conditions. The tank was inoculated with 4.2×10^{10} CFUs. The initial concentration of bacteria in the solution that was treated was 5.4×10^{6} CFU/ml and at the end of the test the concentration was 7.0×10^{7} CFU/ml.

Results demonstrated that the flux reduction in the membrane with linked CSA-121a was less than that of the control (Figure 16). At the end of the test, the flux through the CSA-121a membrane was approximately 30% greater than that of the control.

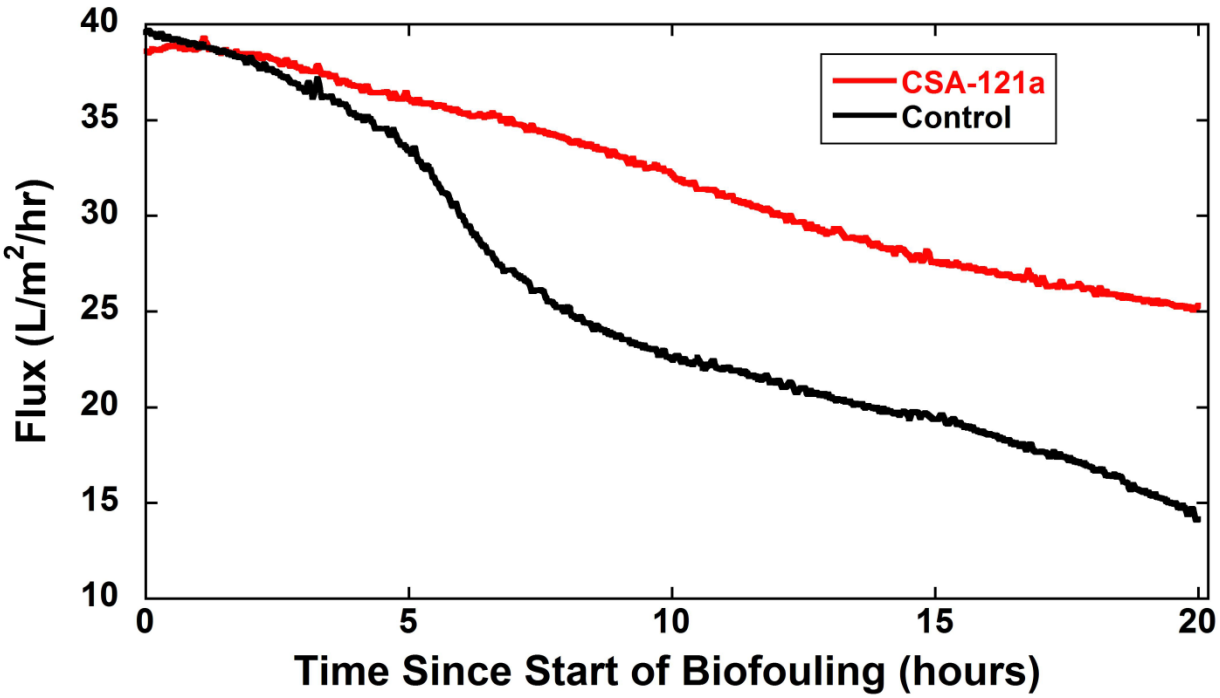

Figure 16: Results of cross-flow membrane testing on membrane with CSA-121a attached using the silane direct attachment method with a 50% CSA-121a solution. Results demonstrate less fouling on membrane with linked CSA-121a in comparison to a typical control.

This test also determined that the linking of the CSA-121a did impact the flux through the membrane. A pressure of on average 296 psi was needed to maintain the same initial flux as the control membrane, which ran with a pressure of on average 199 psi. In other words, a 50% greater pressure was needed to maintain the same initial flux of an untreated membrane.

2.1 Summary and Conclusions

Table 5 presents a summary of the results of the biofouling testing as a function of the attachment method. It is difficult to directly compare between attachment methods as different testing protocols were used for the amine-linked polymer brush method and the silane direct attachment method. The results can be summarized as follows:

- Biofouling reduction is observed in the majority of CDC reactor tests, indicating the ceragenins are a viable solution to biofouling on water treatment membranes.

- Based on ceragenin visualization on the membrane surface, the silane direct attachment method is the most promising attachment method if a high concentration of CSA-121a is used in the ceragenin solution.

- The silane direct attachment method with a solution of 50% CSA-121a demonstrated a 64% reduction in biofouling on the CDC reactor tests.

Table 5: Summary of Biofouling Testing

Attachment Method	Ceragenin	Ninhydrin Visualization	CDC Biofouling Testing Conditions	CDC Biofouling Testing Results
Direct Attachment	CSA-111	Ninhydrin – attachment not observed	N/A	N/A
Amine-Linked Polymer Brush	CSA-113	Ninhydrin – in consistent results Hyperspectral – inconsistent results, attachment spotty at best	Drinking water source of bacteria. Coupons sampled after 7, 14, and 28 days for flow.	0.08 – 0.68 log reduction 17% - 79% biofouling reduction. 11 out of 12 tests show biofouling reduction.
UV-Grafted Polymer Brush	CSA-113	Ninhydrin – light purple Hyperspectral – inconsistent results, attachment spotty at best	Drinking water source of bacteria. Coupons sampled after 7, 14, and 28 days for flow.	-0.29 – 0.67 log reduction -94 – 78% reduction. 9 out of 12 tests show biofouling reduction. UV-grafting damaged membrane
Silane-Linked Polymer Brush	CSA-113	Ninhydrin - Uneven, medium-intensity purple color	N/A	N/A
Silane Direct	CSA-121a	Ninhydrin – dependent on CSA concentration (see Figure 14). Looks promising	Pseudomonas fluorescens source of bacteria in artificial seawater. Tests run for 1 day in batch phase and 1 day in continuous flow phase.	-0.44 – 0.45 log reduction -175% - 64% reduction. 2 out of 5 test show biofouling reduction. Cross-flow testing look promising.

- The silane direct attachment method with a solution of 50% CSA-121a demonstrated approximately 30% less biofouling reduction in the cross-flow membrane test.

- Additional refinement of the attachment methods are needed in order to achieve our goal of a several log-reduction in biofilm cell density.

- Additional refinement of the attachment methods are needed to attach the ceragenins without impacting the membrane flux.

3 CHARACTERIZATION OF SOURCE-WATER BACTERIA

3.1 Introduction

The goal of this study was to isolate bacteria that are potential biofilm growers from relevant water sources for membrane treatment. The sources chosen were:

- Wastewater
- Agricultural drainage
- River water
- Seawater, and
- Brackish groundwater

All of the water samples were selected as potential water sources for desalination.

Wastewater is currently being treated for use as drinking water in countries with sparse water and the resources to do so (e.g., Singapore). In Albuquerque it is being treated for grass irrigation uses. As clean water becomes scarcer, it is likely that RO treatment of wastewater will become more common.

The agricultural drainage sample was chosen because the Bureau of Reclamation currently has a desalting plant built for treating such waters, though the plant is not in use. In this case, the water was going to be treated before discharge into Mexico. With development near the Colorado River, total dissolved solids increased considerably due to irrigation projects, where the water was drained back into the river to minimize water table rise. In response to concerns expressed by officials in Mexico that that the higher TDS was leading to lower crop yields, the U.S. government agreed to control the salinity [*Lohman*, 2003]. The agricultural drainage is now diverted into channels were it can be treated if needed. As the Yuma Desalting Plant is close to the Colorado River and this water can be treated in the research facility there, water from the river was also collected.

RO treatment of seawater is already taking place both in the U.S. (e.g., Carlsbad Desalination Project, Tampa Bay Seawater Desalination Plant) and internationally. Microorganisms are abundant in seawater and seawater can be prone to algal blooms, leading to potential membrane biofouling.

Brackish groundwater is also being treated for drinking water (e.g., the El Paso Water Utilities). It is a potential source of drinking water in inland locations where drinking water may become scarce and a surface water source is not apparent. While biofouling from microorganisms in groundwater is less likely than from surface waters, it was decided that it was worth researching.

3.2 Source Water Descriptions

Water samples were collected at 4 different sites: 1) the waste water treatment plant at Albuquerque (Southside Water Reclamation Plant), 2) the U. S. Bureau of Reclamation, Yuma

Desalting Plant, 3) the Seawater Desalination Test Facility at the Naval Facilities Engineering Command Engineering Service Center in Port Hueneme, CA, and 4) the Brackish Groundwater National Desalination Research Facility (BGNDRF) in Alamogordo, NM. Several samples were collected from each facility as described in Table 6. The highlighted samples, B, D, E, F, H, J, and K are thought to be the most relevant to water treatment. It is likely that wastewater will go through some treatment before membrane treatment, therefore the isolates from the primary effluent in Sample A were not used for extensive analyses. Chlorine can damage polyamide RO membranes, therefore the isolates collected from the chlorinated samples of wastewater were thought to be less relevant. For the same reason, sample G was not used for extensive analyses. Finally, it was thought that there could have been contamination in the tanks from which the samples were collected at BGNDRF (Samples L-O). Therefore, only the initial screening was conducted on these samples. All of the water samples were sent to Brigham Young University (BYU) for bacteria isolation, as described in Section 3.3.1.

Table 6: Summary of Water Samples Collected (highlighted samples are those thought to be most relevant for water treatment).

Sample ID	Water Source	Sample Description
A	Wastewater	Primary effluent
B	Wastewater	Final effluent with chlorine removed
C	Wastewater	Chlorinated final effluent
D	Agricultural Drainage	Collected from a channel with a scooper
E	Colorado River Water	Collected directly from the river
F	Agricultural Drainage	Collected from a different channel
G	Agricultural Drainage	Collected from the WQIC, treated with chloramines, ammonium and sulfuric acid to a pH of 5.5
H	Seawater	Untreated
I	Seawater	Treated with ultrafiltration or microfiltration
J	Groundwater	Well #1
K	Groundwater	Well #2
L	Groundwater stored in a tank	Tank #1 with pipe
M	Groundwater stored in a tank	Tank #1
N	Groundwater stored in a tank	Tanks #2 with pipe
O	Groundwater stored in a tank	Tank #3

3.3 Methods

3.3.1 Bacteria Isolation and Identification

Sample growth, isolation, amplification and 16S rRNA gene sequencing occurred in Paul Savage's laboratory at Brigham Young University. Once it was determined that the isolates could be handled under BSL-1 or BSL-2 containment, they were transported to Steve Branda's laboratory at Sandia National Laboratories. Steve Branda then conducted his own amplification and sequencing on the isolates, to confirm their taxonomic identifications.

At BYU, water samples were serially diluted and plated on TSA. For the saltwater samples, the TSA was mixed with 50% seawater (Sigma Aldrich) and 1.5% agar. Plates were incubated at room temperature (approximately 24 °C) for 48 hours to allow growth. Individual colonies were picked and re-streaked on fresh TSA plates. Colonies were re-plated until clean cultures were obtained.

A single colony of the bacterial isolate was collected from the plate and inoculated in sterile TSB. A 3 mL of each overnight culture was pelleted and washed with TE (Tris, EDTA) buffer in preparation for the DNA analysis. DNA was isolated using an E.Z.N.A genomic DNA isolation kit (Omega Bio-tek; Norcross, GA). Isolated DNA was quantified using a UV spectrophotometer at 260 nm. DNA was then diluted appropriately for PCR use. PCR Primers used (~µg per reaction) were 1) 16S DNA for: ACT CCT ACG GGA GGC AGC AGT (E338F), and 16S DNA rev: CGT CAT CCC CAC CTT CC (E1177R). PCR was performed with Platinum Pfx Polymerase Kit (Invitrogen; Carlsbad. CA) using the following cylces: 1) initial denaturing (95 °C for 10 minutes), 2) denaturing (95 °C for 45 seconds), 3) annealing (55 °C for 45 seconds), elongation (68 °C for 45 seconds), and 5) final elongation (68 °C for 60 seconds). Steps 2 through 4 were repeated 35 times before conducting the final elongation. All PCR reactions were then observed by electrophoresis on a 1% agarose gel.

Samples were prepared for sequencing as suggested by the BYU DNA Sequencing Center (BYU DNASC). Samples were sent to the BYU DNASC for sequencing. Forward and Reverse sequences were read using FinchTV [PerkinElmer, 2010]. Forward and reverse sequences were then aligned with hierarchical clustering using MultAlin [Corpet, 1988]. Aligned sequences were then compared to the greengenes 16S DNA Library [McDonald et al., In press]. Samples were identified based on the % similarity to the greengenes known isolates.

At Sandia National Laboratories, the procedure for DNA extraction, amplification and sequencing is as follows. 200 µl aliquots of water samples were spread on 1X TSB (BD Biosciences, 211768) agar (1.5%; Fisher Scientific, A360-500) and incubated at 25°C for 3 days. Bacterial isolates were further purified by re-streaking on 1X TSB (1.5% agar); colonies generated by single cells were preserved in frozen glycerol (10%) stocks, and used to inoculate liquid (1X TSB) cultures. DNA was extracted from confluent liquid cultures using the QiaPrep Spin MiniPrep kit (Qiagen, 27106). From each DNA extract the 16S rRNA gene variable regions V3-V7 were amplified, using two well-characterized [PLoS ONE 4:e7401] "universal" primers: E338F and E1177R, corresponding to positions 338-358 and 1193-1177 of rrnE in Escherichia coli K-12, respectively. Each 50 µl reaction mixture contained 25 pmol of each primer, 200 µM of each dNTP, 1.5 mM $MgCl_2$, and 1.5 units of Taq polymerase (Applied Biosystems). An initial denaturation step (95°C for 5 min) was followed by 30 cycles of 95°C

for 30 sec, 55°C for 30 sec, and 72°C for 1 min, and a final extension step (72°C for 7 min). Amplicons were purified using the QIAquick PCR Purification kit (Qiagen, 28104) and sent to Quintara Biosciences (Albany, CA) for Sanger sequencing. Taxonomic analyses were made on the basis of BLASTN-mediated comparison of full-length amplicon sequences to the 16S rRNA gene sequences deposited in the NCBI non-redundant nucleotide (nr/nt) database as of May, 2011. The species showing the greatest degree of full-length sequence identity to a bacterial isolate's amplicon was designated the isolate's closest relative. Bacterial nomenclature followed that used by the NCBI taxonomy database as of September, 2011.

3.3.2 High-Throughput Multiwell Plate Screening at SNL

Isolates obtained from BYU that we were able to continue to grow were also tested at Sandia for their biofilm growth potential using a high-throughput multiwall plate screening. The goal of this analysis was to determine the isolates that were most likely to be biofilm formers.

Bacterial isolates were resuscitated from frozen glycerol stocks through growth on 1X TSB (Teknova, T0420) agar (1.5%; Teknova, T0401) at 30°C for 1-2 days, and then grown in liquid culture (1X TSB) at 30°C with shaking for 4-8 hrs, to an OD_{600} of ~1. These starter cultures were used to inoculate 0.1X TSB to an OD_{600} of 0.05, and 300 µl aliquots were transferred to the wells of a sterile, ultra-low attachment 96-well microtiter plate (Costar, 3474), using ≥6 wells *per* bacterial isolate; additionally, ≥8 wells *per* plate received media without bacteria, to serve as negative controls. Each well contained a sterile ¼" x ¼" square coupon of Sepa CF Polyamide reverse-osmosis AG membrane (Spectrum Lab Products, YMAGSP3001). Once wetted by the bacterial cultures, the coupons remained submerged for the duration of the experiment. By design, the coupons were too large to lay flat on the bottom surfaces of the wells; this ensured that both faces of the membrane remained readily accessible to the bacteria in the cultures. The microtiter plates were placed within a 30°C humid chamber and incubated without shaking for 10 days. At this point, each membrane coupon was removed from its bacterial culture and transferred to a new microtiter plate well containing 300 µl of 1% (w/v) crystal violet dye in water. After staining at room temperature (RT) for 10 min, each coupon was transferred to a new microtiter plate well containing 300 µl of water, and allowed to stand at RT for 5 min. This step was repeated, for a total of two washes. Finally, each coupon was transferred to a new microtiter plate well containing 200 µl of 95% ethanol, and the plate incubated at RT with vigorous shaking (Lab-Line Titer Plate Shaker, set at maximum speed) for 10 min. After removing the coupons from the wells, the RT incubation with vigorous shaking was repeated for 5 min, in order to disperse clumps of biofilm material and fully dissolve their associated crystal violet dye. Optical density at 600 nm (OD_{600}) was measured for each well using a SpectraMax 190 microtiter plate reader (Molecular Devices). Absorbance readings were scaled against the "background" absorbance (mean of the OD_{600} readings in the negative-control wells) of the plate; resulting negative values were set to zero. Each bacterial isolate showing robust growth in starter cultures was tested in this way in at least 3 independent experiments (≥6 wells per experiment), and the background-scaled OD_{600} readings from the replicate experiments were pooled for statistical analyses. Mean, median, and standard deviation values were calculated for each isolate.

3.3.3 High-Throughput Multiwell Plate Screening at NDSU

Isolates obtained from the seawater sample that we were able to continue to grow (H2, H3, H4, and H6) were also tested for their biofilm growth potential at the Center for Nanoscale Science and Engineering at North Dakota State University (NDSU). Combinatorial, high-throughput capabilities at NDSU are well established for the testing of antifouling marine coatings for naval applications. Having NDSU test the seawater isolates allows for comparison with the high-throughput testing at Sandia.

The silicone elastomer, Dow Corning Silastic® T2, served as the test surface for assessing the biofilm growth characteristics of the bacterial isolates and was prepared in 24-well plates as described previously [*S J Stafslien et al.*, 2006]. Several different growth conditions were investigated and included variations in the initial inoculum concentration (1% or 10% of a 0.4 OD_{600} suspension in artificial sea water), incubation temperature (18°C or 28°C), duration of incubation (24 hrs or 72 hrs) and the carbon and energy source utilized in the growth medium (0.5 g/l of peptone or dextrose). One milliliter of each bacterial suspension was added in triplicate to a 24-well plate of Silastic T2. Upon incubating at the desired set of growth conditions, the plates were quantified for biofilm growth using a high-throughput crystal violet colorimetric assay [*S Stafslien et al.*, 2007]. Briefly, the spent media and planktonic growth were discarded from the wells of the plates by inverting them over a plastic container. The plates were then rinsed three times with 1.0 ml of sterile artificial sea water, inverted and tapped on a paper towel and dried at ambient laboratory conditions for approximately 1 hour. Upon drying, 0.5 ml of the biomass indicator dye, crystal violet (0.3% wt/v in deionized water), was added to the wells of the plates for 15 minutes and the excess dye was removed using the rinsing procedure described above. Digital images were captured of each plate after crystal violet staining and each well was subsequently treated with 0.5 ml of 33% glacial acetic acid for 15 minutes to elute the crystal violet dye bound to the biofilms attached to the Silastic T2 coating surface. 0.15 ml of the resulting eluates were transferred to a 96-well plate and measured for absorbance at 600 nm using a multi-well plate spectrophotometer. The absorbance values obtained were considered to be directly proportionally to the amount of biofilm growth obtained on the surface of the Silastic T2. The biofilm growth obtained for each isolate is reported as the mean of all of the measurements of all the growth conditions. In addition, Appendix B presents the results for each individual growth condition as the mean absorbance value of three replicate samples. Error bars represent one standard deviation of the mean crystal violet absorbance value.

3.3.4 Tube Reactor Experiments

Tube reactor experiments were conducted at the Standardized Biofilm Methods Laboratory at the Center for Biofilm Engineering (CBE) at Montana State University. These tests were meant to further test the ability of isolates to form biofilms. Isolates were selected from each source water based the results of the testing described in Section 3.3.2 and results described in Section 3.4.2. The goal during methods development was to include relevant conditions to the extent possible to encourage the bacteria to form biofilms. Site water was used as the medium so any trace elements and nutrients the bacteria needed for growth were present. A concern with using the site water only was the low carbon concentration; therefore, the decision was made to supplement the water with 10 mg/L TSB. The remaining test conditions, such as temperature and time in the incubator during biofilm growth, were consistent for all 12 isolates.

3.3.4.1 Isolate Preparation

Table 7 lists the isolates evaluated and associated site water. The isolates were streaked for isolation on TSA and R2A media. The plates were incubated at 23°C and the growth examined at 24 and 48 hours. Isolates that did not grow well at 23°C were moved to a 30°C incubator to encourage growth. The growth was more consistent on TSA than R2A, and so TSA was used for the remainder of the plating. After sufficient colonies grew, isolated colonies were streaked on TSA for confluent growth. The confluent growth was harvested with cryofreeze solution (2% peptone/20% glycerol in water) for frozen stocks.

Table 7: List of isolates evaluated for biofilm growth.

Source Water	Isolate	Isolate ID
Wastewater	*Pseudomonas* spp.	B2
Wastewater	*Nocardia coeliaca* *Rhodococcus* spp.	B4
Agricultural Drainage	*Pseudomonas fluorescens*	D1
Agricultural Drainage	*Pseudomonas* spp.	D4
Agricultural Drainage	*Hydrogenophaga palleronii*	D5
Colorado River Water	*Pseudomonas* spp.	E6
Seawater	*Sulfitobacter donghicola*	H2
Seawater	*Rhodococcus fascians*	H3
Seawater	*Rhodobacter katedanii*	H4
Seawater	*Paracoccus marcusii*	H5
Seawater	*Rhodococcus fascians*	H6
Ground water	*Sphingopyxis* spp.	J1

3.3.4.2 Reactor Design

Experiments were conducted in batch reactors with recycle. The reactor vessel was a 1 liter Erlenmeyer flask topped with a rubber stopper plumbed with five ports: two effluent ports, two influent ports and an air exchange port. Size 16 tubing (ID = 0.32 cm) was connected to the bottom of each effluent port. The tubing went to the bottom of the flask. Additional sections of size 16 tubing were connected to the top of each effluent port. This tubing was spliced into two lines and each line was fed through a pump head. Following the pump, the tubing was rejoined into single lines that were connected to the top of each influent port. The air exchange port was fitted with a 0.2 μm filter for sterile air exchange. The pump was operated so that the recycle flow rate was equal to 80 mL/min/tubing section, which resulted in a 1 minute residence time in the tubing. For these settings, the calculated Reynolds Number was equal to 540 (laminar flow).

3.3.4.3 Reactor Operation

Each reactor was assembled and sterilized. 750 mL of filter sterilized site water was aseptically poured into the reactor followed by the addition of TSB to a final concentration equal to 10 mg/L. The reactor was then inoculated with individual colonies from a streak plate. The entire system was placed in a 23°C incubator and the pump was turned on briefly to circulate the inoculated site water. The pump was left off while the system incubated for 24 hours. At the end

of 24 hours, the pump was started. On day 3, three of the four sections of the tubing were sampled for biofilm growth. 5 cm sections of tubing were cut with sterile scissors before the tubing went through the pump. TSB was again added to the bulk water to a final concentration of 10 mg/L, and the pump was started for another four days. On day 7, three final biofilm samples and a sample for imaging were collected. The entire experiment was repeated three times for each isolate.

3.3.4.4 Biofilm Samples

The interior of each removed section of tubing was scraped with a sterile wooden applicator stick into 9 mL sterile buffered water. The tubing was rinsed with 1 mL of sterile buffered dilution water which was pipetted through the tubing into the dilution tube containing the removed biofilm. The biofilm sample was vortexed for 30 seconds, sonicated for 30 seconds at 25 kHz (100% power on sweep mode), vortexed for 30 seconds, sonicated and vortexed one final time. The disaggregated sample was serially diluted and plated. The plates were incubated at 23°C or 30°C, depending upon the isolate, for up to 7 days. Results for each experiment are reported as the mean log biofilm density ($Log_{10}(cfu/cm^2)$).

3.3.4.5 Total Protein Assay with Biofilm Samples

1.5 mL of each 10^0 disaggregated biofilm sample was aliquoted into sterile microcentrifuge tubes. The aliquots were frozen at -70°C for a minimum of 30 minutes. Once the samples were removed from the freezer, the tubes were placed in a container of ice to keep them cool. The contents of each tube were sonicated at medium to high power using a probe sonicator in 3 – 20 second bursts with a 10 – 20 second rest between each burst to allow cooling of the sample and probe. Between each sample, the probe was rinsed with laboratory reagent grade water and wiped with a Kimwipe. The tubes containing the lysed cells were centrifuged @ 14,000 RPM for 5 minutes to pellet the cells. 1 mL of the supernatant was pipetted into a sterile microcentrifuge tube. 1N (1X) Folin-Ciocalteu Phenol Reagent was prepared by diluting the supplied 2N (2X) reagent 1:1 with reagent grade water. Because the diluted Phenol Reagent was unstable, only the minimum amount was prepared. 0.2 mL of each prepared sample was added to a test tube. 1.0 mL of the Modified Lowry Reagent was added to each test tube and the contents vortexed with 15 sec intervals between each tube. The samples were incubated for 10 minutes at room temperature. 0.1 mL 1N Phenol Reagent was added to each test tube and the tube was vortexed. These samples were incubated for 30 minutes at room temperature. The spectrophotometer was zeroed with water, and the absorbance of each sample measured at 750 nm. The protein concentration of each unknown sample was calculated using the following equation:

$$\text{Concentration} = (\text{Absorbance} - 0.0352)/0.0022$$

This concentration was transformed from μg/mL to $\mu g/cm^2$ by multiplying by 10 mL (original volume scraped into) and dividing by the surface area scraped (5.0265 cm^2). The limit of detection was found by substituting 0.0353 in as the lowest possible absorbance that would give a meaningful result, then dividing this number by 2, as shown below:

$$\text{Limit of detection} = [(0.0353-0.0352)/0.0022*10/5.0265]/2 = 0.0452\ \mu g/cm^2$$

The results are reported as the mean of three samples for each experiment.

3.3.4.6 Analysis

The variance components (among and within experiment variability) were calculated in Minitab 16 using a general linear model ANOVA. For this analysis, the day 3 and day 7 results were pooled, sample day was a fixed factor and experiment was a random factor. The mean and repeatability standard deviations (per sample day) were calculated in Excel.

3.3.5 CDC Reactor Experiments

CDC reactor experiments were conducted at the Biofilms Laboratory and Sandia National Laboratories. The method used to quantify biofouling on the membrane surface is based on a standard method [*ASTM*, E 2562-07]. The bulk water chemistry and flow rate differed from the standard method. Experiments were carried out using Centers for Disease Control and Prevention (CDC) biofilm reactors (BioSurface Technologies, Corporation). Prior to running each experiment, the reactor and carboys were autoclaved at 121°C for 30 minutes. Different water chemistries were used for different isolates (Table 8) based on analyses of the original waters from which the isolates were obtained (Table 9). Seawater samples used a generic artificial seawater chemistry. Isolates, B4, D1, and E6 had a 24 hour batch phase with 300 mg/L TSB. The seawater samples were batched for at least 72 hours in 300 mg/L TSB. Different flow rates and therefore residence times were used for the continuous flow phase of the experiments (Table 8). 100 mg/L TSB was used as the nutrient during the continuous flow phase. Reactors were continually mixed during the batch and flow phase at 150 rpm. All experiments were incubated at room temperature.

Table 8: Summary of Testing Conditions for Biofilm Growth in a CDC Reactor.

Date Flow Initiated	Isolate ID	Concentration of Elements in the Medium (mg/L)	Flow Rate (Residence Time)	Sampling Times (Days after Flow)
9/21/2011	B4	92 Na, 60 Ca, 24 Mg, 20 K, 122 HCO_3, 212 Cl, 96 SO_4, 0.95 PO_4, 9.0 NH_4	5.6 mL/min (1.2 hrs)	1 and 3
8/30/2011	D1	690 Na, 40 Ca, 2.4 Mg, 3.9 K, 366 HCO_3, 518 Cl, 586 SO_4, 0.95 PO_4, 9.0 NH_4	5.6 mL/min (1.2 hrs)	1 and 3
9/13/2011	E6	103 Na, 80 Ca, 49 Mg, 9.8 K, 214 HCO_3, 204 Cl, 192 SO_4, 0.95 PO_4, 9.0 NH_4	5.6 mL/min (1.2 hrs)	1 and 3
8/8/2011	H4	11,088 Na, 401 Ca, 729 Mg, 391 K, 140 HCO_3, 18,099 Cl, 2,882 SO_4, 0.95 PO_4, 9.0 NH_4	1.0 mL/min (6.7 hrs)	1, 2, 3, and 4
8/1/2011	H5	11,088 Na, 401 Ca, 729 Mg, 391 K, 140 HCO_3, 18,099 Cl, 2,882 SO_4, 0.95 PO_4, 9.0 NH_4	1.0 mL/min (6.7 hrs)	1, 2, 3, and 4
8/15/2011	H6	11,088 Na, 401 Ca, 729 Mg, 391 K, 140 HCO_3, 18,099 Cl, 2,882 SO_4, 0.95 PO_4, 9.0 NH_4	1.0 mL/min (6.7 hrs)	1, 2, 3, and 4

Table 9: Water Analysis Results on Source Waters.

Element	Concentration (mg/L)			
	Waste Water	Agricultural Drainage	River Water	Seawater
F	1.2	---	---	---
Cl	105.8	548.5	148.0	18,711
NO_2	3.9	---	---	---
Br	0.3	---	---	---
NO_3	42.9	---	9.5	---
PO_4	2.0	---	---	---
SO_4	126.8	786.1	322.9	2,586
Al	0.05	---	---	---
B	0.287	52	0.6	14
Ba	0.017	25	0.28	14
Ca	56.0	31	94.2	848
K	17.8	---	1.36	---
Mg	8.06	---	31.5	981
Na	101.3	674	145.8	10,240
Sr	0.374	---	1.21	---
Charge Balance Error	0.5%	9.2%	2.6%	1.3%

The reactor was inoculated with 1 mL of overnight growth in TSB for isolates B4, D1, and E6. Seawater isolates were grown on TSA and scraped with an inoculating loop. The reactor was inoculated with an inoculating loop full of the isolates.

Biofilm was scraped from reactor coupons with a polypropylene cell lifter (Corning) and placed into 10 mL of DI. The solution was then sonicated for 5 to 10 minutes to reduce cell clumping [*Heersink*, 2003] vortexed, and serially diluted. Cell concentrations in the diluted samples were quantified using pour plating. Samples were plated onto TSA. Plates were incubated at 30°C for approximately 48 h prior to counting. Three plates were counted for each sample.

Protein analyses were conducted using the same methods described in Section 3.3.4.5. Differences include that the aliquots were frozen at -20°C instead of -70°C. The calibration curves and limit of detection also differed:

$$\text{Concentration} = 336.7(\text{Absorbance}) - 4.52 \qquad R^2 = 0.997$$

3.4 Results

3.4.1 Bacteria Isolation and Identification

The results of the bacterial isolation and identification work performed at both BYU and SNL are presented in detail in Appendix A, and summarized in Figure 17 and Table 10. Sixty nine isolates were identified. 72% of the isolates were Gram-negative bacteria, nearly all belonging to the phylum Proteobacteria (26% α-class, 26% β-class, 46% γ-class), with a single Flavobacteria isolate proving the exception. The majority of γ-proteobacteria isolates (78%) were most closely related to Pseudomonas species. Of the Gram-positive isolates, 84% belonged to the class Actinobacteria, the rest to Bacilli. The majority of actinobacteria isolates were most closely related to Rhodococcus (50%), Microbacterium (19%), or Arthrobacter (19%) species.

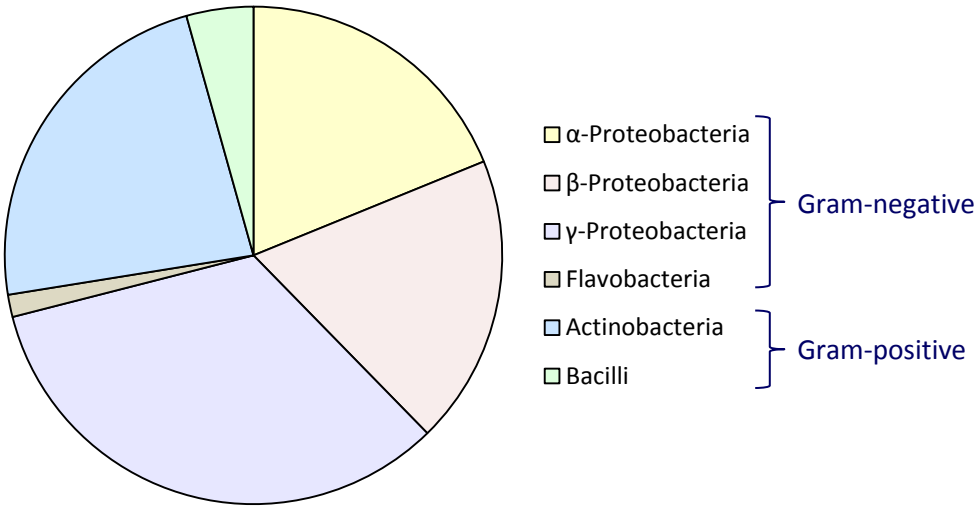

Figure 17: Identities of isolates by taxonomic class.

Table 10: Summary of Isolate Identification Result

Water Source	Isolate ID	Class	Closest Relative	Sequence Identity (%)
primary effluent CABQ	A1	Actinobacteria	*Nocardia globerula* *Rhodococcus globerulus*	100
	A2	Actinobacteria	*Nocardia globerula* *Rhodococcus globerulus*	85
	A5	Actinobacteria	*Microbacterium oxydans*	99
	A6	α-Proteobacteria	*Aminobacter aminovorans*	94
	A7	α-Proteobacteria	*Brevundimonas bullata*	100
	A8	Actinobacteria	*Rhodococcus erythropolis*	99
	A9	β-Proteobacteria	*Pusillimonas noertemanni*	92
re-use water CABQ w/o chlorine	B1	γ-Proteobacteria	*Pseudomonas meridiana*	99
	B2	γ-Proteobacteria	*Pseudomonas brenneri* *P. collierea* *P. fluorescens*	100
	B3	Actinobacteria	*Microbacterium oxydans* *M. maritypicum*	100
	B4	Actinobacteria	*Nocardia coeliaca* *Rhodococcus boritolerans* *R. erythropolis* *R. globerulus* *R. qingshengii*	99
	B5	γ-Proteobacteria	*Pseudomonas putida*	98
	B6	γ-Proteobacteria	*Pseudomonas migulae*	97

Table 10: Summary of Isolate Identification Result

Water Source	Isolate ID	Class	Closest Relative	Sequence Identity (%)
re-use water CABQ w/ chlorine	C1	γ-Proteobacteria	*Pseudomonas marginalis* *P. meridiana* *P. veronii*	100
	C2	Actinobacteria	*Rhodococcus erythreus* *R. erythropolis*	99
	C3	Actinobacteria	*Microbacterium oxydans*	90
	C4	γ-Proteobacteria	*Pseudomonas putida*	100
	C5	γ-Proteobacteria	*Pseudomonas migulae*	88
	C6	γ-Proteobacteria	*Pseudomonas fluorescens* *P. putida*	98
	C7	γ-Proteobacteria	*Enterobacter cowanii*	99
	C8	γ-Proteobacteria	*Acinetobacter haemolyticus* *A. schindleri*	94
YDP mode (1)	D1	γ-Proteobacteria	*Pseudomonas fluorescens*	99
	D2	γ-Proteobacteria	*Pseudomonas aeruginosa*	86
	D3	Actinobacteria	*Micrococcus luteus*	100
	D4	γ-Proteobacteria	*Pseudomonas fluorescens* *P. peli*	99
	D5	β-Proteobacteria	*Hydrogenophaga palleronii*	99
	D6	β-Proteobacteria	*Limnobacter thiooxidans*	99
YDP-CR2	E1	Bacilli	*Exiguobacterium antarcticum*	97
	E2	γ-Proteobacteria	*Acinetobacter johnsonii*	97
	E3	Bacilli	*Exiguobacterium undae*	100
	E4	γ-Proteobacteria	*Aeromonas media*	99
	E5	β-Proteobacteria	*Janthinobacterium lividum*	98

Table 10: Summary of Isolate Identification Result

Water Source	Isolate ID	Class	Closest Relative	Sequence Identity (%)
	E6	γ-Proteobacteria	*Pseudomonas constantinii* *P. lurida*	99
	E7	β-Proteobacteria	*Acidovorax avenae*	93
	E8	Actinobacteria	*Arthrobacter oxydans*	98
	E9	β-Proteobacteria	*Burkholderia cepacia*	100
	E10	α-Proteobacteria	*Caulobacter tundrae*	97
	E11	Flavobacteria	*Flavobacterium johnsoniae*	97
	E12	β-Proteobacteria	*Acidovorax facilis*	93
YDP mode	F1	γ-Proteobacteria	*Pseudomonas fluorescens*	100
	F2	γ-Proteobacteria	*Pseudomonas fluorescens* *P. peli*	98
YDP WQIC	-	-	-	-
SDTF SW	H1	β-Proteobacteria	*Limnobacter thiooxidans*	98
	H2	α-Proteobacteria	*Sulfitobacter donghicola*	98
	H3	Actinobacteria	*Rhodococcus fascians*	98
	H4	α-Proteobacteria	*Rhodobacter katedanii*	96
	H5	α-Proteobacteria	*Paracoccus marcusii*	99
	H6	Actinobacteria	*Rhodococcus fascians*	99
SDTF UF 29	I2	γ-Proteobacteria	*Marinobacter koreensis*	99
	I4	α-Proteobacteria	*Oceanibulbus indolifex*	95
BGNDRF Well #1	J1	α-Proteobacteria	*Sphingopyxis alaskensis* *S. macrogoltabida*	99
	J2	Bacilli	*Bacillus mycoides*	79
BGNDRF Well #2	K1	γ-Proteobacteria	*Pseudomonas mendocina* *P. pseudoalcaligenes*	97
BNNDRF Tank #1 with pipe	L1	α-Proteobacteria	*Brevundimonas nasdae*	97

Table 10: Summary of Isolate Identification Result

Water Source	Isolate ID	Class	Closest Relative	Sequence Identity (%)
	L2	α-Proteobacteria	*Sphingomonas koreensis*	94
	L3	α-Proteobacteria	*Afipia lausannensis*	100
BNNDRF Tank #1	M1	α-Proteobacteria	*Sphingopyxis alaskensis*	100
	M2	β-Proteobacteria	*Acidovorax facilis*	99
	M3	Actinobacteria	*Micromonospora marina*	100
	M4	β-Proteobacteria	*Herbaspirillum seropedicae*	78
BNNDRF Tank #2 with pipe	N1	γ-Proteobacteria	*Pseudomonas mendocina* *P. pseudoalcaligenes*	95
	N2	γ-Proteobacteria	*Pseudomonas mendocina* *P. pseudoalcaligenes*	96
	N3	β-Proteobacteria	*Hydrogenophaga intermedia*	98
	N4	Actinobacteria	*Arthrobacter bergerei*	99
	N5	Actinobacteria	*Pimelobacter simplex* *Rhodococcus boritolerans* *R. erythreus* *R. erythropolis*	100
	N6	Actinobacteria	*Arthrobacter polychromogenes* *A. scleromae*	100
	N7	γ-Proteobacteria	*Pseudomonas mendocina* *P. pseudoalcaligenes*	96
BNNDRF Tank #1 with pipe	O1	β-Proteobacteria	*Acidovorax facilis*	97
	O2	α-Proteobacteria	*Paracoccus thiocyanatus*	87
	O3	β-Proteobacteria	*Limnobacter thiooxidans*	100

3.4.2 High-Throughput Multiwell Plate Screening at SNL

The results of the high throughput screening are summarized in Table 11. Rows shaded in Table 11 are the isolates that were chosen for further characterization of biofilm growth using both tube and CDC reactors. Isolates with measured biofilm growth above 6 were chosen, with a few exceptions (Figure 18). Groundwater samples collected from tanks (Samples L – O) were not selected because it was thought that contamination in the tanks from which the samples were collected was possible. In addition, sample C2 was not selected because it was isolated from a chlorinated water sample and 2 other waste water samples that were not from chlorinated samples had good growth. Finally, despite low biofilm growth, it was decided to further analyze all of the seawater isolates, as the seawater source was of the most interest.

Table 11: Results of High-Throughput Multiwell Plate Screening at Sandia.

Isolate	Closest Relative	Biofilm Assays (n)	Biomass on Membrane (OD_{600})		
			Mean	Median	Std Dev
A5	*Microbacterium oxydans*	40	5.3	3.8	4.8
A6	*Aminobacter aminovorans*	30	2.9	2.5	2.3
A7	*Brevundimonas bullata*	31	1.7	0.6	3.0
A8	*Rhodococcus erythropolis*	40	4.4	1.6	7.2
B1	*Pseudomonas meridiana*	31	1.2	0.7	1.3
B2	*Pseudomonas* spp.	30	6.7	6.8	3.2
B3	*Microbacterium* spp.	40	4.1	2.1	4.8
B4	*Nocardia coeliaca* *Rhodococcus* spp.	32	7.4	2.1	13.7
B5	*Pseudomonas putida*	24	1.7	1.3	1.3
B6	*Pseudomonas migulae*	23	0.8	0.8	0.7
C1	*Pseudomonas* spp.	39	1.7	0.7	2.9
C2	*Rhodococcus* spp.	36	7.2	5.3	6.7
C3	*Microbacterium oxydans*	38	4.5	3.1	4.4
C4	*Pseudomonas putida*	39	4.1	4.4	2.4
C5	*Pseudomonas migulae*	30	1.7	1.4	1.5
C6	*Pseudomonas* spp.	24	1.5	1.1	1.4
D1	*Pseudomonas fluorescens*	39	6.3	5.4	4.5
D3	*Micrococcus luteus*	32	1.8	1.6	1.5
D4	*Pseudomonas* spp.	31	16.8	15.4	12.8
D5	*Hydrogenophaga palleronii*	24	9.1	0.9	14.5
E1	*Exiguobacterium antarcticum*	32	2.0	0.6	3.2

Table 11: Results of High-Throughput Multiwell Plate Screening at Sandia.

Isolate	Closest Relative	Biofilm Assays (n)	Biomass on Membrane (OD_{600})		
			Mean	Median	Std Dev
E3	*Exiguobacterium undae*	31	1.3	0.9	1.2
E4	*Aeromonas media*	24	1.9	1.8	0.7
E6	*Pseudomonas* spp.	32	16.4	13.6	12.4
E7	*Acidovorax avenae*	31	2.1	1.0	2.4
E8	*Arthrobacter oxydans*	31	0.6	0.3	0.8
E10	*Caulobacter tundrae*	23	0.3	0.0	0.5
E11	*Flavobacterium johnsoniae*	24	0.7	0.0	3.2
E12	*Acidovorax facilis*	24	2.9	2.3	2.9
F1	*Pseudomonas fluorescens*	23	1.6	1.5	0.6
F2	*Pseudomonas* spp.	30	8.8	6.0	7.7
H2	*Sulfitobacter donghicola*	---	---	---	---
H3	*Rhodococcus fascians*	23	3.1	2.1	3.1
H4	*Rhodobacter katedanii*	37	1.2	0.7	1.7
H5	*Paracoccus marcusii*	---	---	---	---
H6	*Rhodococcus fascians*	31	1.4	0.6	2.0
J1	*Sphingopyxis* spp.	37	14.0	4.6	17.6
L1	*Brevundimonas nasdae*	29	0.5	0.2	0.8
L2	*Sphingomonas koreensis*	31	5.3	4.2	5.3
M2	*Acidovorax facilis*	31	4.6	2.9	5.0
M4	*Herbaspirillum seropedicae*	22	1.0	0.3	1.6
N1	*Pseudomonas* spp.	24	10.6	6.2	9.3
N2	*Pseudomonas* spp.	24	17.4	16.1	16.5
N3	*Hydrogenophaga intermedia*	39	11.4	3.4	15.5
N4	*Arthrobacter bergerei*	40	9.1	5.2	10.3
N5	*Pimelobacter simplex* *Rhodococcus* spp.	30	6.1	4.7	6.1
N6	*Arthrobacter* spp.	24	2.4	1.5	2.5
N7	*Pseudomonas* spp.	22	6.6	5.6	3.4
O1	*Acidovorax facilis*	31	38.8	42.1	27.1

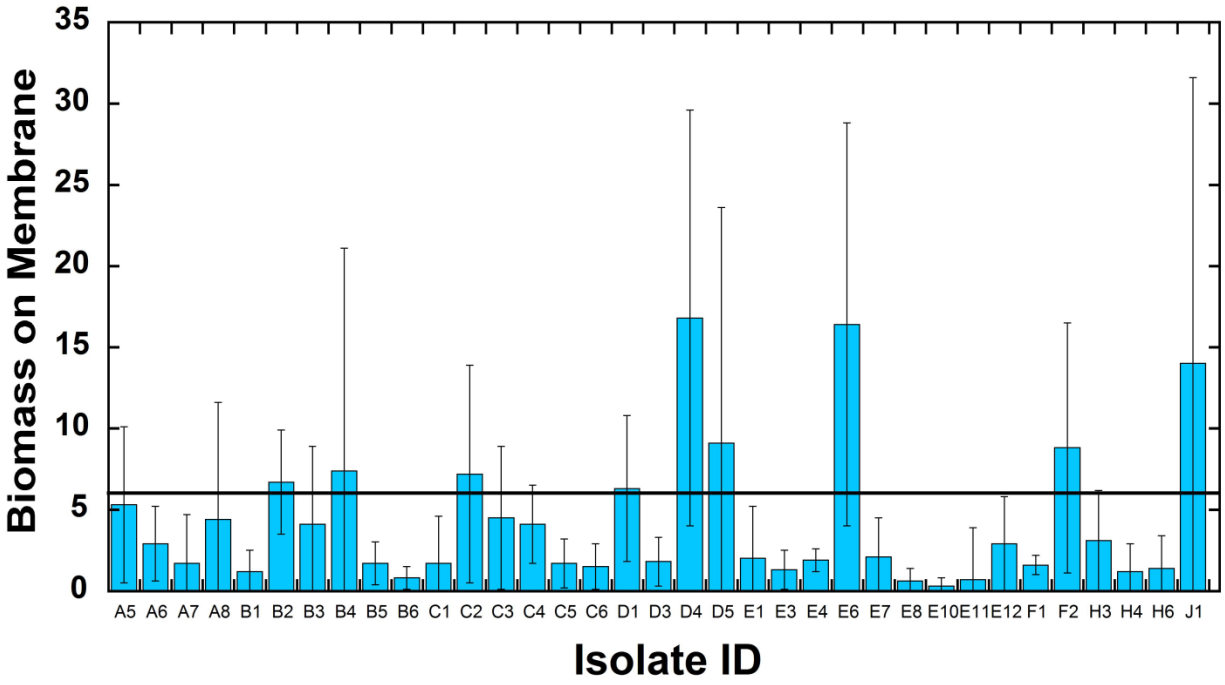

Figure 18: Results of high-throughput biofilm growth screening performed at Sandia National Laboratories. Isolates obtained from samples L - O) are not show as they are thought to be less relevant for membrane treatment. Horizontal line at 6 shows the cut-off used to select isolates for further analysis.

3.4.3 High-Throughput Multiwell Plate Screening at NDSU

The results of the high-throughput screening conducted at are summarized in Table 12 and Figure 19. Biofilm growth was clearly greatest with isolates H2 and H5. Unfortunately, these were the two isolates that were not tested by the high-throughput multiwell plate screening at Sandia. For the three isolates that were tested at Sandia, H3 had the most growth, followed by H6 and then H4. This same trend was observed for the NDSU testing (see Figure 19). What is most important to observe is that the growth for isolates H3, H4, and H6 was low compared to H2 and H5.

Table 12: Results of High-Throughput Multiwell Plate Screening at NDSU (Crystal Violet Absorbance at 600 nm (AU)).

Isolate ID	Closest Relative	n	24 Hours of Growth		72 Hours of Growth	
			Mean	Std Dev	Mean	Std Dev
H2	*Sulfitobacter donghicola*	24	0.61	0.19	0.79	0.15
H3	*Rhodococcus fascians*	24	0.18	0.03	0.27	0.04
H4	*Rhodobacter katedanii*	24	0.09	0.08	0.12	0.08
H5	*Paracoccus marcusii*	24	0.76	0.18	0.79	0.72
H6	*Rhodococcus fascians*	48	0.16	0.13	0.14	0.09

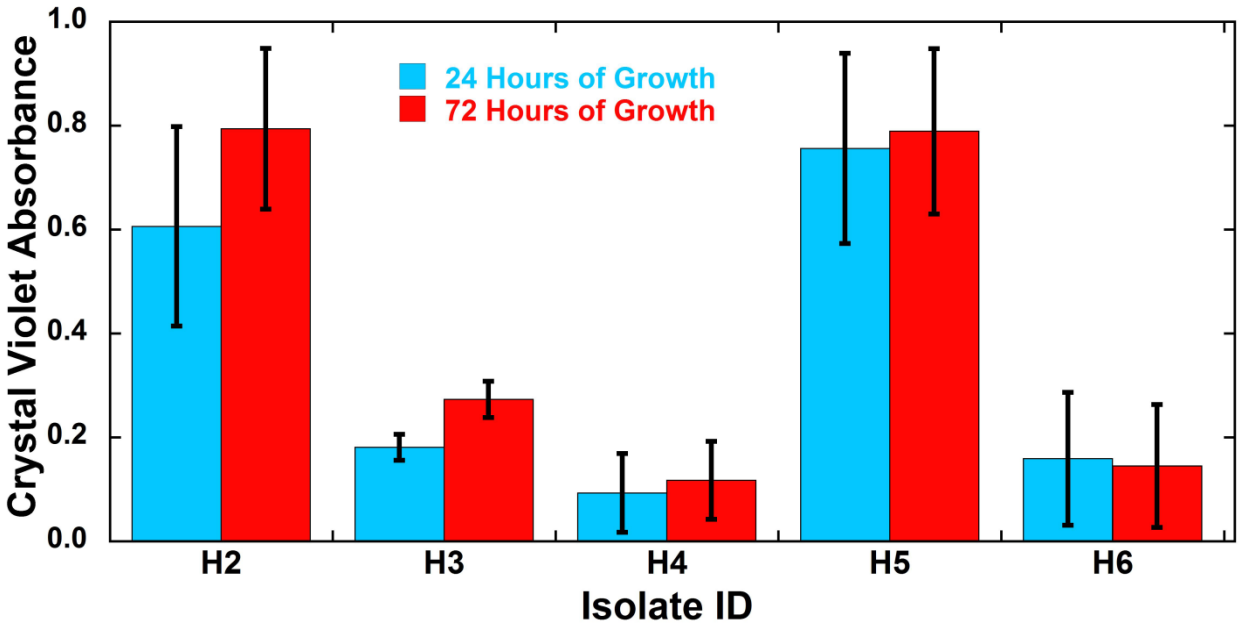

Figure 19: Results of high-throughput biofilm growth screening performed at North Dakota State University.

3.4.4 Tube Reactor Experiments

The viable cells results are shown in two different ways in Figures 20 and 21. Figure 20 is an individual value plot of the mean log densities (also known as a "TestLD" in the literature) for each sample day within each experiment for each isolate evaluated. One symbol is the mean of the three samples collected. Figure 21 is a summary plot where one bar is the mean of nine data points (three samples x three replicate experiments). These data are also presented in Table 12. The error bars represent the repeatability standard deviation (SD) of the mean Test LD. This plot is consistent with the presentation of the other tests presented in Sections 3.4.2, 3.4.3, and 3.4.5. Table 13 listed the pooled repeatability standard deviation and percent of the variability that is attributed to between and within experimental error.

Isolate H6 had the largest biofilm density at day 7 (6.50 $Log_{10}(cfu/cm^2)$), followed by the J1 isolate with a mean density equaled 6.10 $Log_{10}(cfu/cm^2)$. Isolate D4 had the lowest mean log density on day 7 at 4.29 $Log_{10}(cfu/cm^2)$. The rest of the isolates had mean densities between 4.7 and 5.7 logs. The largest variability in the data was found for isolate H3. For this isolate, most of the variability is attributed to experiment-to-experiment error. Isolates E6 and J1 had the smallest variability in the data. For J1, 100% of the variability was attributed to within experiment error, which means the results were highly repeatable from experimental-to-experiment, but that within an experiment the biofilm was really heterogeneous. This same interpretation may be made for isolate B4.

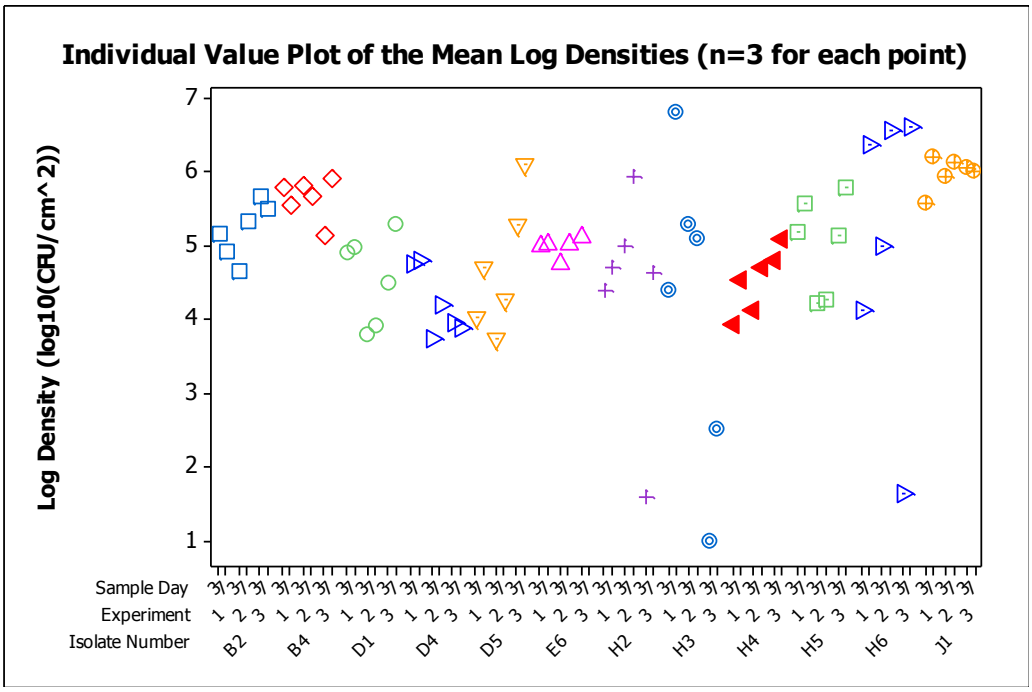

Figure 20: Individual value plot of the TestLD for each isolate. Each symbol is the mean of the three samples collected for each test day within an experiment for each isolate. For clarity, each isolate was given a unique color/symbol combination.

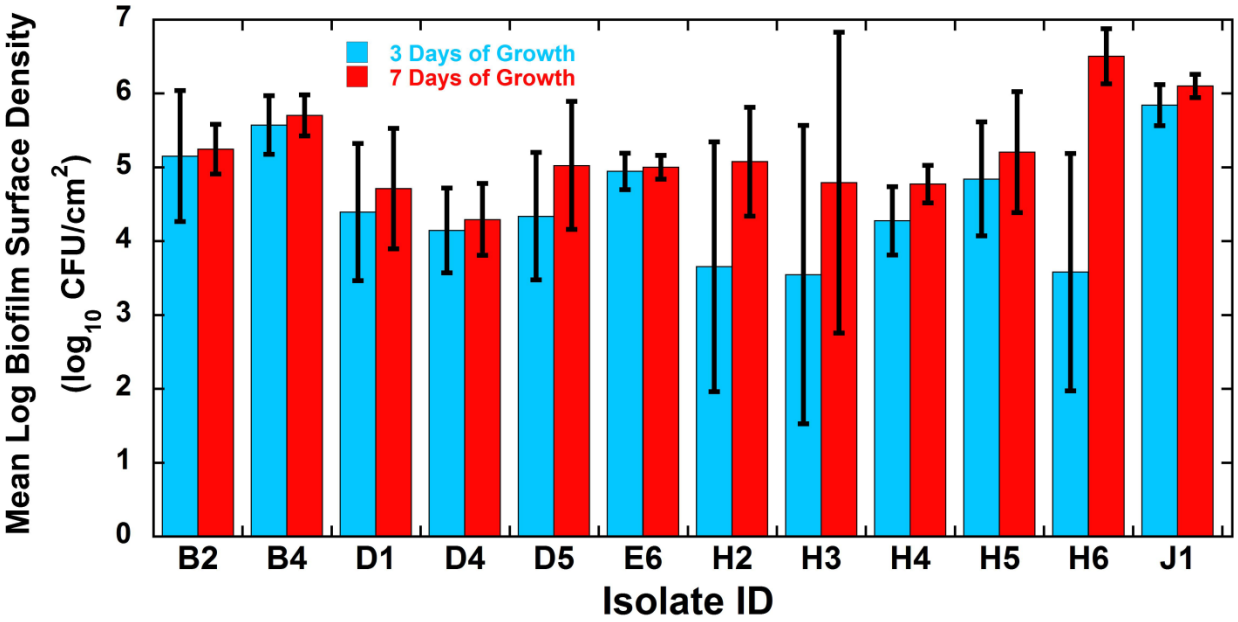

Figure 21: Summary plot of the overall mean density for each isolate evaluated in tube reactors. The error bars represent the repeatability standard deviation of the TestLD.

Table 13: The pooled repeatability SD and percent of the variability that is attributed to between and within experimental error for each isolate.

Isolate ID	Isolate Name	Pooled Repeatability SD	Percent Variability	
			Between Exp	Within Exp
B2	*Pseudomonas* spp.	0.68	9.3%	90.7%
B4	*Nocardia coeliaca* *Rhodococcus* spp.	0.35	0.0%	100.0%
D1	*Pseudomonas fluorescens*	0.91	34.3%	65.7%
D4	*Pseudomonas* spp.	0.58	60.2%	39.8%
D5	*Hydrogenophaga palleronii*	0.97	80.8%	19.2%
E6	*Pseudomonas* spp.	0.22	18.3%	81.7%
H2	*Sulfitobacter donghicola*	1.42	63.1%	36.9%
H3	*Rhodococcus fascians*	2.28	82.2%	17.8%
H4	*Rhodobacter katedanii*	0.41	74.5%	25.5%
H5	*Paracoccus marcusii*	0.86	55.0%	45.0%
H6	*Rhodococcus fascians*	1.23	37.1%	62.9%
J1	*Sphingopyxis* spp.	0.23	0.0%	100.0%

Table 14: Results of Tube Reactor Experiments – Biofilm Surface Density (CFU/cm^2)

Isolate ID	Closest Relative	n	3 Days of Growth		7 Days of Growth	
			Mean	Std Dev	Mean	Std Dev
B2	*Pseudomonas fluorescens*	9	5.2	0.9	5.2	0.3
B4	*Rhodococcus erythropolis*	9	5.6	0.4	5.7	0.3
D1	*Pseudomonas fluorescens*	9	4.4	0.9	4.7	0.8
D4	*Pseudomonas anguilliseptica*	9	4.1	0.6	4.3	0.5
D5	*Hydrogenophaga palleronii*	9	4.3	0.9	5.0	0.6
E6	*Pseudomonas constantinii*	9	4.9	0.2	5.0	0.2
H2	*Sulfitobacter donghicola*	9	3.7	1.7	5.1	0.7
H3	*Rhodococcus fascians*	9	3.5	2.0	4.8	2.0
H4	*Rhodobacter katedanii*	9	4.3	0.5	4.8	0.3
H5	*Paracoccus marcusii*	9	4.8	0.8	5.2	0.8
H6	*Rhodococcus fascians*	9	3.6	1.6	6.5	0.4
J1	*Sphingopyxis macrogoltabida*	9	5.8	0.3	6.1	0.2

Figure 22 shows the increase in the mean log density from day 3 to day 7. The mean increase across all 12 isolates was equal to 0.68 logs, with the greatest increase occurring for three of the sea water isolates H2 and H3 and H6.

Figure 23 is a summary plot of the mean protein concentration found for each isolate per sample day. The error bars are the standard deviation of the mean protein concentration for each experiment per sample day (analogous to the Test LD). On day 7, isolates D5 and H6 had the greatest protein concentration at 17.9 and 17.8 $\mu g/cm^2$, respectively. Figure 24 shows the change in protein concentration per isolate from day 3 to day 7. The concentration increased for half of the isolates and decreased for the other half. Due to the large variability associated with this data, no additional analysis was done.

Figure 25 is a comparison of the mean log density and protein concentration on day 3. Figure 24 visually demonstrates that the isolates with the greatest biofilm density did not necessarily correlate with the isolates that had the highest protein concentration, as shown by the results for B4 and D1.

3.4.4.1 Discussion

The goal of this research was to evaluate 12 environmental isolates for their ability to form biofilm as determined by viable plate counts, protein analysis and imaging. Not surprisingly, all of the isolates did form biofilms. The average density for all 12 isolates was equal to 5.2 logs, and in general, the biofilm coverage was sparse. The average biofilm density would most likely increase if the amount of TSB added to the site water was greater than 10 mg/L. For most of the isolates, the average the biofilm density did not increase too much from day 3 to day 7, suggesting that a three day experiment would have been sufficient. For the isolates that did show an increase in growth between days 3 and day 7, most likely they would have a smaller increase in biofilm density over time if the incubation temperature had been greater than 23°C.

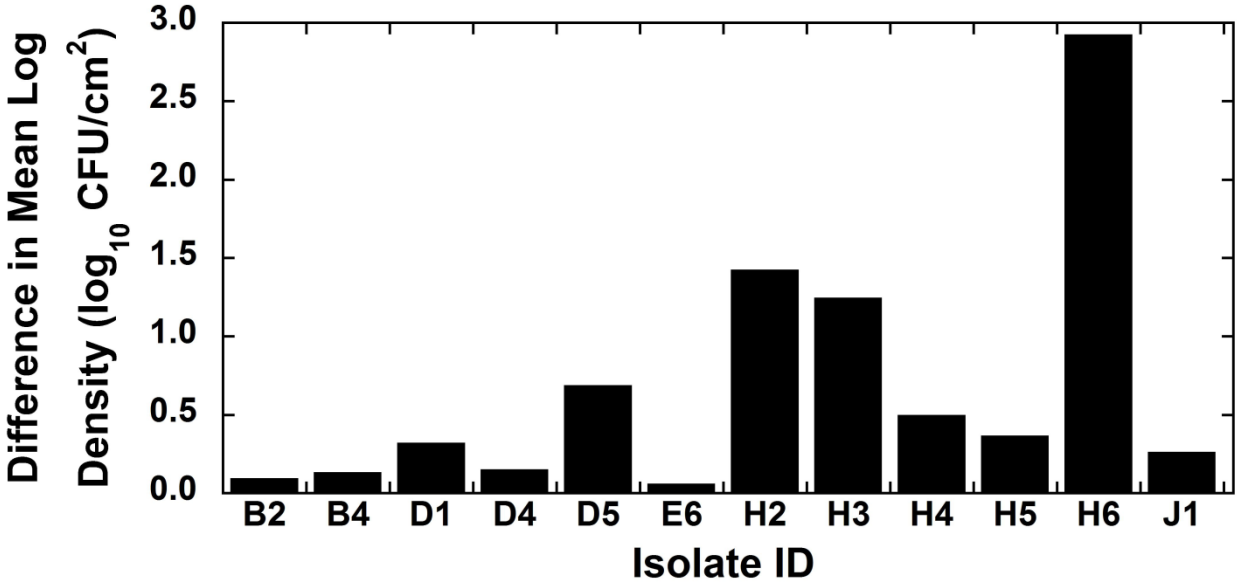

Figure 22: Increase in mean log density from day 3 to day 7 for each isolate for tube reactor experiments.

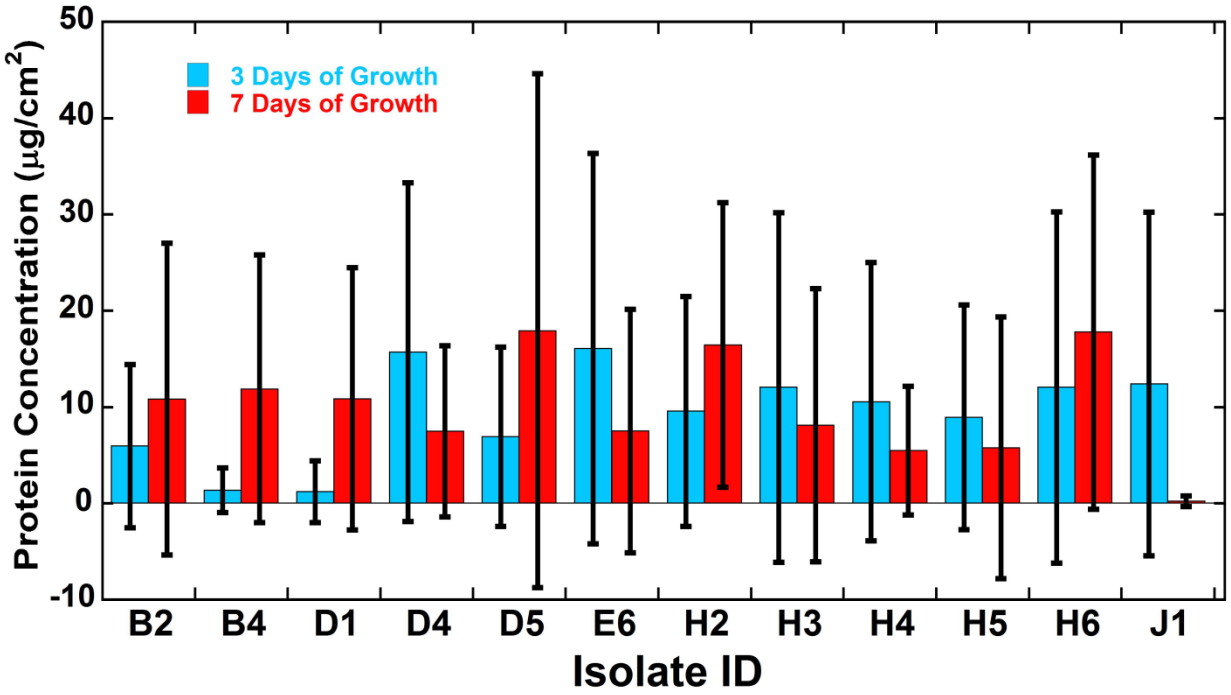

Figure 23: Summary plot of the mean protein concentration found for each isolate per sample day for tube reactor experiments. The error bars are the standard deviation of the mean protein concentration for each experiment per sample day.

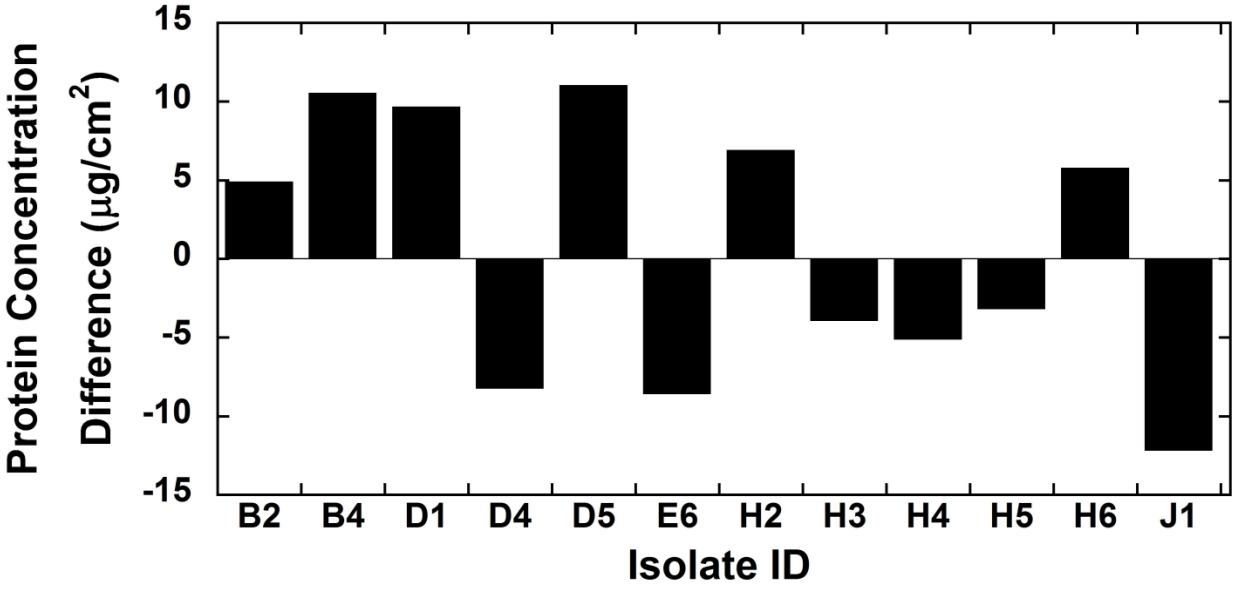

Figure 24: Change in protein concentration from day 3 to day 7 for each isolate grown in tube reactors.

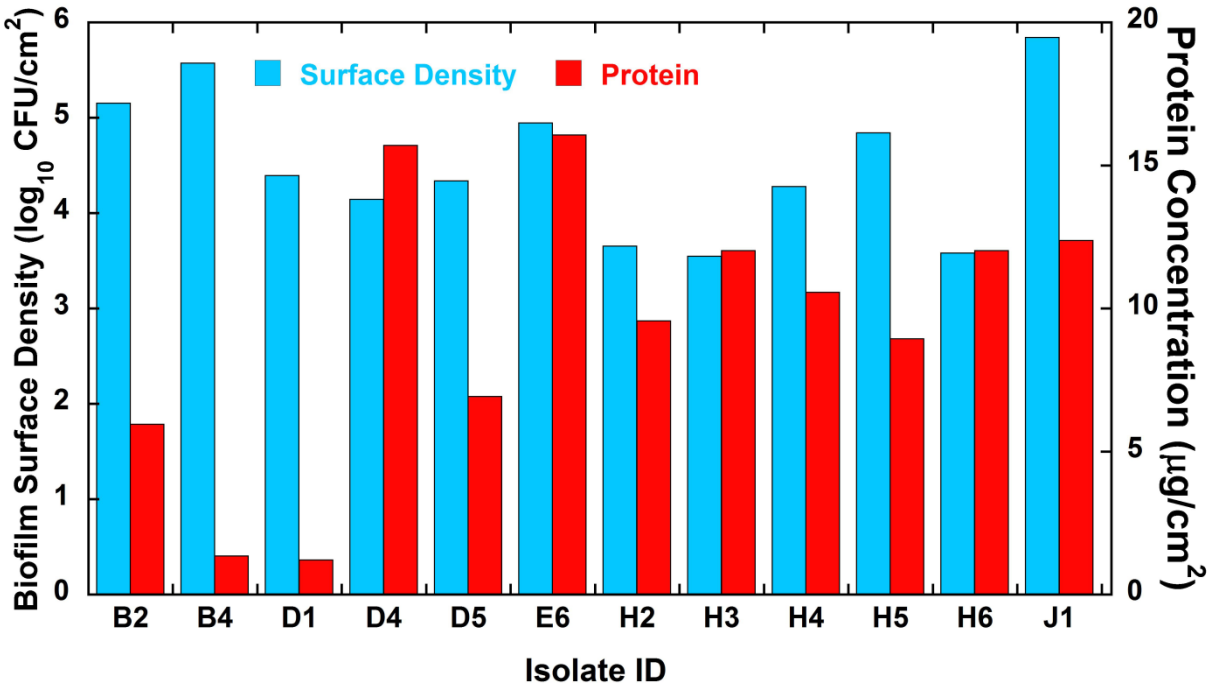

Figure 25: A comparison of the mean log density and protein concentration for each isolate after 3 days of growth for tube reactor experiments.

The repeatability standard deviation is an important parameter to consider when determining which isolate to choose for incorporation into more routine testing. From this perspective, at least four isolates showed promise (B4, E6, H4 and J1) with a SD_r less than 0.5. Of these four isolates, two (B4 and J1) had all of their variability attributed to within experiment variability, meaning that from experiment-to-experiment the results were highly repeatable.

The protein results were highly variable, and the isolates with the greatest biofilm density did not necessarily correlate with the isolates that had the highest protein concentration. Potentially, these isolates were putting all of their energy into making new cells.

As would be expected, no general statements may be made about the day 7 images captured for each of the isolates (Appendix C). Visually, B4 produced a more robust biofilm than J1. The images collected from isolate H6 show fairly homogeneous coverage within an experiment, but change in biofilm architecture from experiment-to-experiment (although 63% of the variability was attributed to within-experiment variability based upon the viable plate counts). This demonstrates the challenge in directly trying to correlate qualitative images to quantitative data.

Finally, none of the isolates posed any particular challenges in the laboratory. They all would be reasonable to use in future experiments.

3.4.5 CDC Reactor Experiments

Figure 26 and Table 15 present a summary of the results of the experiments conducted in CDC reactors at Sandia National Laboratories. Biofilm cell density was greater in the isolates collected from the non-seawater samples (B4, D1 and E6) than the seawater sample isolates.

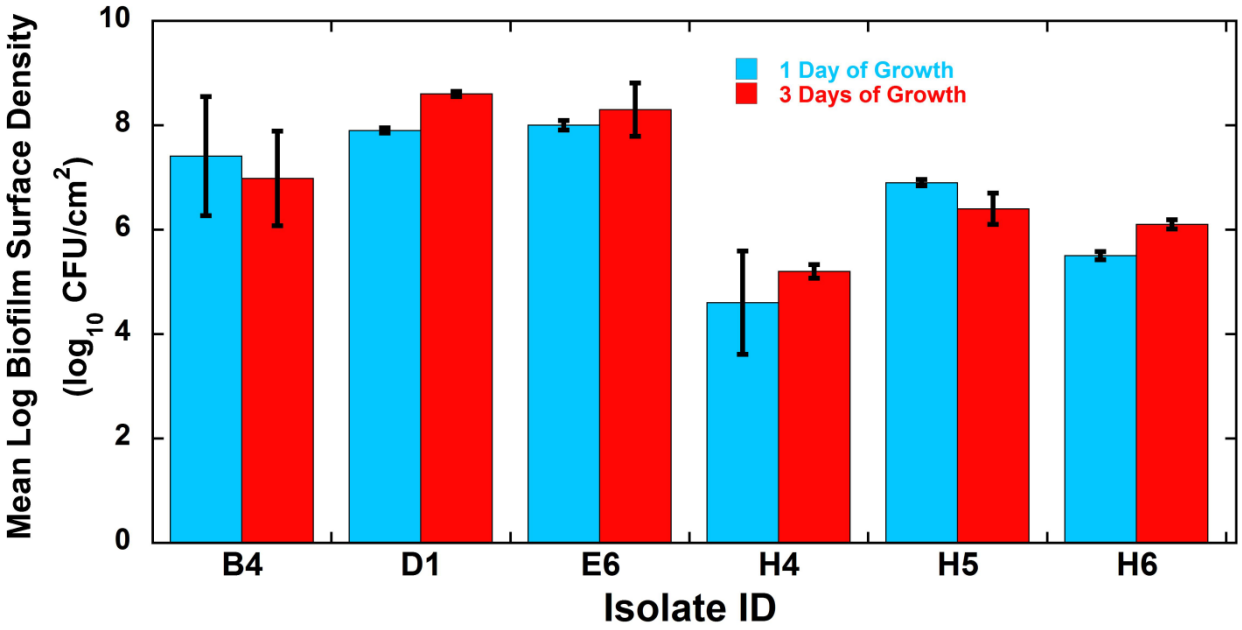

Figure 26: Summary plot of the overall mean density for each isolate evaluated in CDC reactors. The error bars represent the standard deviation of 12 counts (4 coupons, 3 plates per coupon) for B4, D1, and E6 and 6 counts (2 coupons, 3 plates per coupon) for the H isolates.

Table 15: Results of CDC Reactor Experiments – Biofilm Surface Density (CFU/cm^2)

Isolate ID	Closest Relative	n	1 Day of Growth		3 Days of Growth	
			Mean	Std Dev	Mean	Std Dev
B4	*Rhodococcus erythropolis*	12	7.4	1.1	7.0	0.91
D1	*Pseudomonas fluorescens*	12	7.9	0.05	8.6	0.05
E6	*Pseudomonas constantinii*	12	8.0	0.09	8.3	0.51
H4	*Rhodobacter katedanii*	6	4.6	0.99	5.2	0.13
H5	*Paracoccus marcusii*	6	6.9	0.06	6.4	0.30
H6	*Rhodococcus fascians*	6	5.5	0.08	6.1	0.09

Differences are significant using a student's t-test except for the comparison of H3 and B4. Within the seawater sample isolates, H5 appeared to have the greatest growth, though it was not much higher than H6. In comparing the differences between the seawater sample isolates, the only difference that is not statistically significant is between H4 and H6 with 1 day of growth, most likely due to the high variability in the counts for the H4 sample.

Figure 27 shows the increase in the mean log biofilm cell density from day 1 to day 3. The greatest growth occurred in isolate D1. A decrease in biofilm surface density was observed in isolates B4 and H5.

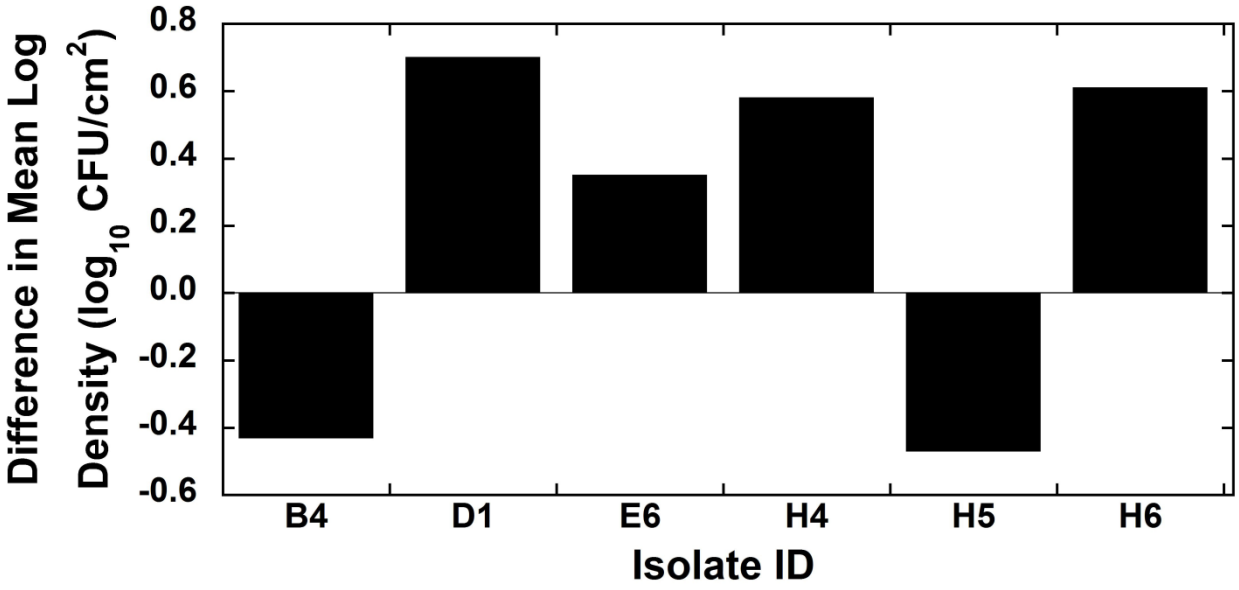

Figure 27. Increase in mean log density from day 1 to day 3 for each isolate for CDC reactor experiments.

In comparison to the tube reactor experiments, there was more variability in biofilm surface density after days of growth in the CDC reactors (Figure 28). The CDC reactors showed a 3.4 order of magnitude range in biofilm surface density between experiments in comparison to the 2 order of magnitude range for the same samples in the tube reactor experiments. This may be due to the CDC reactors being run with an order of magnitude more carbon than the tube reactors. Researchers at the Center for Biofilm Engineering have found better repeatability if carbon is slightly limited. In addition, the CDC reactor experiments clearly demonstrate less growth in the seawater samples isolates. This trend is not observed in the tube reactor experiments.

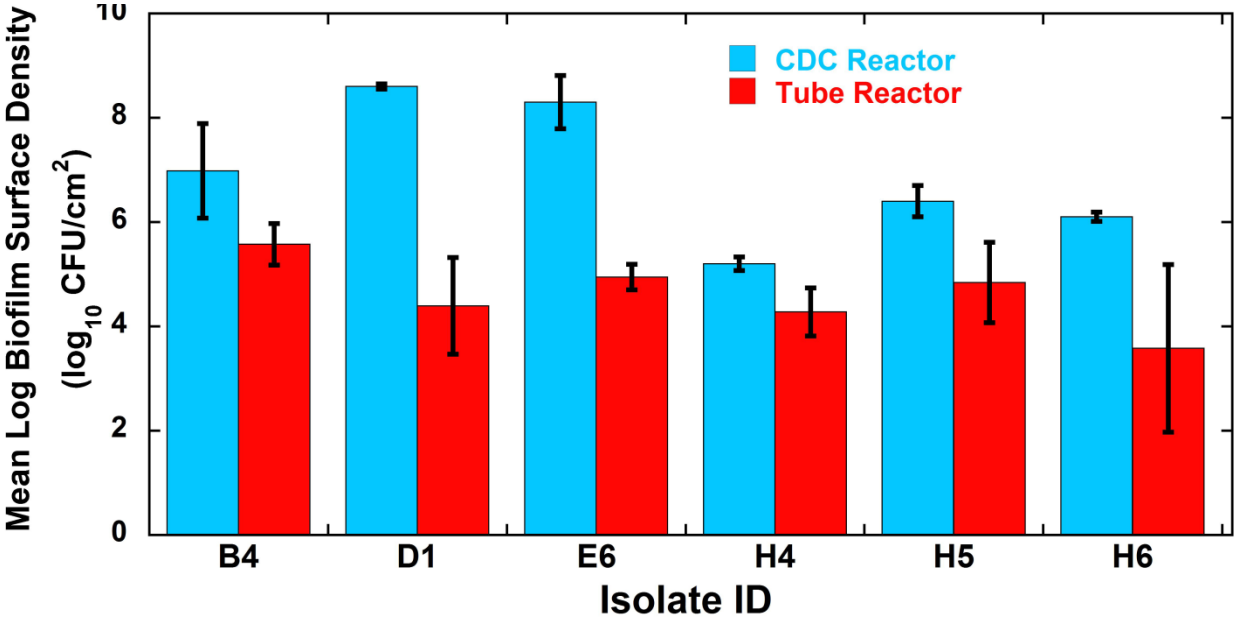

Figure 28. Comparison of biofilm surface density as measured in the CDC reactors and the tube reactors after 3 days of growth.

Differences between the tube reactor and CDC reactor experiments include that the tube reactors used the actual waters from which the isolates were obtained, the CDC reactors were run with less carbon, and the tube reactor experiments were batch systems with recycle whereas the CDC reactors had a continuous flow of nutrients. Any of these factors could explain the differences.

Greater protein concentrations were also found for the non-seawater isolates (B4, D1 and E6) in comparison to the seawater isolates (Figure 29). Isolate E6 had the greatest protein

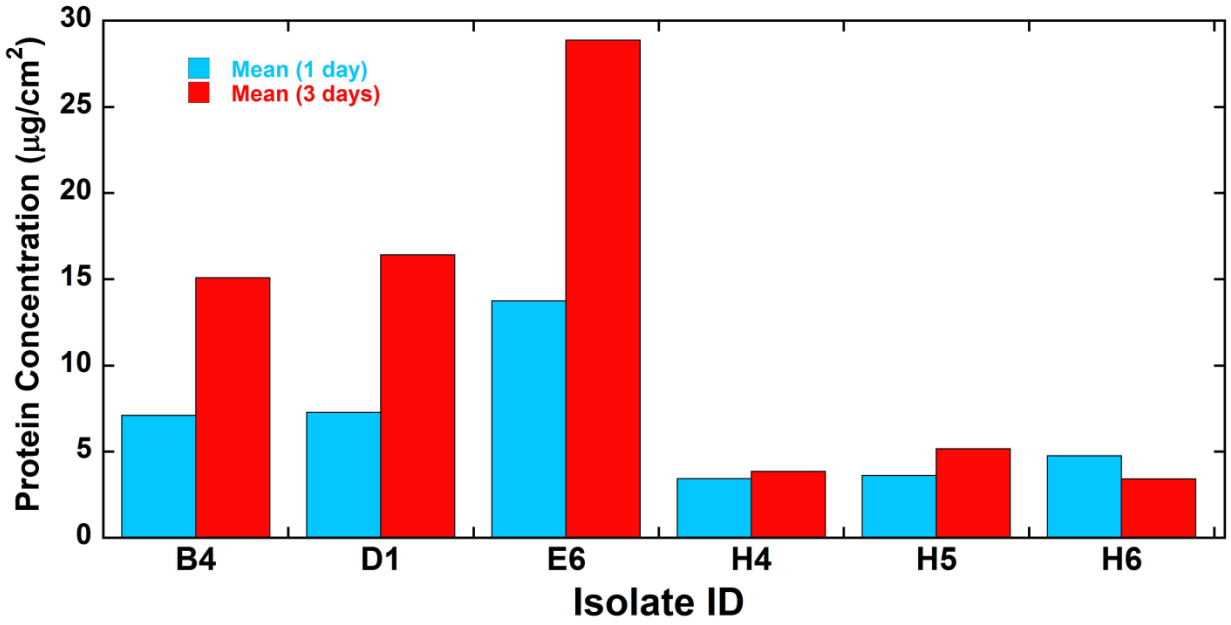

Figure 29. Summary plot of the protein concentration found for each isolate per sample day for CDC reactor experiments.

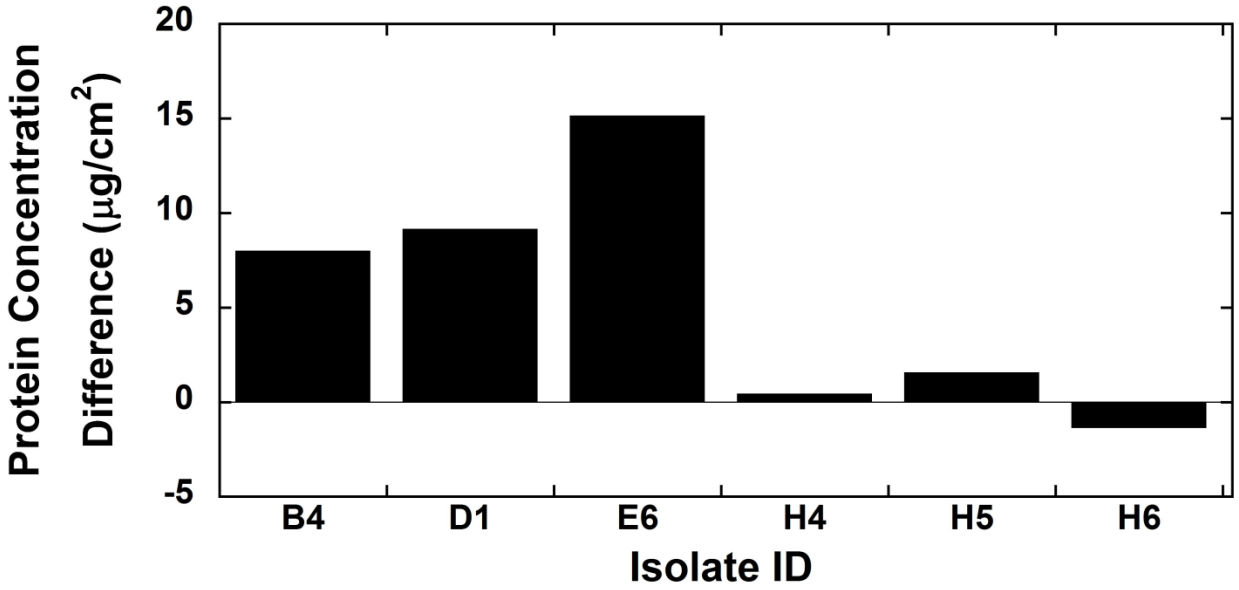

Figure 30. Change in protein concentration from day 1 to day 3 for each isolate for CDC reactor experiments.

concentration at 13.7 µg/cm^2 after 1 day of growth and 28.9 µg/cm^2 after 3 days of growth. Protein concentrations ranged from 3.4 to 5.2 µg/cm^2 for the seawater sample isolate. Protein concentrations increase by 8.0 to 15.1 µg/cm^2 between 1 and 3 days for growth for the non-seawater isolates with the largest concentration increase for isolate E6 (Figure 30). Changes in protein concentrations for the seawater isolates was minimal.

While both the tube reactor and CDC reactor experiments show the highest protein concentration in biofilms grown from isolate E6, the similarities end there (Figure 31). The tube reactor experiments showed the next highest concentrations in the seawater samples, where the CDC reactor experiments showed the lowest protein concentrations in the seawater samples. Due to the high variability in the tube reactor experiment data (Figure 23) we do not attempt to interpret these comparisons.

Figure 32 is a comparison of the mean log density and protein concentration after 3 days of growth. Figure 24 visually demonstrates that the isolates with the greatest biofilm density do correlate with the isolates that had the highest protein concentration. This is most clearly seen in comparing the seawater isolates to those obtained from the other water samples.

3.5 Summary and Conclusions

This study has demonstrated that

- Methods to isolate and culture microorganisms from natural waters were demontrated
- Many of these isolates can be used to grow biofilms

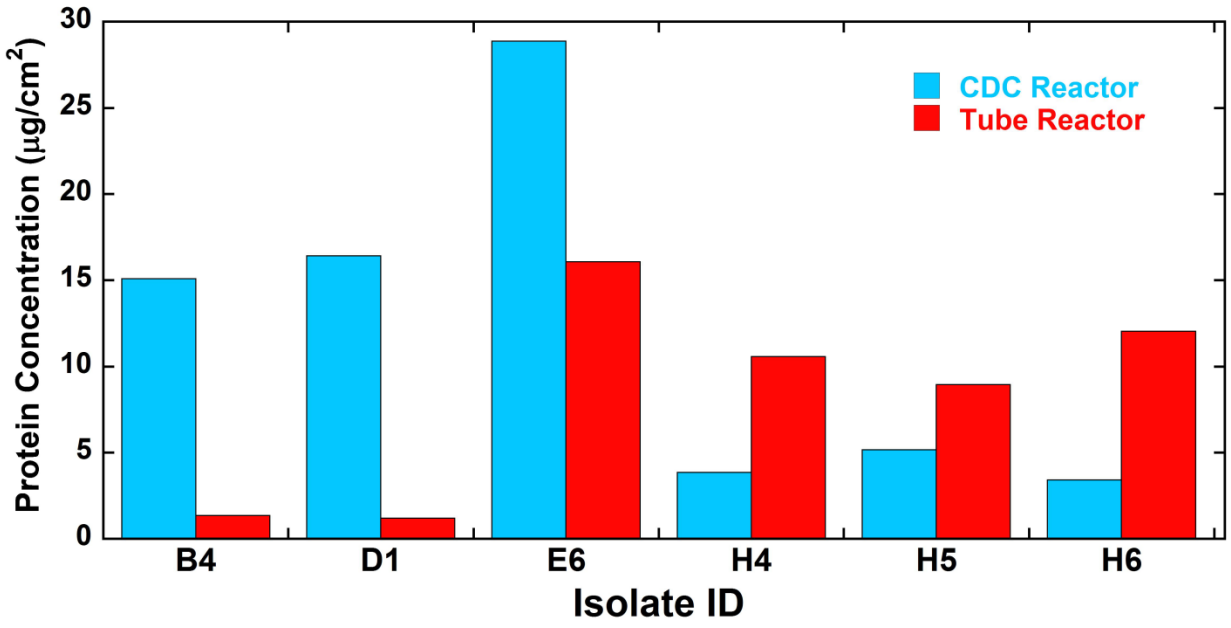

Figure 31. Comparison of protein concentrations for biofilms grown in CDC reactors and the tube reactors after 3 days of growth.

- The biofilms can be grown in different reactors and under different conditions
- Use of the actual source water versus waters produced in the laboratory that mimic the major ion chemistry did not appear to make much of a difference in biofilm growth, with the possible exception of the seawater samples
- We now have many isolates relevant that can be used to conduct controlled biofilm growth experiments (at least 1 from each source water).
- Some isolates are easier to work with than others, but most seem feasible for use for future experiments.

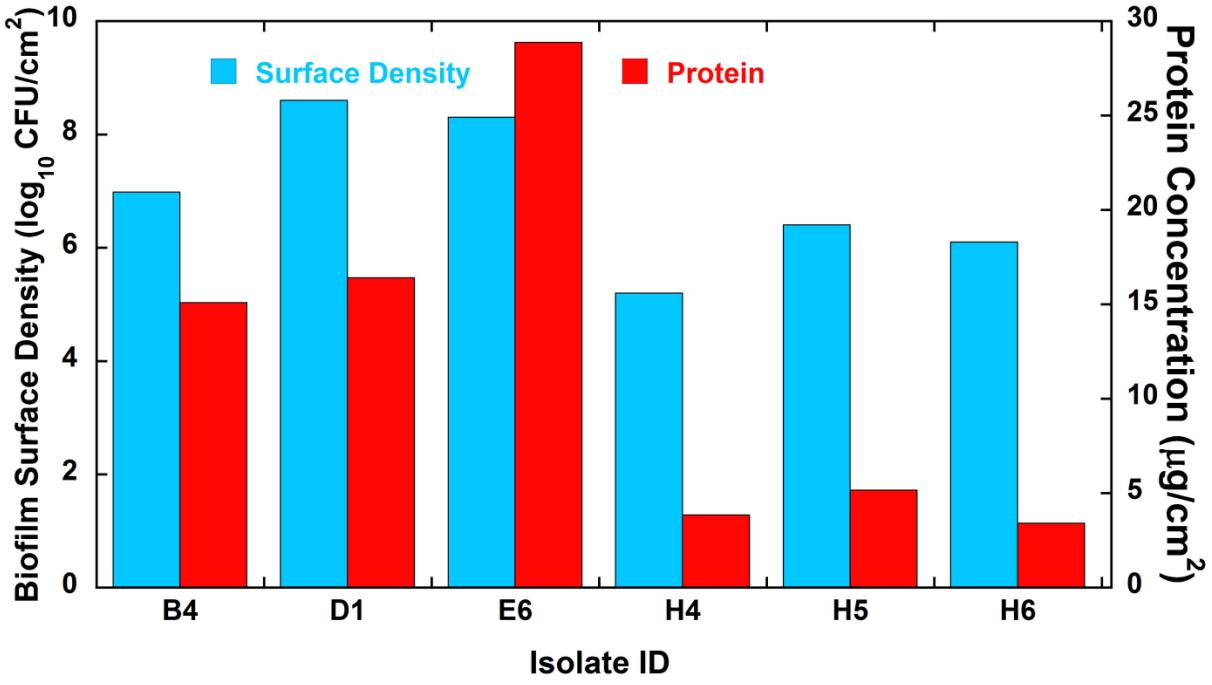

Figure 32. A comparison of the mean log density and protein concentration for each isolate after 3 days of growth in CDC reactor experiments.

REFERENCES

Altman, S. J., L. K. McGrath, H. D. T. Jones, A. Sanchez, R. Noek, P. Clem, A. Cook, and C. K. Ho (2010), Systematic analysis of micromixers to minimize biofouling on reverse osmosis membranes, Water Res, 44(12), 3545-3554.

ASTM (E 2562-07), Standard test method for quantification of Pseduomonas aeruginosa biofilm grown with high shear and continuous flow using CDC biofilm reactorRep.

Belfer, S., Y. Purinson, R. Fainshtein, Y. Radchenko, and O. Kedem (1998), Surface modification of commercial composite polyamide reverse osmosis membranes, J. Membr. Sci., 139(2), 175-181.

Chin, J. N., M. J. Rybak, C. M. Cheung, and P. B. Savage (2007), Antimicrobial activities of ceragenins against clinical isolates of resistant Staphylococcus aureus, Antimicrobial Agents and Chemotherapy, 51(4), 1268-1273.

Chin, J. N., R. N. Jones, H. S. Sader, P. B. Savage, and M. J. Rybak (2008), Potential synergy activity of the novel ceragenin, CSA-13, against clinical isolates of Pseudomonas aeruginosa, including multidrug-resistant P. aeruginosa, Journal of Antimicrobial Chemotherapy, 61(2), 365-370.

Corpet, F. (1988), Multiple sequence alignment with hierarchical clustering, Nucl. Acids Res., 16(22), 10881-10890.

Haaland, D. M., et al. (2009), Hyperspectral Confocal Fluorescence Imaging: Exploring Alternative Multivariate Curve Resolution Approaches, Applied Spectroscopy, 63(3), 271-279.

Heersink, J. (2003), Basic Biofilm Analytical Methods, in The Biofilm Laboratory: Step-by-Step Protocols for Experimental Design, Analysis, and Data Interpretation, edited by M. Hamilton, J. Heersink, K. Buckingham-Meyer and D. Goeres, Cytergy Publishing, Bozeman.

Hightower, M., and S. A. Pierce (2008), The energy challenge, Nature, 452(7185), 285-286.

Ho, C. K., S. J. Altman, H. D. T. Jones, S. S. Khalsa, L. K. McGrath, and P. G. Clem (2008), Analysis of micromixers to reduce biofouling on reverse-osmosis membranes, Environ. Prog., 27(2), 195-203.

Jones, H. D. T., D. M. Haaland, M. B. Sinclair, D. K. Melgaard, M. H. Van Benthem, and M. C. Pedroso (2008), Weighting hyperspectral image data for improved multivariate curve resolution results, Journal Of Chemometrics, 22(9-10), 482-490.

Kotula, P. G., M. R. Keenan, and J. R. Michael (2003), Automated analysis of SEM X-ray spectral images: A powerful new microanalysis tool, Microscopy and Microanalysis, 9(1), 1-17.

Lohman, E. (2003), Yuma Desalting Plant: 2003, edited.

McDonald, D., M. N. Price, J. Goodrich, E. P. Nawrocki, T. Z. DeSantis, A. Probst, G. L. Andersen, R. Knight, and P. Hugenholtz (In press), An improved Greengenes taxonomy with explicit ranks for ecological and evolutionary analyses of bacteria and archaea, International Society for Microbial Ecology Journal.

Meyer, H. (1957), Ninhydrin reaction and its analytical applications, Biochemical Journal, 67, 333-340.

Mickols, W. E. (2001), Composite membrane with polyalkylene oxide modified polyamide surface, edited, p. 6, Dow Chemical Company, U.S. Pat. 6 280 853.

Moore, E. R. B., B. J. Tindall, V. A. P. Martins Dos Santos, D. H. Pieper, J.-L. Ramos, and N. J. Palleroni (2006), Nonmedical: Pseudomonas, in The Prokaryotes, edited by M. Dworkin, S. Falkow, E. Rosenberg, K.-H. Schleifer and E. Stackebrandt, pp. 646-703, Springer, New York.

NRC, and N. R. C. o. t. N. Academies (2008), Desalination A National Perspective, The National Academies Press, Washington D. C.

Ohlhausen, J. A. T., M. R. Keenan, P. G. Kotula, and D. E. Peebles (2004), Multivariate statistical analysis of time-of-flight secondary ion mass spectrometry images using AXSIA, Appl. Surf. Sci. (Netherlands), 231, 230-234.

PerkinElmer (2010), FinchTV, edited, p. free DNA sequencing chromatogram trace viewer, PerkinElmer, http://www.geospiza.com/Products/finchtv.shtml.

Ridgway, H. F., A. Kelly, C. Justice, and B. H. Olson (1983), Microbial fouling of reverse-osmosis membranes used in advanced wastewater-treatment technology - chemical, bacteriological, and ultrastructural analyses, Appl Environ Microbiol, 45(3), 1066-1084.

Savage, P. B. (2002), Cationic steroid antibiotics, Current Medicinal Chemistry - Anti-Infective Agents, 1(3), 293-304.

Sinclair, M. B., J. A. Timlin, D. M. Haaland, and M. Werner-Washburne (2004), Design, construction, characterization, and application of a hyperspectral microarray scanner, Applied Optics, 43(10), 2079-2088.

Stafslien, S., J. Daniels, B. Chisholm, and D. Christianson (2007), Combinatorial materials research applied to the development of new surface coatings III. Utilisation of a high-throughput multiwell plate screening method to rapidly assess bacterial biofilm retention on antifouling surfaces, BIOFOULING, 23(1), 37-44.

Stafslien, S. J., J. A. Bahr, J. M. Feser, J. C. Weisz, B. J. Chisholm, T. E. Ready, and P. Boudjouk (2006), Combinatorial materials research applied to the development of new surface coatings I: A multiwell plate screening method for the high-throughput assessment of bacterial biofilm retention on surfaces, Journal of Combinatorial Chemistry, 8(2), 156-162.

Van Benthem, M. H., and M. R. Keenan (2004), Fast algorithm for the solution of large-scale non-negativity-constrained least squares problems, Journal of Chemometrics, 18(10), 441-450.

Van Benthem, M. H., M. R. Keenan, and D. M. Haaland (2002), Application of equality constraints on variables during alternating least squares procedures, Journal Of Chemometrics, 16(12), 613-622.

Watson, I. C., J. Morin, O. J., and L. Henthorne (2003), Desalting Handbook for PlannersRep. 72, 233 pp, United States Department of the Interior, Bureau of Reclamation, Denver, CO.

APPENDIX A: SUMMARY OF BACTERIA ISOLATION AND IDENTIFICATION

Isolate #	Date Plated	Photograph	BYU Identification	BYU % Reliability	SNL Identification	SNL % Reliability
A1	02/26/2010		*Nocardia globerula* *Rhodococcus globerulus* *Corynebacterineae*	100 100 100	*Nocardia globerula* *Rhodococcus globerulus*	100
A2	02/26/2010	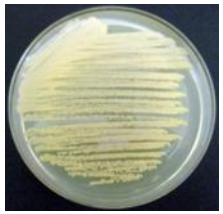	*Nocardia globerula* *Rhodococcus globerulus* *Corynebacterineae*	85.0 85.0 85.0	*Nocardia globerula* *Rhodococcus globerulus*	85
A3	02/26/2010		No DNA	---	---	---
A4	02/27/2010	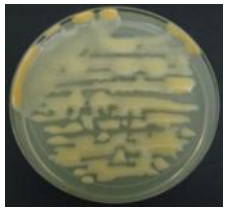	No DNA	---	---	---
A5	02/26/2010		*Microbacterium oxydans* *Erwinia*	98 – 99 99.0	*Microbacterium oxydans*	99

Isolate #	Date Plated	Photograph	BYU Identification	BYU % Reliability	SNL Identification	SNL % Reliability
A6	02/25/2010	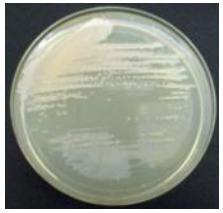	*Pseudomonas aminovorans* *Mesorhizobium*	94.0 93.0	*Aminobacter aminovorans*	94
A7	02/26/2010		*Brevundimonas bullata* *Brevundimonas terrea* *Brevundimonas diminuta* *Caulobacter*	100 92.7 91.3 95.4	*Brevundimonas bullata*	100
A8	02/27/2010		*Rhodococcus erythropolis*	99.0	*Rhodococcus erythropolis*	99
A9	02/26/2010	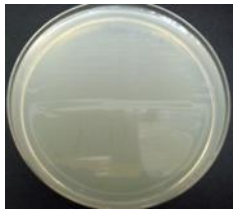	*Alcaligenes defragrans* *Bordetella avium* *Bordetella trematum* *Bordetella hinzii* *Castellaniella defragrans* *Pusillimonas noertemanni* *Burkholderia* *Denitrobacter permanens*	86.6 83.8 85.2 84.0 86.6 92.2 89.0 84.5	*Pusillimonas noertemanni*	92

Isolate #	Date Plated	Photograph	BYU Identification	BYU % Reliability	SNL Identification	SNL % Reliability
B1	02/26/2010		*Pseudomonas meridian* *Pseudomonas veronii* *Pseudomonas fluorescens* *Pseudomonas marginalis* *Pseudomonas extremoaustralis* *Pseudomonas rhodesiae*	99.2 98.7 98.5 98.5 98.5 98.4	*Pseudomonas meridiana*	99
B2	02/26/2010	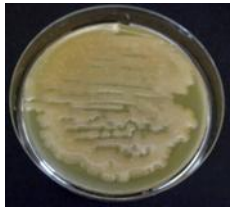	*Pseudomonas fluorescens* *Pseudomonas brenneri* *Pseudomonas collierea*	100 100 100	*Pseudomonas brenneri* *Pseudomonas collierea* *Pseudomonas fluorescens*	100
B3	02/26/2010		*Microbacterium hydrocarbonoxydans* *Microbacterium oxydans* *Microbacterium saperdae* *Microbacterium phyllosphaerae* *Microbacterium shrimpcida* *Microbacterium maritypicum* *Microbacterium foliorum*	98.8 99.6 98.8 98.8 98.8 99.6 98.8	*Microbacterium oxydans* *Microbacterium maritypicum*	100
B4	02/26/2010		*Rhodococcus erythropolis*	100	*Nocardia coeliaca* *Rhodococcus boritolerans* *Rhodococcus erythropolis* *Rhodococcus globerulus* *Rhodococcus qingshengii*	99

Isolate #	Date Plated	Photograph	BYU Identification	BYU % Reliability	SNL Identification	SNL % Reliability
B5	02/26/2010		*Pseudomonas fragi* *Pseudomonas psychrophila* *Pseudomonas syringae* *Pseudomonas fluorescens* *Pseudomonas putida*	96.9 97.4 97.4 97.5 97.9	*Pseudomonas putida*	98
B6	02/25/2010		*Pseudomonas fluorescens* *Pseudomonas putida* *Pseudomonas migulae* *Pseudomonas madelii*	96.5 96.4 97.0 96.5	*Pseudomonas migulae*	97

Isolate #	Date Plated	Photograph	BYU Identification	BYU % Reliability	SNL Identification	SNL % Reliability
C1	02/26/2010	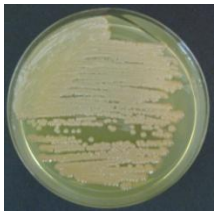	*Pseudomonas fluorescens* *Pseudomonas veronii* *Pseudomonas marginalis* *Pseudomonas extremoaustralis* *Pseudomonas meridiana* *Pseudomonas rhodesiae*	99.2 100.0 100.0 99.2 100.0 99.2	*Pseudomonas marginalis* *P.meridiana* *P. veronii*	100
C2	02/26/2010		*Rhodococcus erythreus* *Rhodococcus erythropolis*	98.9% 98.9%	*Rhodococcus erythreus* *R. erythropolis*	99
C3	02/26/2010	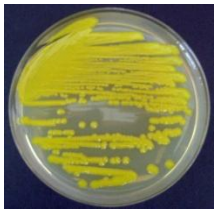	*Microbacterium oxydans* *Microbacterium maritypicum* *Microbacterium hydrocarbonoxydans* *Erwinia*	90.3 89.8 89.5 90.3	*Microbacterium oxydans*	90
C4	02/26/2010	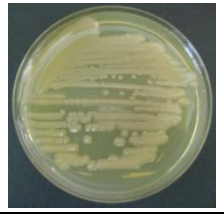	*Pseudomonas aurantiaca* *Pseudomonas fluorescens* *Pseudomonas putida* *Pseudomonas brassicacearum* *Pseudomonas kilonensis* *Pseudomonas migulae*	97.6 97.2 100.0 97.6 96.6 97.2	*Pseudomonas putida*	100

Isolate #	Date Plated	Photograph	BYU Identification	BYU % Reliability	SNL Identification	SNL % Reliability
C5	02/26/2010	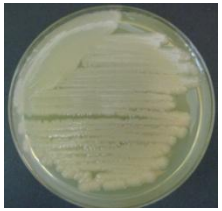	*Pseudomonas fluorescens* *Pseudomonas putida* *Pseudomonas migulae*	87.6 87.2 88.2	*Pseudomonas migulae*	88
C6	02/26/2010		*Pseudomonas putida* *Pseudomonas fluorescens* *Pseudomonas fragi* *Pseudomonas psychrophila* *Pseudomonas syringae*	98.1 98.1 96.8 97.3 97.3	*Pseudomonas fluorescens* *P. putida*	98
C7	02/26/2010	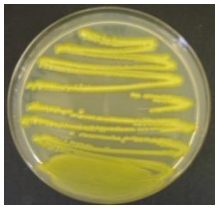	*Enterobacter cloacae* *Enterobacter cowanii* *Escherichia hermannii* *Escherichia coli* *Escherichia senegalensis* *Pantoea* *Salmonella typhimurium* *Salmonella enterica* *Salmonella bongori* *Shigella sonnei* *Enterobacteriaceae* *Yersinia*	95.3 99.1 97.5 95.6 96.1 93.8 93.3 93.6 92.9 92.6 96.4 95.5	*Enterobacter cowanii*	99
C8	02/26/2010		*Acinetobacter johnsonii* *Acinetobacter haemolyticus* *Acinetobacter schindleri*	83.7 94.0 94.0	*Acinetobacter haemolyticus* *A. schindleri*	94

Isolate #	Date Plated	Photograph	BYU Identification	BYU % Reliability	SNL Identification	SNL % Reliability
D1	02/26/2010	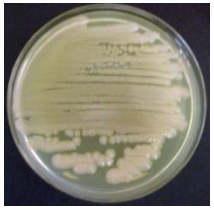	*Pseudomonas fluorescens*	97.1	*Pseudomonas fluorescens*	99
D2	02/26/2010		*Agrobacterium agile* *Pseudomonas aeruginosa* *Pseudomonas mendocina*	85.9 86.0 83.2	*Pseudomonas aeruginosa*	86
D3	02/26/2010		*Micrococcus luteus*	100.0	*Micrococcus luteus*	100
D4	02/26/2010	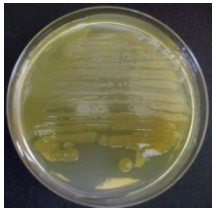	*Pseudomonas aeruginosa* *Pseudomonas mendocina* *Pseudomonas guinea* *Pseudomonas alcaliphila* *Pseudomonas anguilliseptica* *Pseudomonas pseudoalcaligenes*	92.0 88.1 92.0 87.4 93.1 87.1	*Pseudomonas fluorescens* *P. peli*	99

Isolate #	Date Plated	Photograph	BYU Identification	BYU % Reliability	SNL Identification	SNL % Reliability
D5	02/26/2010	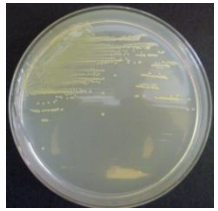	*Hydrogenophaga palleronii* *Hydrogenophaga taeniospiralis* *Hydrogenophaga defluvii* *Hydrogenophaga atypical*	94.5 91.1 94.5 94.6	*Hydrogenophaga palleronii*	99
D6	02/26/2010	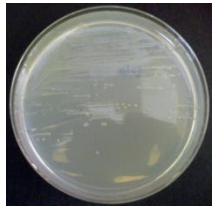	*Limnobacter thiooxidans*	99.1	*Limnobacter thiooxidans*	99

Isolate #	Date Plated	Photograph	BYU Identification	BYU % Reliability	SNL Identification	SNL % Reliability
E1	03/01/2010	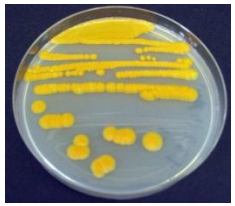	*Exiguobacterium undae* *Exiguobacterium antarcticum* *Exiguobacterium sibiricum* *Exiguobacterium oxidotolerans*	92.2 97.3 96.4 96.5	*Exiguobacterium antarcticum*	97
E2	03/01/2010		*Acinetobacter johnsonii*	97.2	*Acinetobacter johnsonii*	97
E3	03/01/2010	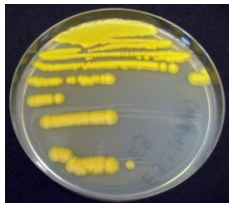	*Exiguobacterium undae* *Exiguobacterium antarcticum* *Exiguobacterium sibiricum* *Exiguobacterium oxidotolerans*	99.9 97.7 97.0 97.1	*Exiguobacterium undae*	100
E4	03/01/2010		*Aeromonas popoffii* *Aeromonas culicicola* *Aeromonas punctata* *Aeromonas hydrophila* *Aeromonas media* *Aeromonas veronii* *Aeromonas jandaei* *Aeromonas bestiarum* *Aeromonas salmonicida*	97.4 97.7 97.9 97.8 98.9 98.3 97.7 97.4 97.4	*Aeromonas media*	99

Isolate #	Date Plated	Photograph	BYU Identification	BYU % Reliability	SNL Identification	SNL % Reliability
E5	03/01/2010	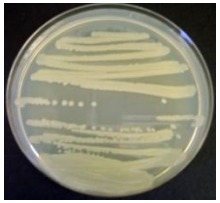	*Janthinobacterium lividum* *Pseudomonas mephitica*	98.4 97.4	*Janthinobacterium lividum*	98
E6	03/01/2010	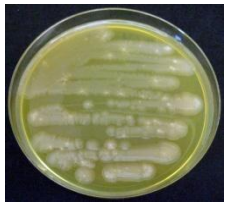	*Pseudomonas poae* *Pseudomonas trivialis* *Pseudomonas simiae* *Pseudomonas costantinii* *Pseudomonas tolaasii* *Pseudomonas lurida*	97.4 97.4 97.4 99.1 97.2 99.1	*Pseudomonas constantinii* *P. lurida*	99
E7	03/01/2010		*Acidovorax avenae* *Acidovorax konjaci* *Pseudacidovorax intermedius*	93.2 91.4 91.3	*Acidovorax avenae*	93
E8	03/01/2010		*Arthrobacter polychromogenes* *Arthrobacter oxydans*	97.9 98.3	*Arthrobacter oxydans*	98
E9	03/01/2010	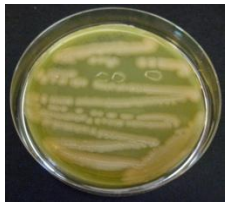	*Burkholderia cepacia* *Pseudomonas fluorescens*	99.8 99.8	*Burkholderia cepacia*	100

Isolate #	Date Plated	Photograph	BYU Identification	BYU % Reliability	SNL Identification	SNL % Reliability
E10	03/01/2010		*Brevundimonas* *Caulobacter vibrioides* *Caulobacter crescentus* *Caulobacter tundrae* *Caulobacter segnis* *Caulobacter henricii*	89.5 93.7 94.1 97.1 95.6 90.3	*Caulobacter tundrae*	97
E11	03/01/2010	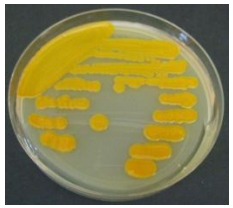	*Chryseobacterium* *Flavobacterium columnare* *Flavobacterium antarctica* *Flavobacterium pectinovorum* *Flavobacterium johnsoniae*	95.0 93.3 96.1 95.0 97.3	*Flavobacterium johnsoniae*	97
E12	03/01/2010		*Acidovorax avenae* *Acidovorax facilis* *Acidovorax valerianellae*	92.2 93.2 92.8	*Acidovorax facilis*	93

Isolate #	Date Plated	Photograph	BYU Identification	BYU % Reliability	SNL Identification	SNL % Reliability
F1	03/10/2010	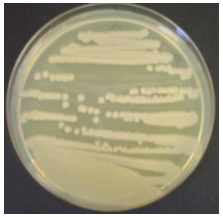	*Pseudomonas fluorescens* *Pseudomonas syringae* *Pseudomonas savastanoi* *Pseudomonas tremae* *Pseudomonas veronii*	100.0 96.6 96.6 96.4 96.2	*Pseudomonas fluorescens*	100
F2	03/01/2010	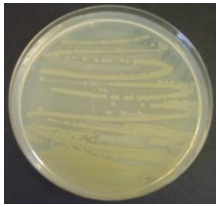			*Pseudomonas fluorescens* *P. peli*	98

Isolate #	Date Plated	Photograph	BYU Identification	BYU % Reliability	SNL Identification	SNL % Reliability
H1	03/01/2010	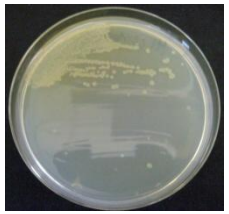	*Limnobacter thiooxidans*	97.9	*Limnobacter thiooxidans*	98
H2	03/01/2010		*Antarctobacter heliothermus* *Pseudomonas*	87.1 99.1	*Sulfitobacter donghicola*	98
H3	03/01/2010	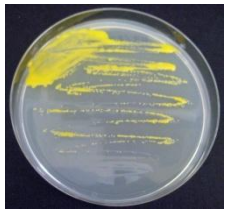	*Rhodococcus fascians* *Rhodococcus yunnanensis* *Rhodococcus erythropolis*	95.4 95.5 87.8	*Rhodococcus fascians*	98
H4	03/01/2010		*Bacillus subtilis* *Paracoccus haeundaensis* *Paracoccus marcusii* *Paracoccus carotinifaciens* *Pseudorhodobacter incheonensis* *Rhodobacter litoralis* *Rhodobacter katedanii* *Rhodobacter sphaeroides* *Rhodobacter sphaeroides*	86.6 85.3 86.5 85.3 86.0 83.5 85.7 83.3 82.9	*Rhodobacter katedanii*	96

Isolate #	Date Plated	Photograph	BYU Identification	BYU % Reliability	SNL Identification	SNL % Reliability
H5	03/01/2010	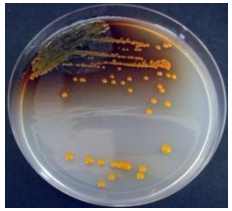	*Bacillus subtilis* *Paracoccus haeundaensis* *Paracoccus marcusii* *Paracoccus carotinifaciens* *Pseudomonas*	99.0 98.0 98.9 97.6 97.8	*Paracoccus marcusii*	99
H6	03/08/2010	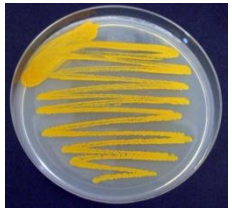	*Rhodococcus fascians* *Rhodococcus yunnanensis* *Rhodocuccus fascians* *Rhodococcus kyotonensis* *Rhodococcus cercidiphyllus*	93.7 95.4 93.7 93.0 95.4	*Rhodococcus fascians*	99

Isolate #	Date Plated	Photograph	BYU Identification	BYU % Reliability	SNL Identification	SNL % Reliability
I1	03/08/2010	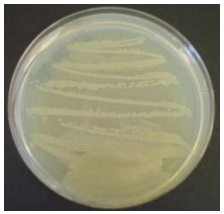				
I2	03/08/2010	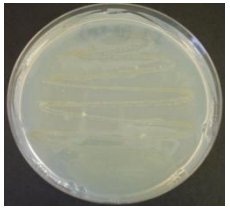	*Marinobacter aquaeolei* *Sulfitobacter* *Halomonas* *Marinobacter algicola* *Marinobacter koreensis* *Marinobacter salsuginis*	97.1 93.1 96.7 97.6 98.9 92.4	*Marinobacter koreensis*	99
I3	03/08/2010	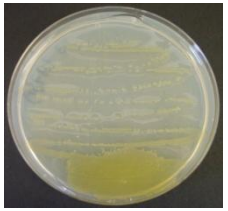				
I4	03/08/2010	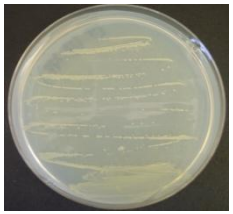	*Oceanibulbus indolifex* *Sulfitobacter*	94.6 100.0	*Oceanibulbus indolifex*	95

Isolate #	Date Plated	Photograph	BYU Identification	BYU % Reliability	SNL Identification	SNL % Reliability
J1	01/21/2010	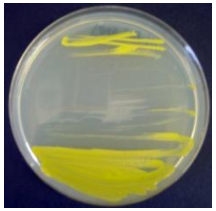	*Novosphingobium* *Sphingomonas adhaesiva* *Sphingomonas taejonensis* *Sphingopyxis composta* *Sphingopyxis alaskensis* *Sphingopyxis panaciterrae* *Sphingopyxis ginsengisoli* *Sphingopyxis macrogoltabida*	94.9 91.6 93.0 92.0 97.1 95.5 94.1 97.8	*Sphingopyxis alaskensis* *S. macrogoltabida*	99
J2	01/21/2010	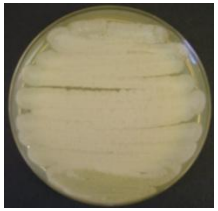	*Bacillus anthracis* *Bacillus cereus* *Bacillus thuringiensis* *Bacillus mycoides*	79.0 79.0 79.0 79.3	*Bacillus mycoides*	79

Isolate #	Date Plated	Photograph	BYU Identification	BYU % Reliability	SNL Identification	SNL % Reliability
K1	03/01/2010		*Pseudomonas pseudoalcaligenes* *Pseudomonas mendocina* *Pseudomonas alcaliphila*	96.5 96.5 94.3	*Pseudomonas mendocina* *P. pseudoalcaligenes*	97
K2	03/01/2010		*Flavobacillus indica* *Flavobacterium saliodium* *Flavobacterium aquatile* *Flavobacterium cucumis* *Flavobacterium kamogawaensis* *Flavobacterium frigoris* *Flavobacterium degerlachei* *Flavobacterium gelidilacus*	78.9 75.2 75.3 81.5 85.8 74.9 74.8 79.2		
K3	03/01/2010		*Limnobacter* *Limnobacter thiooxidans*	100.0 99.0		

Isolate #	Date Plated	Photograph	BYU Identification	BYU % Reliability	SNL Identification	SNL % Reliability
L1	03/01/2010	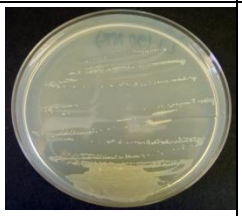	*Brevundimonas mediterranea* *Brevundimonas nasdae* *Brevundimonas intermedia* *Brevundimonas vesicularis* *Brevundimonas aurantiaca* *Caulobacter* *Burkholderia*	96.2 96.6 94.8 95.9 93.2 93.5 94.8	*Brevundimonas nasdae*	97
L2	03/01/2010	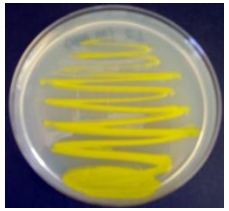	*Caulobacter leidyia* *Caulobacter subvibrioides* *Sphingomonas melonis* *Sphingomonas koreensis* *Sphingomonas aquatilis* *Sphingomonas asaccharolytica* *Sphingomonas kwangyangensis* *Asticcacaulis excentricus* *Asticcacaulis biprosthecium*	90.2 88.0 88.2 93.7 87.4 89.8 92.2 90.2 90.0	*Sphingomonas koreensis*	94
L3	03/01/2010	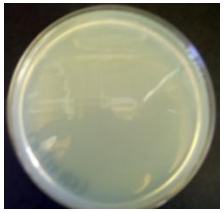	*Burkholderia* *Oligotropha carboxidovoran* *Rhodopseudomonas* *Nitrobacter vulgaris* *Nitrobacter hamburgensis* *Bradyrhizobium lupine* *Bradyrhizobium japonicum* *Afipia massiliensis* *Afipia broomeae* *Afipia lausannensis*	95.1 93.6 92.3 91.1 91.4 91.1 91.0 98.1 98.5 100.0	*Afipia lausannensis*	100

Isolate #	Date Plated	Photograph	BYU Identification	BYU % Reliability	SNL Identification	SNL % Reliability
M1	03/03/2010	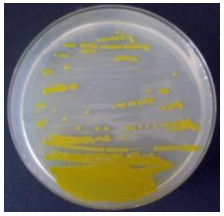	*Novosphingobium* *Sphingomonas* *Sphingopyxis alaskensis* *Sphingopyxis panaciterrae* *Sphingopyxis ginsengisoli* *Sphingopyxis macrogoltabida*	93.2 90-99 100.0 98.4 94.0 95.9	*Sphingopyxis alaskensis*	100
M2	03/03/2010		*Acidovorax facilis* *Acidovorax*	98.7 94-97	*Acidovorax facilis*	99
M3	03/03/2010	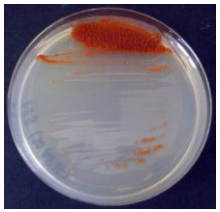	*Actinomycetales* *Micromonospora marina* *Micromonospora coxensis* *Micromonospora aurantiaca* *Micromonospora floridensis* *Micromonospora purpureochromogenes* *Micromonospora chalcea*	100.0 100.0 97.7 100.0 96.8 97.7 98.1	*Micromonospora marina*	100
M4	03/03/2010	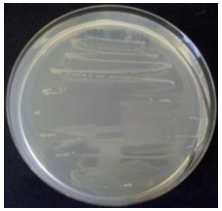	*Limnobacter* *Herbaspirillum seropedicae*	100.0 78.1	*Herbaspirillum seropedicae*	78

Isolate #	Date Plated	Photograph	BYU Identification	BYU % Reliability	SNL Identification	SNL % Reliability
N1	03/10/2010		*Pseudomonas pseudoalcaligenes* *Pseudomonas mendocina* *Pseudomonas alcaliphila*	94.98 94.98 94.25	*Pseudomonas mendocina* *P. pseudoalcaligenes*	95
N2	03/10/2010		*Pseudomonas pseudoalcaligenes* *Pseudomonas mendocina* *Pseudomonas alcaliphila*	95.83 95.83 95.05	*Pseudomonas mendocina* *P. pseudoalcaligenes*	96
N3	03/10/2010	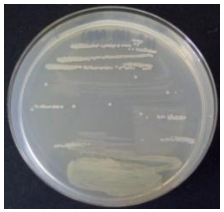	*Comamonas* *Hydrogenophaga bisanensis* *Hydrogenophaga intermedia* *Hydrogenophaga pseudoflava* *Hydrogenophaga flava* *Hydrogenophaga defluvii* *Hydrogenophaga atypica*	86.25 89.95 98.20 88.56 89.20 87.92 87.53	*Hydrogenophaga intermedia*	98
N4	03/10/2010	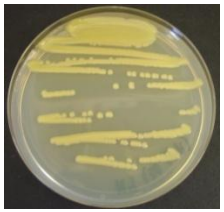	*Arthrobacter mysorens* *Arthrobacter arilaitensis* *Arthrobacter mysorens* *Arthrobacter bergerei* *Arthrobacter protophormiae* *Arthrobacter nicotianae* *Arthrobacter ardleyensis* *Arthrobacter arilaitensis*	95.71 94.91 95.71 99.20 95.84 95.71 97.86 94.90	*Arthrobacter bergerei*	99

Isolate #	Date Plated	Photograph	BYU Identification	BYU % Reliability	SNL Identification	SNL % Reliability
N5	03/10/2010		*Rhodococcus erythropolis* *Rhodococcus erythreus* *Rhodococcus boritolerans* *Pimelobacter simplex*	100 100 100 100	*Pimelobacter simplex* *Rhodococcus boritolerans* *R. erythreus* *R. erythropolis*	100
N6	03/10/2010	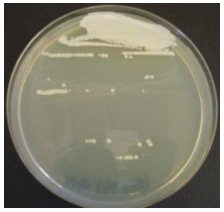	*Arthrobacter oxydans* *Arthrobacter polychromogenes* *Arthrobacter scleromae*	99.50 100 100	*Arthrobacter polychromogenes* *A. scleromae*	100
N7	03/10/2010	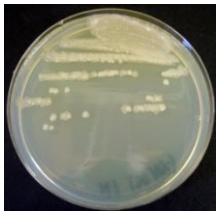	*Pseudomonas pseudoalcaligenes* *Pseudomonas mendocina* *Pseudomonas alcaliphila*	95.60 95.60 94.77	*Pseudomonas mendocina* *P. pseudoalcaligenes*	96

Isolate #	Date Plated	Photograph	BYU Identification	BYU % Reliability	SNL Identification	SNL % Reliability
O1	03/10/2010		*Acidovorax facilis* *Acidovorax defluvii*	97.1 92.7	*Acidovorax facilis*	97
O2	03/10/2010		*Saccharomonospora* *Albidovulum inexpectatum* *Rhodobacter* *Paracoccus denitrificans* *Paracoccus pantotrophus* *Paracoccus thiocyanatus*	88.7 84.5 96.0 85.9 84.9 86.9	*Paracoccus thiocyanatus*	87
O3	03/10/2010		*Limnobacter*	100.0	*Limnobacter thiooxidans*	100

APPENDIX B: RESULTS OF HIGH-THROUGHPUT MULTIWELL PLATE SCREENING AS ORIGINALLY REPORTED TO SANDIA BY NDSU

Optimization of *in vitro* Biofilm Growth Conditions for Marine Bacteria Isolates
Sandia National Laboratories (Susan Altman)

BMRL ID: Sandia-BO-1

Report by: Shane Stafslien
6-3-11

Center for Nanoscale Science and Engineering
North Dakota State University
Fargo, ND 58102

Evaluation of Biofilm Growth – Isolate H4

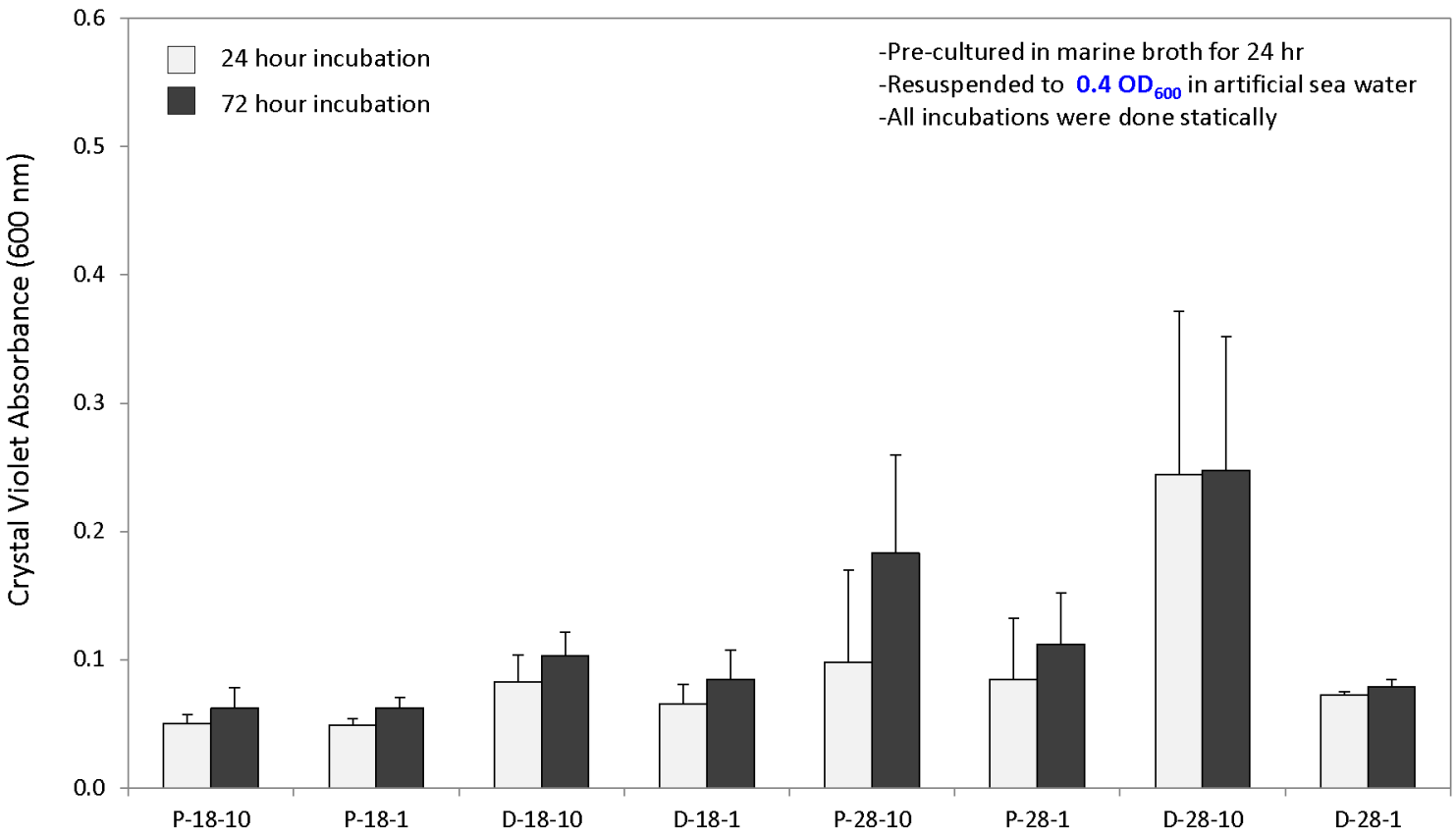

P = Peptone
D = Dextrose

18 = 18°C
28 = 28°C

10 = 10% inoculum
1 = 1% inoculum

2

Evaluation of Biofilm Growth – Isolate H6 (Trial 1)

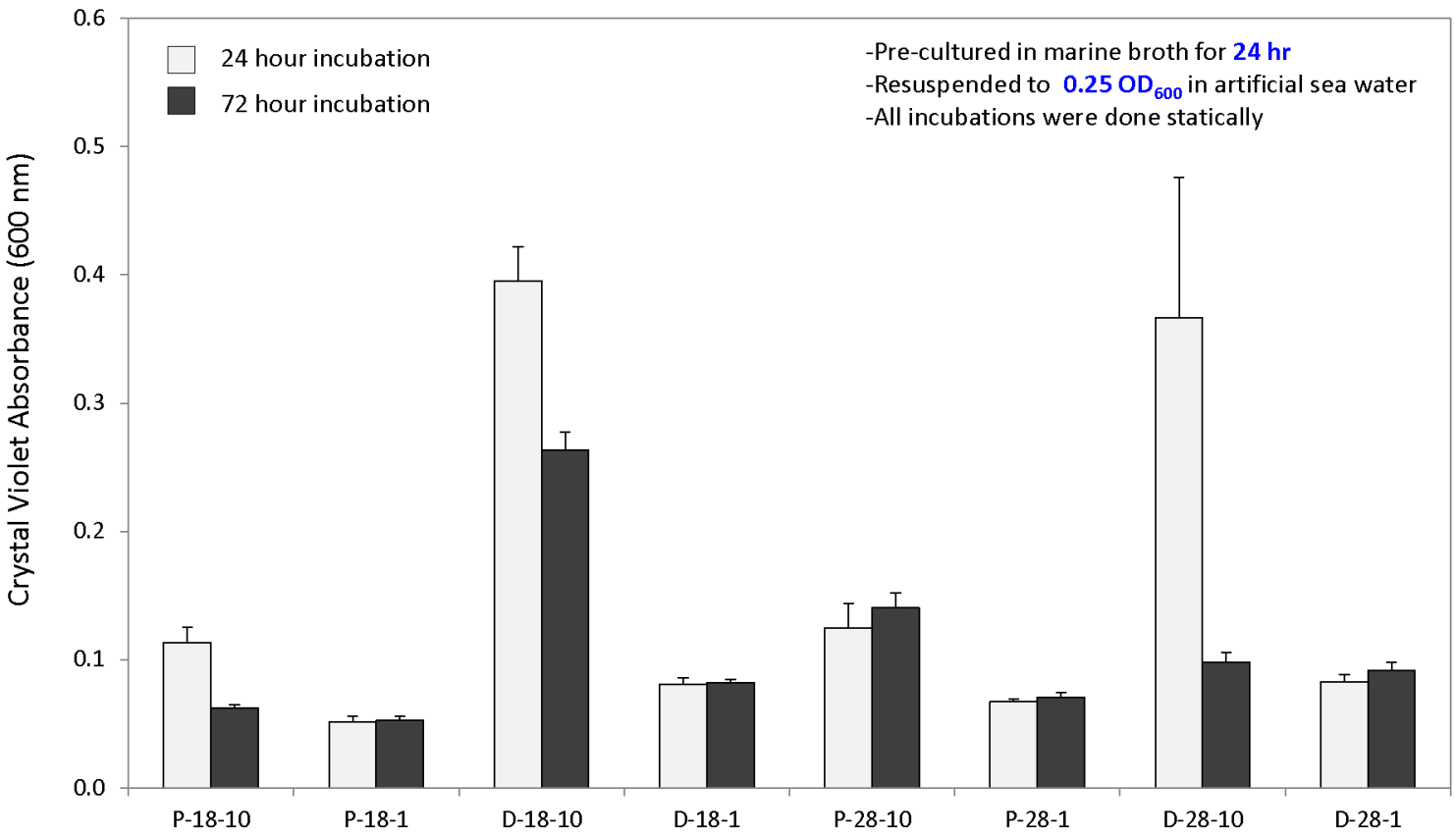

P = Peptone
D = Dextrose

18 = 18°C
28 = 28°C

10 = 10% inoculum
1 = 1% inoculum

3

Images of Bacterial Biofilm Growth after Crystal Violet Staining

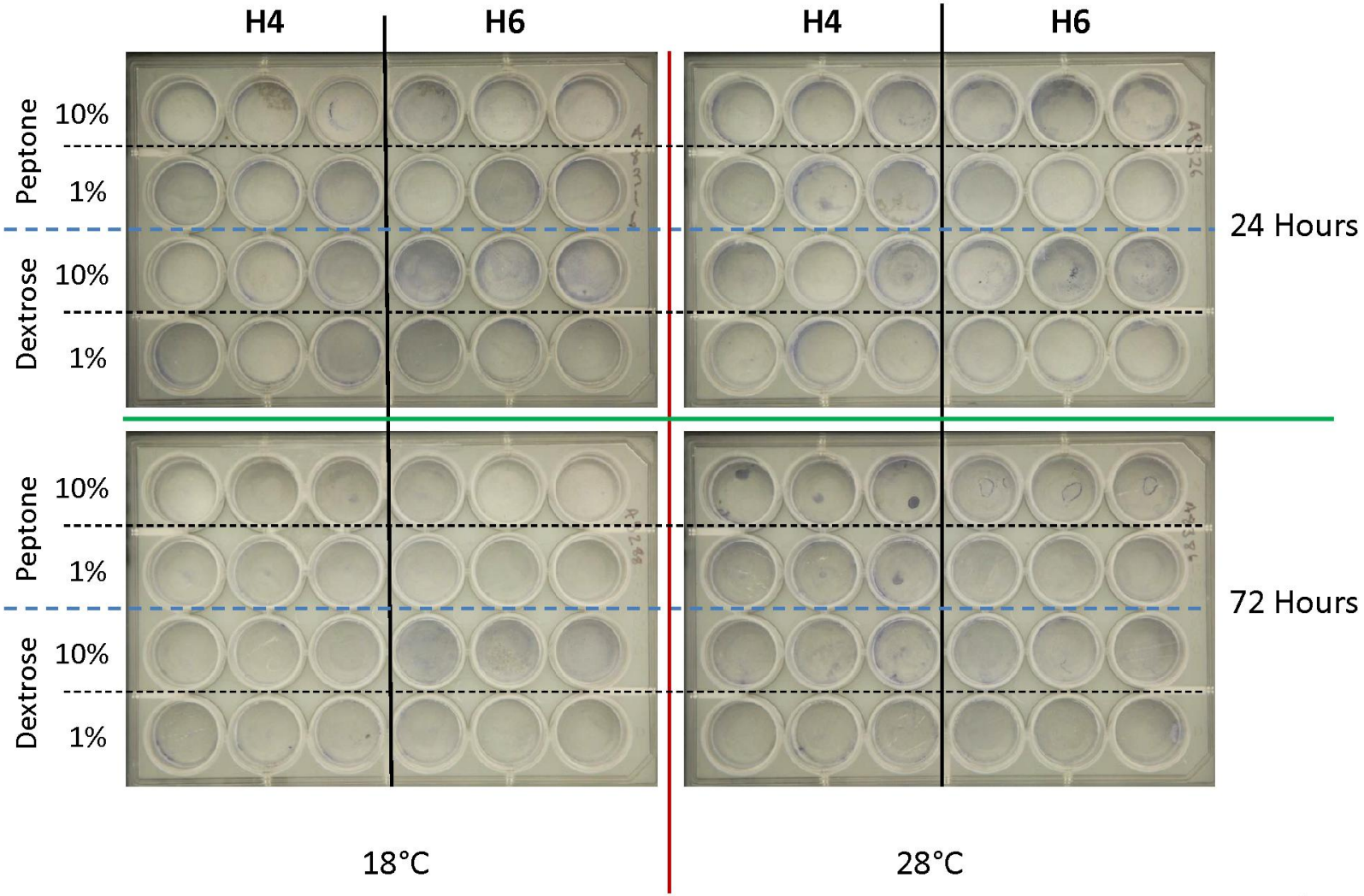

4

Evaluation of Biofilm Growth – Isolate H3

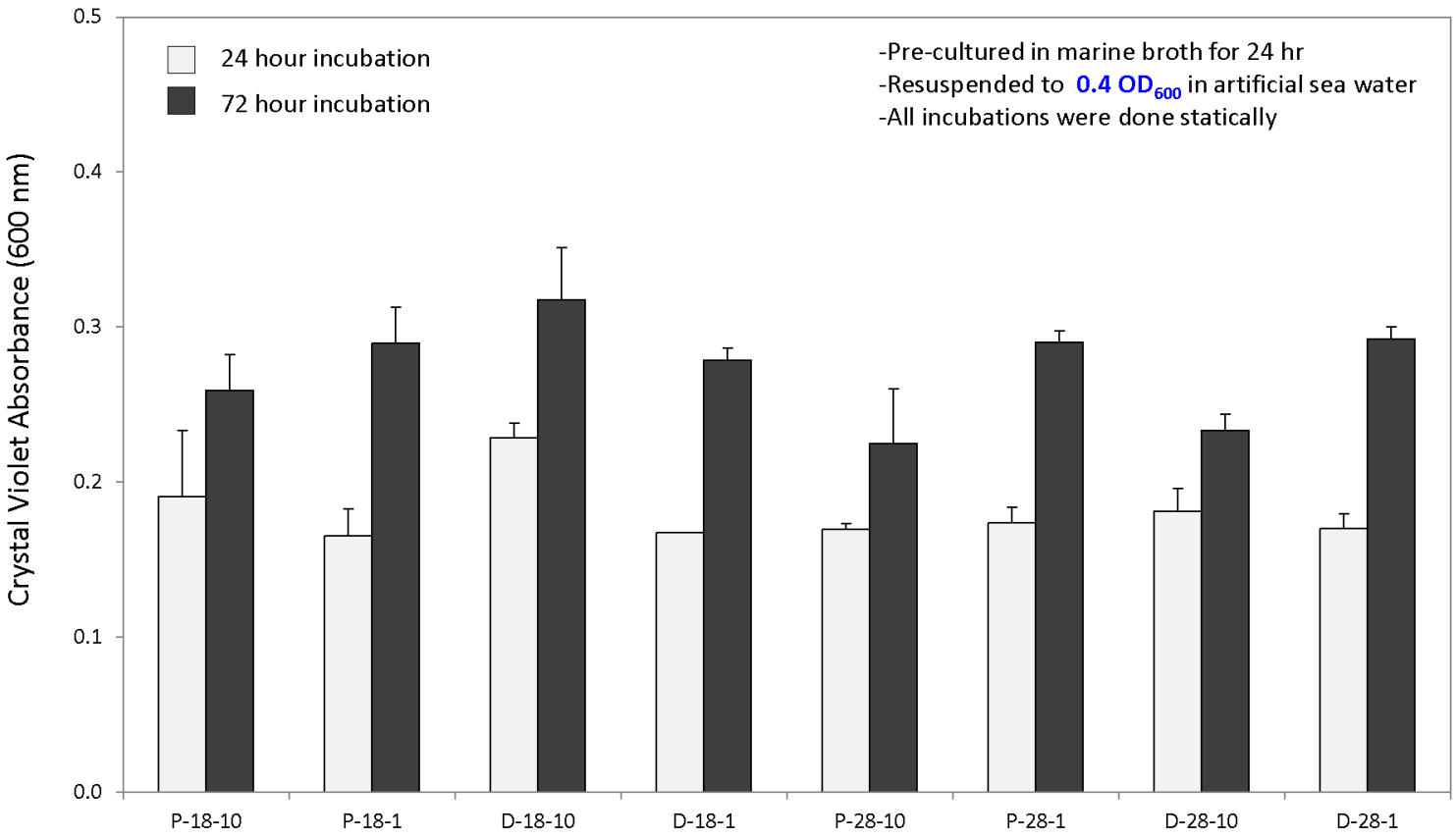

P = Peptone
D = Dextrose

18 = 18°C
28 = 28°C

10 = 10% inoculum
1 = 1% inoculum

Evaluation of Biofilm Growth – Isolate H6 (Trial 2)

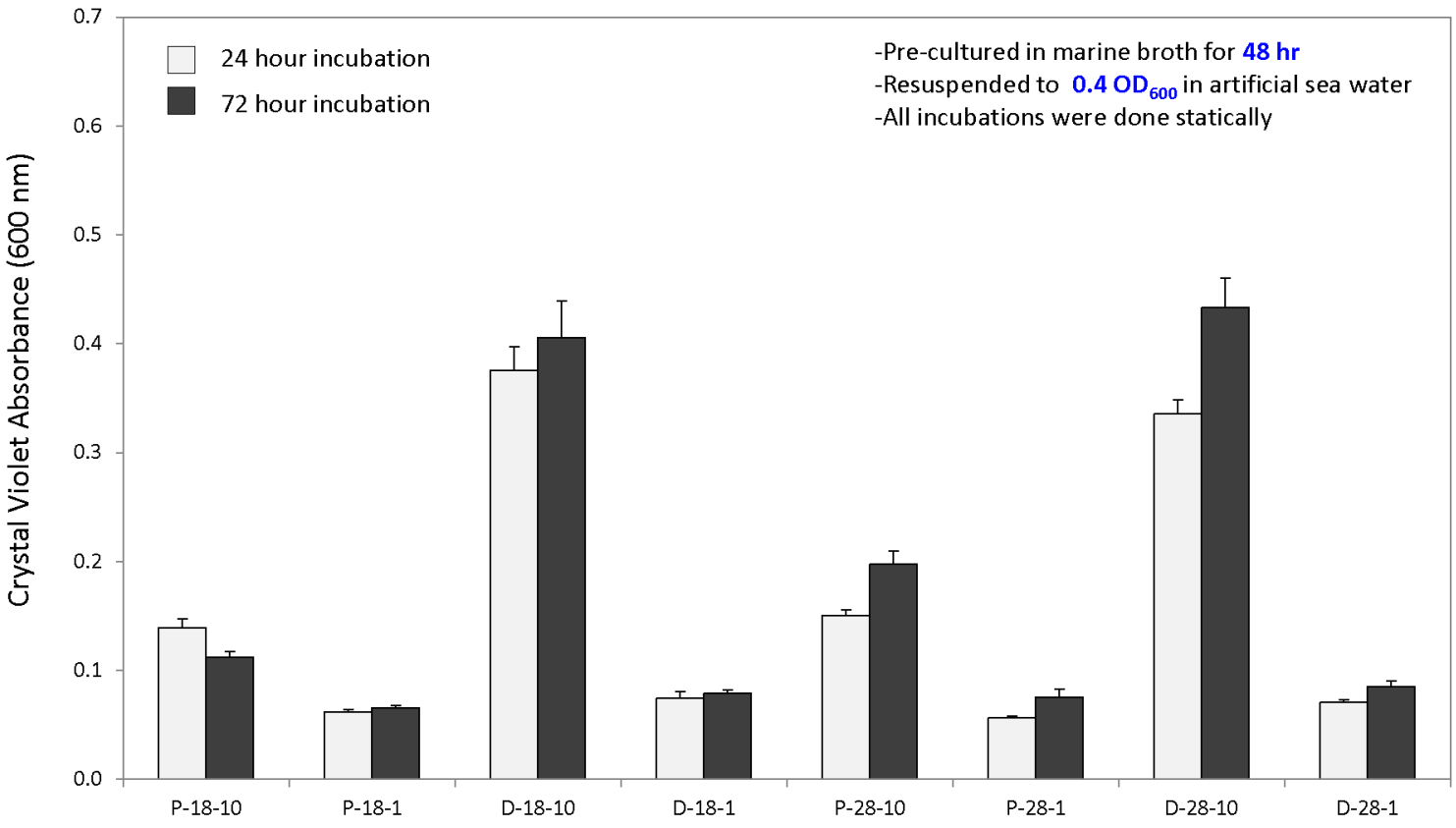

P = Peptone
D = Dextrose

18 = 18°C
28 = 28°C

10 = 10% inoculum
1 = 1% inoculum

Images of Bacterial Biofilm Growth after Crystal Violet Staining

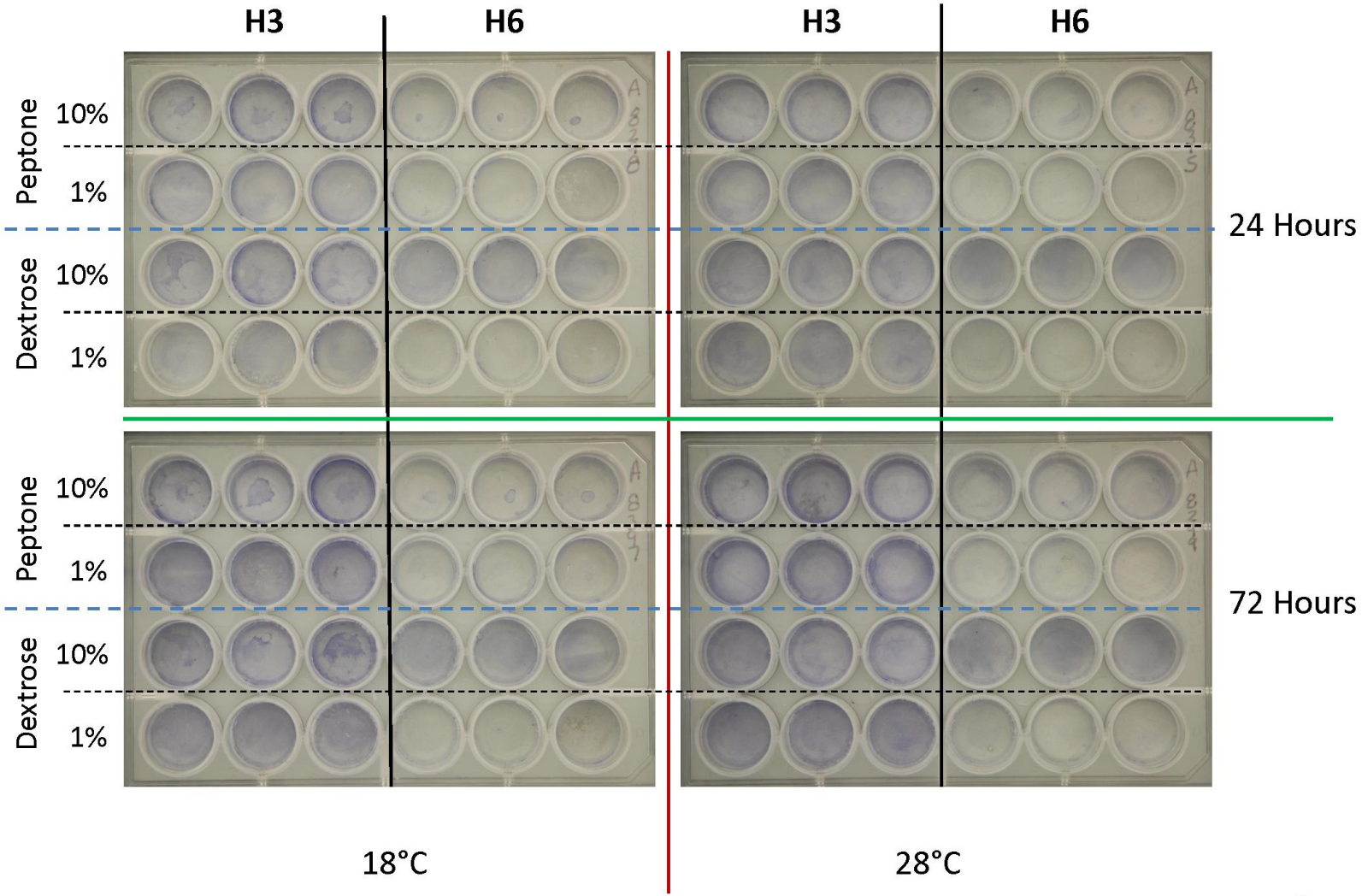

7

Evaluation of Biofilm Growth – Isolate H2

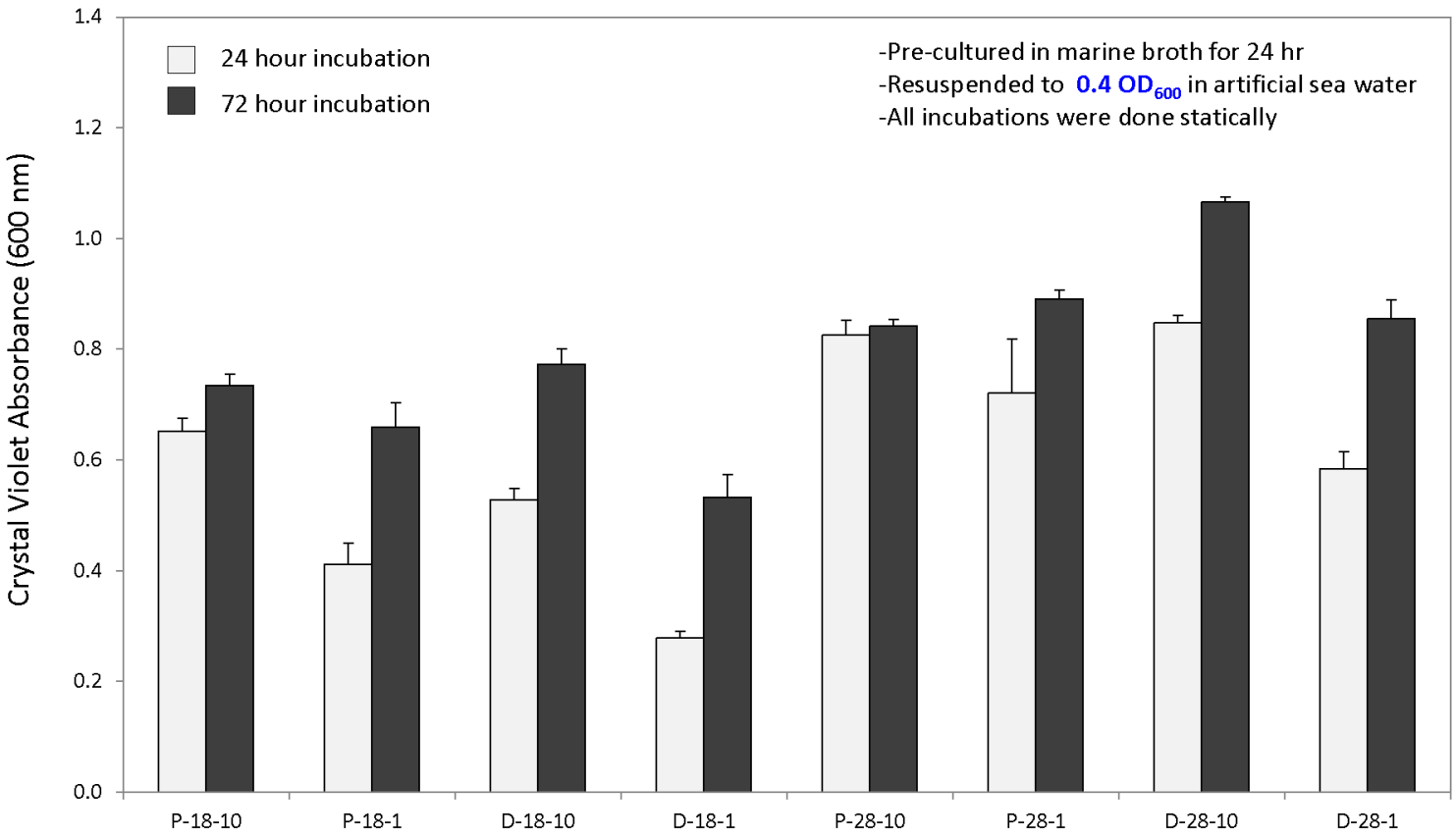

P = Peptone
D = Dextrose

18 = 18°C
28 = 28°C

10 = 10% inoculum
1 = 1% inoculum

Evaluation of Biofilm Growth – Isolate H5

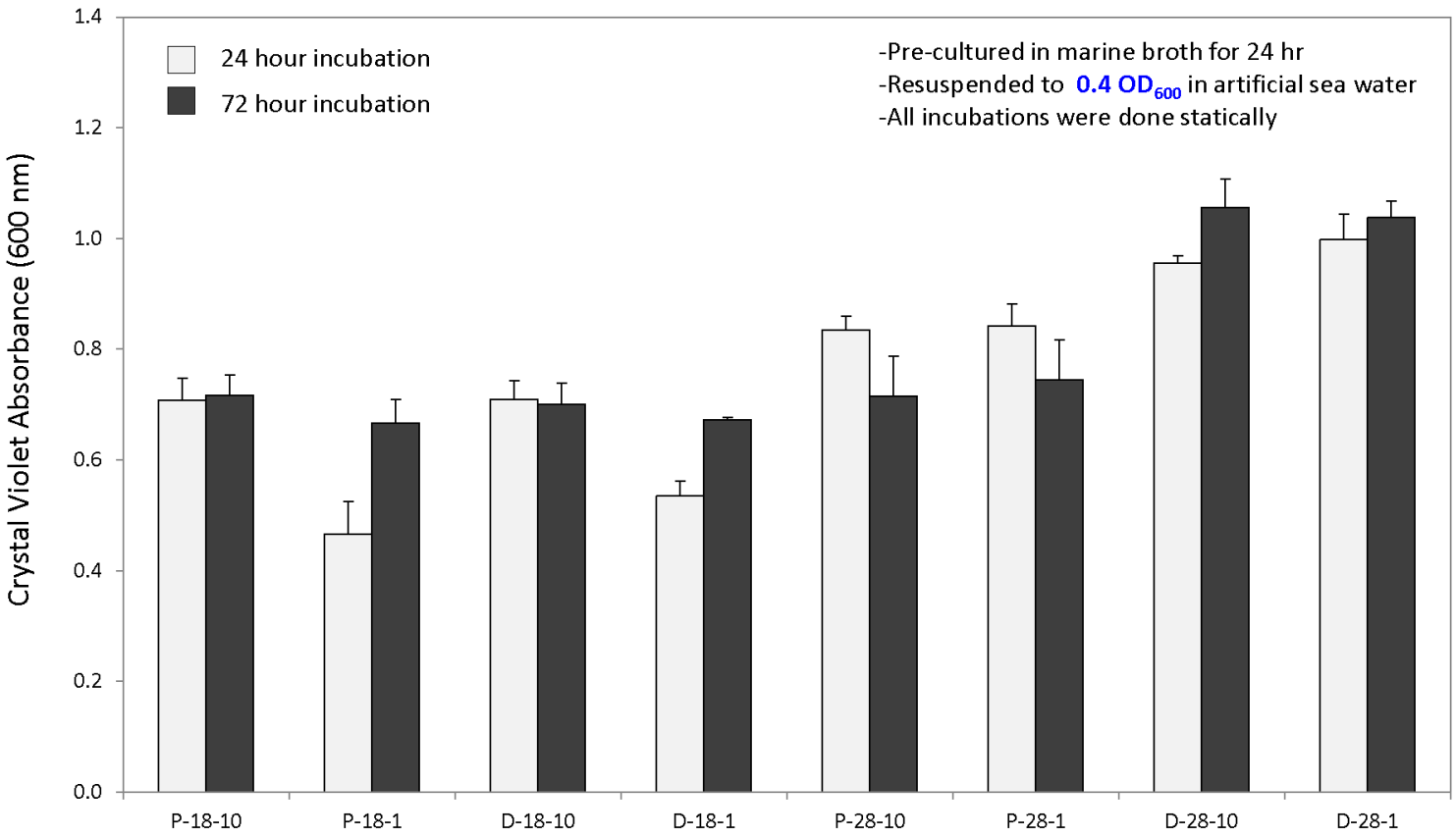

P = Peptone
D = Dextrose

18 = 18°C
28 = 28°C

10 = 10% inoculum
1 = 1% inoculum

Images of Bacterial Biofilm Growth after Crystal Violet Staining

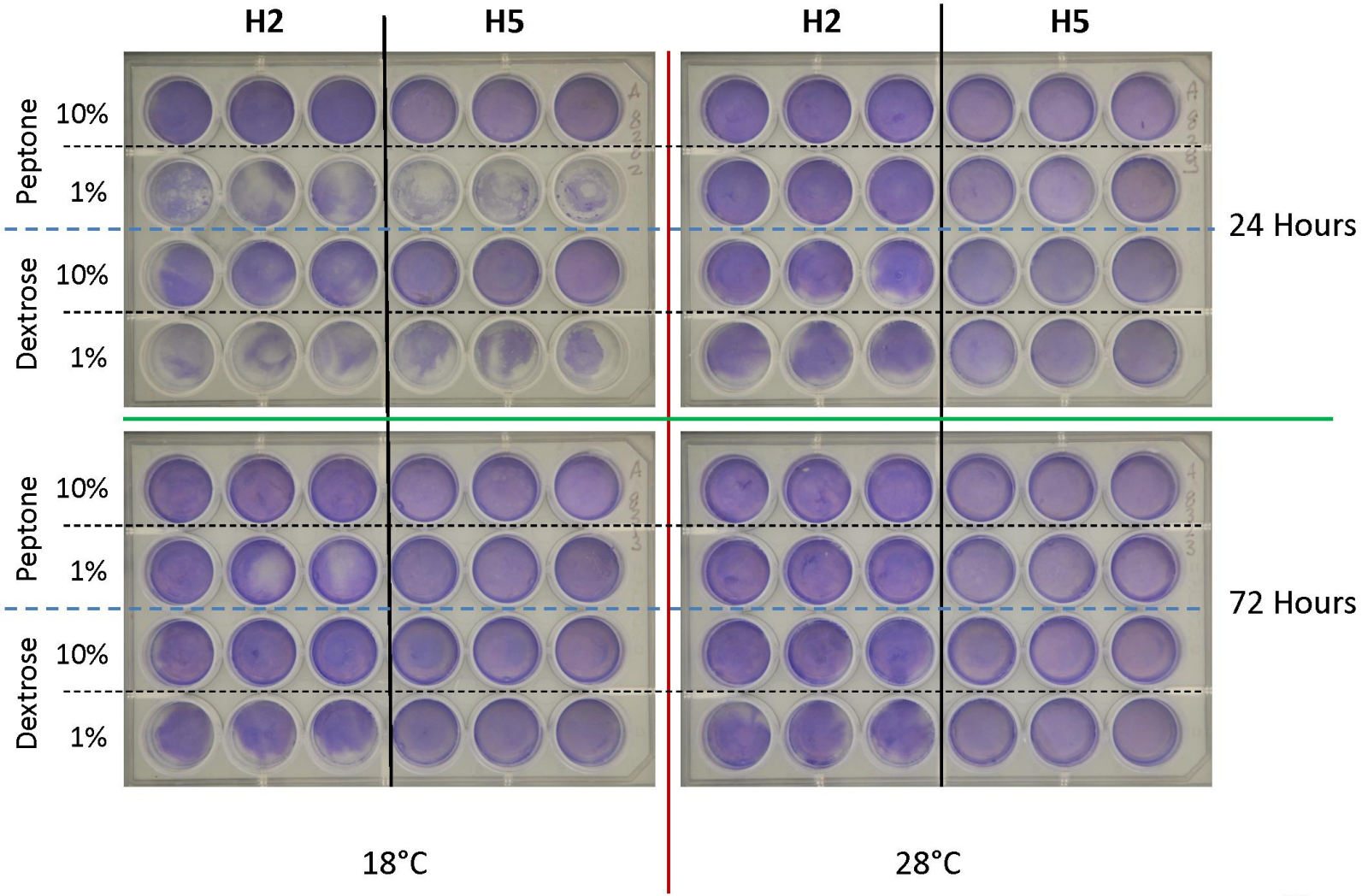

10

APPENDIX C: STERIOSCOPIC IMAGES AND OBSERVATIONS FROM TUBE REACTOR EXPERIMENTS

Experiment 1 Stereoscopic Images: *Pseudomonas fluorescens* B2 Isolate

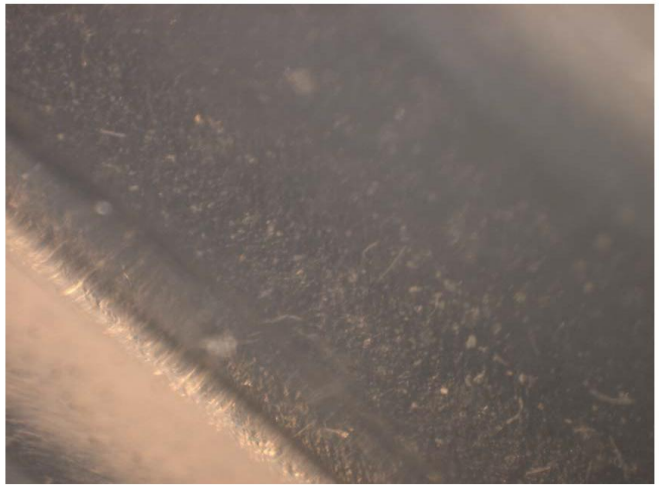

Pseudomonas fluorescens B2 biofilm on silicone tubing at 20x magnification

Pseudomonas fluorescens B2 biofilm on silicone tubing at 40x magnification

Observations:

- Small white colonies with some stringy structures
- Colonies relatively uniform in size
- Heterogenous coverage
- Sparse in some areas

Experiment 1 Stereoscopic Images: *Rhodococcus erythropolis* B4 Isolate

Rhodococcus erythropolis B4 biofilm on silicone tubing at 10x magnification

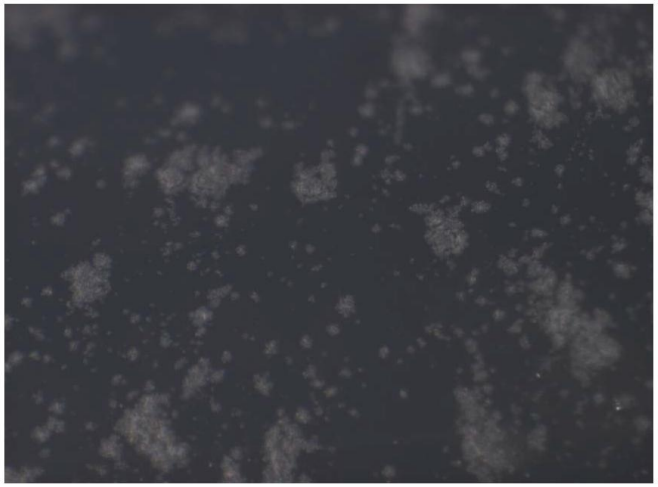

Rhodococcus erythropolis B4 biofilm on silicone tubing at 80x magnification

Observations:

- White semi-transparent colonies
- More large colonies than small
- Heterogenous coverage
- Colonies look similar to those grown on R2A agar

Experiment 1 Stereoscopic Images: *Pseudomonas fluorescens* D1 Isolate

Pseudomonas fluorescens D1 biofilm on silicone tubing at 20x magnification

Pseudomonas fluorescens D1 biofilm on silicone tubing at 50x magnification

Observations:

- White semi-transparent colonies with flock-like appearance
- A few larger clumps but mostly smaller
- Heterogenous & sparse coverage

Experiment 2 Stereoscopic Images: *Pseudomonas anguilliseptica* D4 Isolate

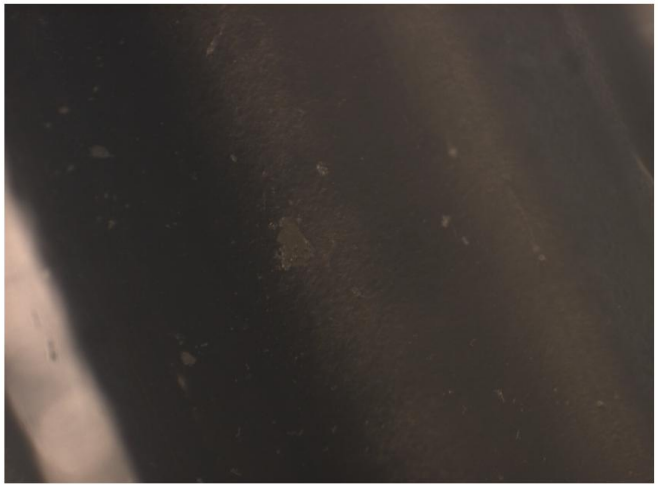

Pseudomonas anguilliseptica D4 biofilm on silicone tubing at 40x magnification

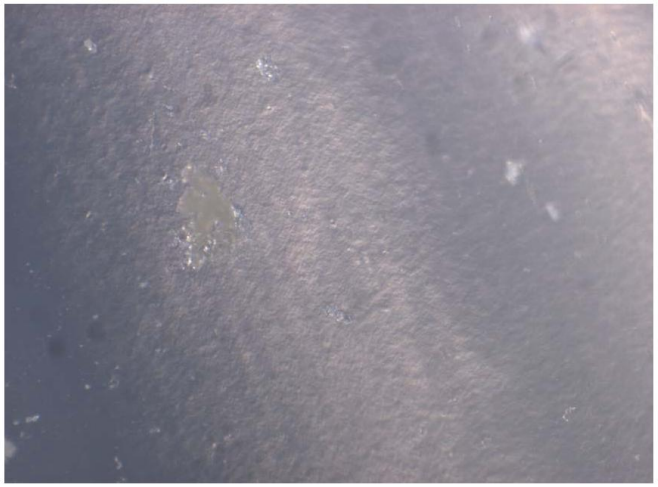

Pseudomonas anguilliseptica D4 biofilm on silicone tubing at 80x magnification

Observations:

- White opaque colonies
- Mostly large clumps
- Heterogenous & sparse coverage

Experiment 3 Stereoscopic Images: *Hydrogenophaga palleronii* D5 Isolate

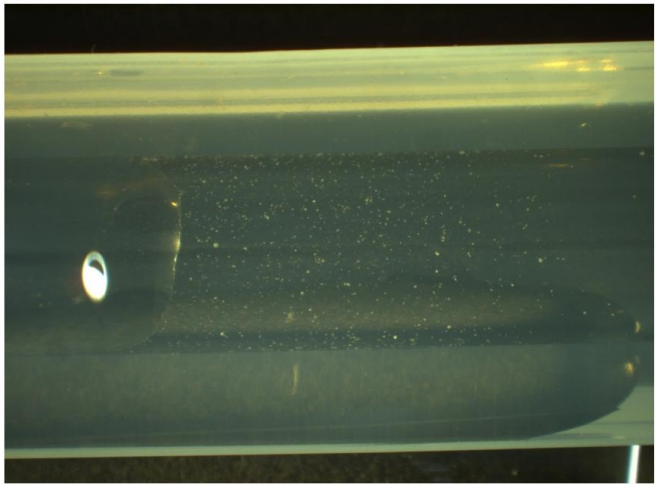

Hydrogenophaga palleronii D5 biofilm on silicone tubing at 10x magnification

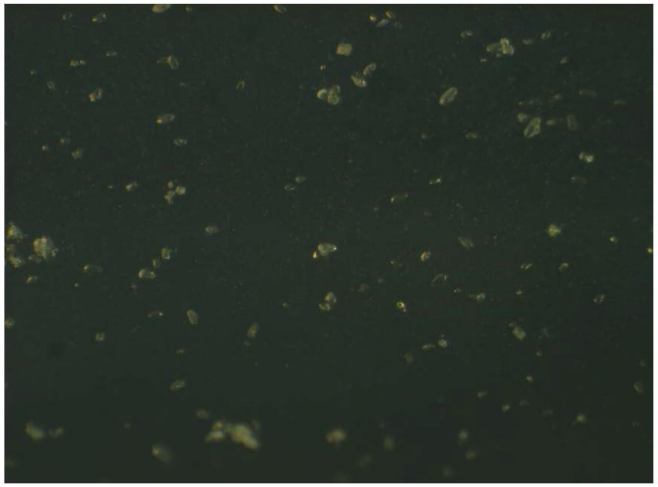

Hydrogenophaga palleronii D5 biofilm on silicone tubing at 80x magnification

Observations:

- Small cream opaque colonies
- Mostly large clumps
- Fairly homogenous coverage
- Colonies uniform in size

Experiment 4 Stereoscopic Images: *Pseudomonas constantinii* E6 Isolate

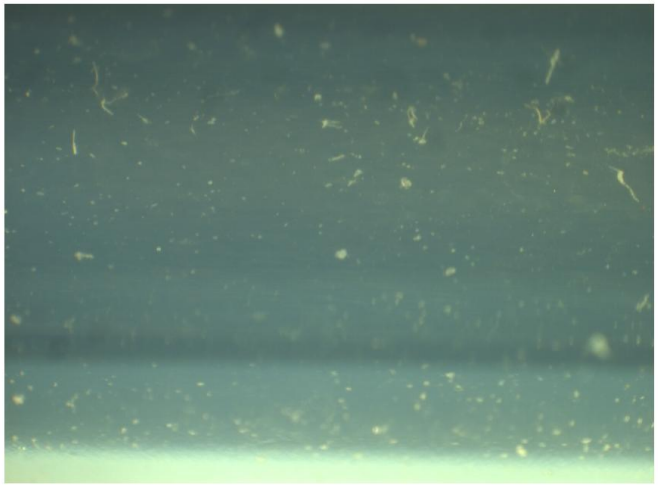

Pseudomonas constantinii E6 biofilm on silicone tubing at 20x magnification

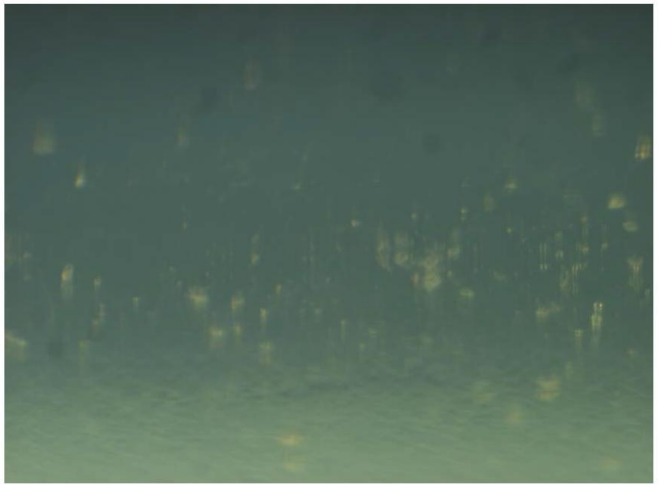

Pseudomonas constantinii E6 biofilm on silicone tubing at 80x magnification

Observations:

- Yellow opaque colonies
- Variety of clump sizes
- Fairly homogenous coverage
- Colonies uniform in size

Experiment 4 Stereoscopic Images: *Antarcticobacter heliothermus* H2 Isolate

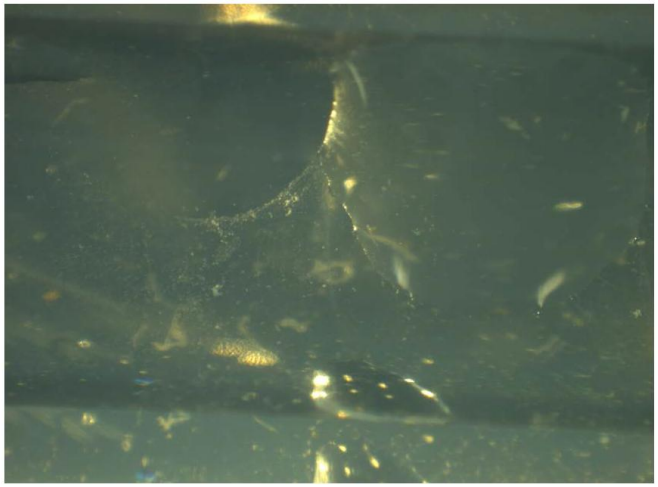

Antarcticobacter heliothermus H2
biofilm on silicone tubing at 20x magnification

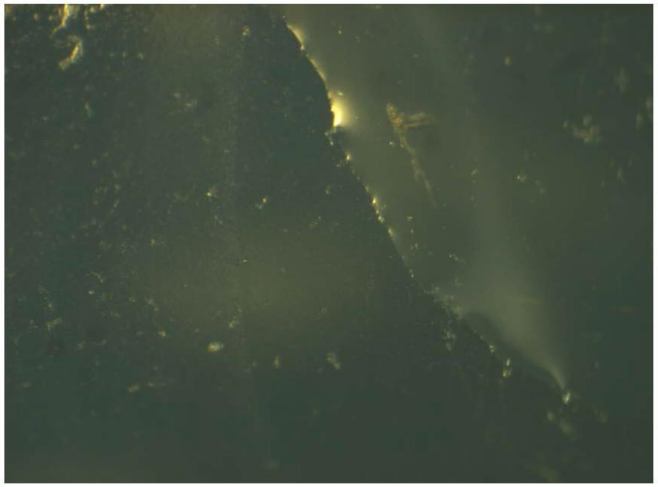

Antarcticobacter heliothermus H2
biofilm on silicone tubing at 80x magnification

Observations:

- Cream semi-transparent colonies with some stringy structures
- Variety of clump sizes
- Images demonstrated both homogenous & hetergenous coverage
- Colonies uniform in size

Experiment 4 Stereoscopic Images: *Rhodococcus yunnanensis* H3 Isolate

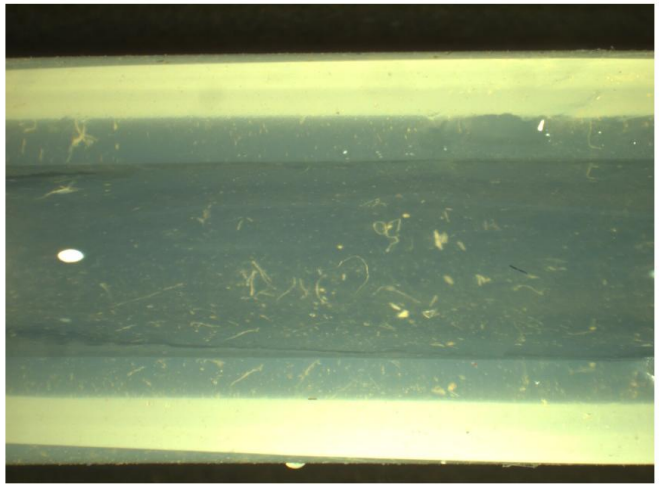

Rhodococcus yunnanensis H3 biofilm on silicone tubing at 10x magnification

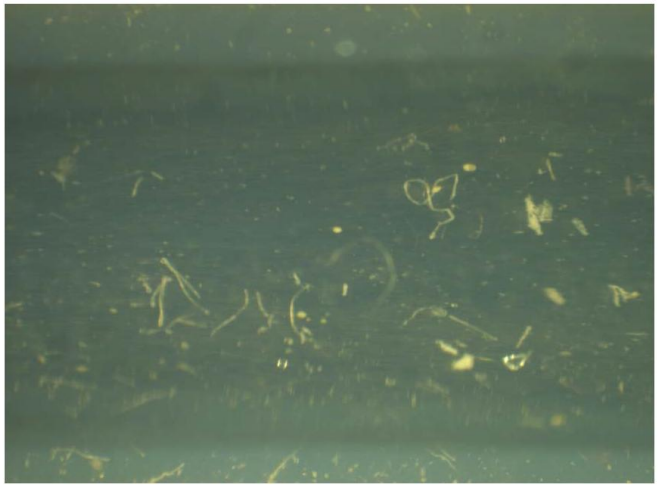

Rhodococcus yunnanensis H3 biofilm on silicone tubing at 20x magnification

Observations:

- Images demonstrated different biofilm structures between experiments (see next slide)
- Cream opaque colonies with some stringy structures
- A few big clumps
- Heterogenous coverage

Experiment 3 Stereoscopic Images: *Rhodococcus yunnanensis* H3 Isolate

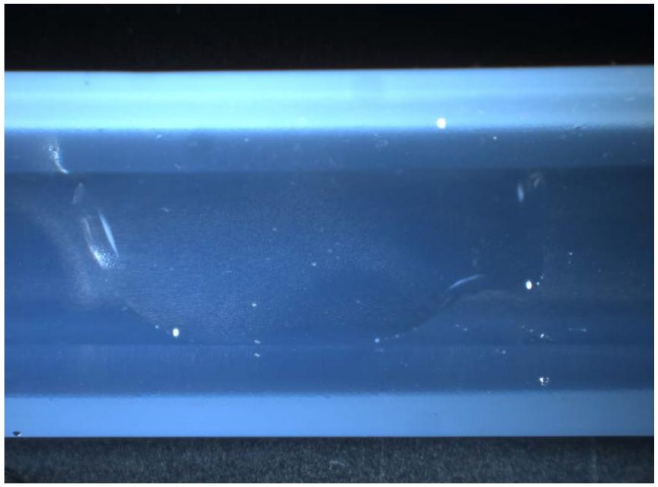

Rhodococcus yunnanensis H3 biofilm on silicone tubing at 10x magnification

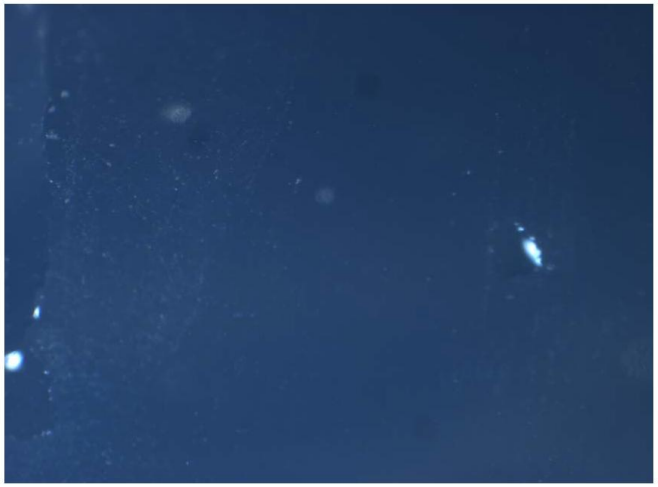

Rhodococcus yunnanensis H3 biofilm on silicone tubing at 50x magnification

Observations:

- Images demonstrated different biofilm structures between experiments (see previous slide)
- Tiny white semi-transparent colonies
- A few big clumps
- Heterogenous coverage

Experiment 2 Stereoscopic Images: *Bacillus subtilis* H4 Isolate

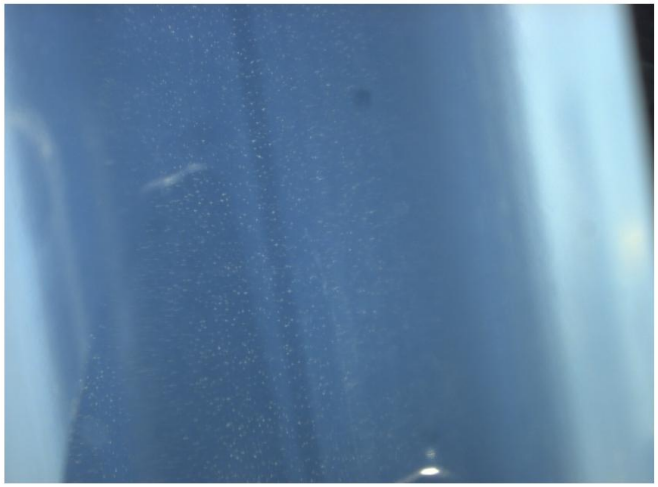

Bacillus subtilis H4 biofilm on silicone tubing at 20x magnification

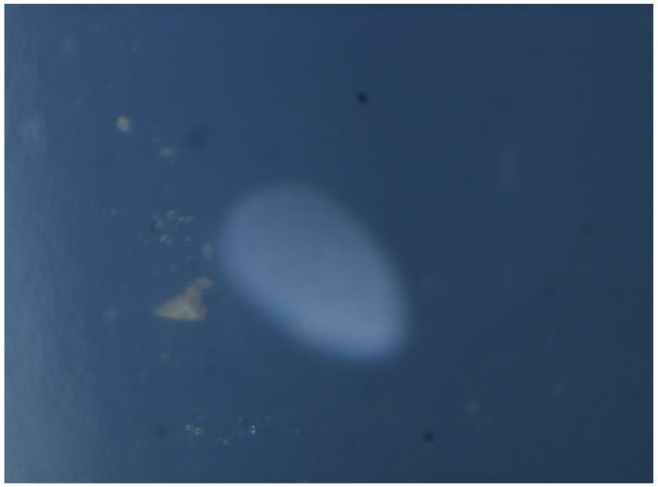

Bacillus subtilis H4 biofilm on silicone tubing at 80x magnification

Observations:

- Tiny cream semi-transparent colonies
- A few big clumps
- Fairly homogenous coverage

Experiment 2 Stereoscopic Images: *Bacillus subtilis* H5 Isolate

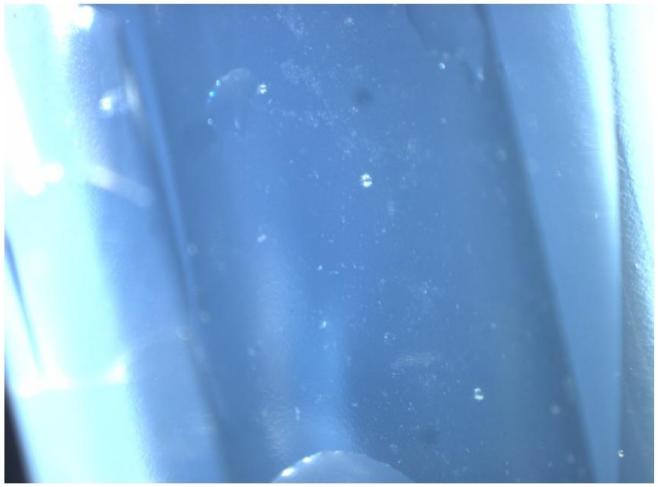

Bacillus subtilis H5 biofilm on silicone tubing at 20x magnification

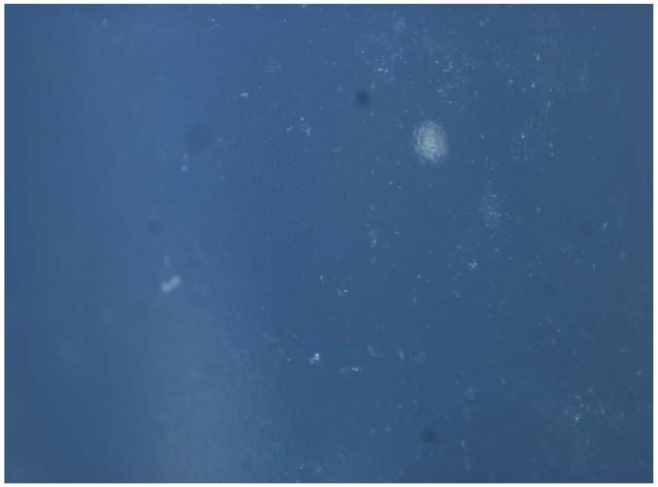

Bacillus subtilis H5 biofilm on silicone tubing at 50x magnification

Observations:

- Tiny cream semi-transparent colonies
- A few larger clumps
- Evenly distributed but heterogenous coverage

Experiment 4 Stereoscopic Images: *Rhodococcus yunnanensis* H6 Isolate

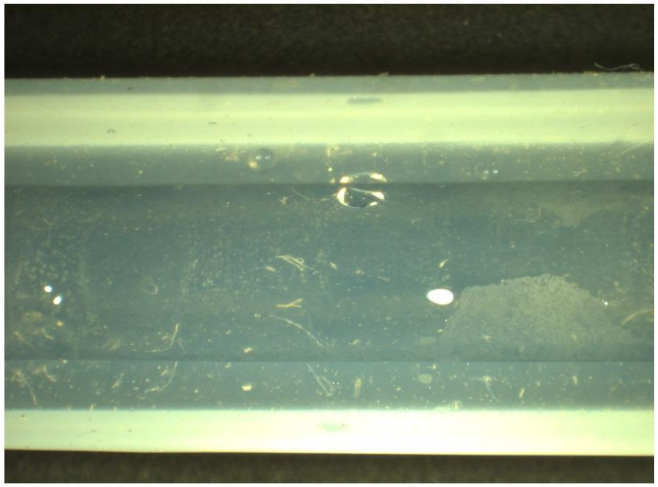

Rhodococcus yunnanensis H6 biofilm on silicone tubing at 10x magnification

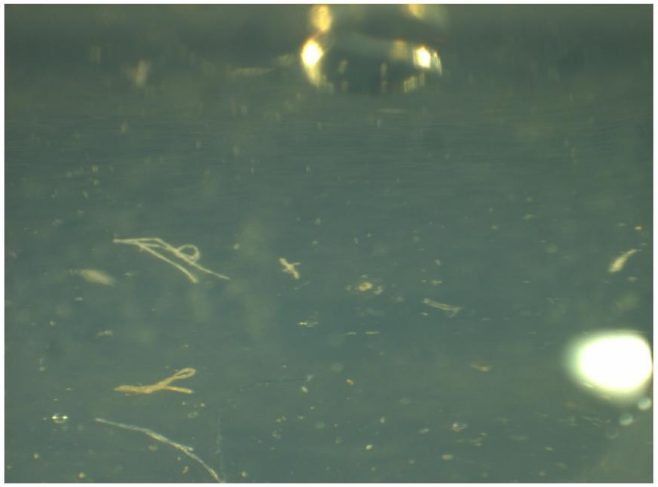

Rhodococcus yunnanensis H6 biofilm on silicone tubing at 30x magnification

Observations:

- Images demonstrated different biofilm structures between experiments (see next slide)
- Yellow semi-transparent colonies with some stringy structures
- Fairly homogenous coverage

Experiment 3 Stereoscopic Images: *Rhodococcus yunnanensis* H6 Isolate

Rhodococcus yunnanensis H6 biofilm on silicone tubing at 50x magnification

Rhodococcus yunnanensis H6 biofilm on silicone tubing at 100x magnification

Observations:

- Images demonstrated different biofilm structures between experiments (see previous slide)
- Tiny white semi-transparent colonies
- Tiny colonies make up larger colonies
- Fairly homogenous coverage

Experiment 2 Stereoscopic Images: *Sphingopyxis macrogoltabida* J1 Isolate

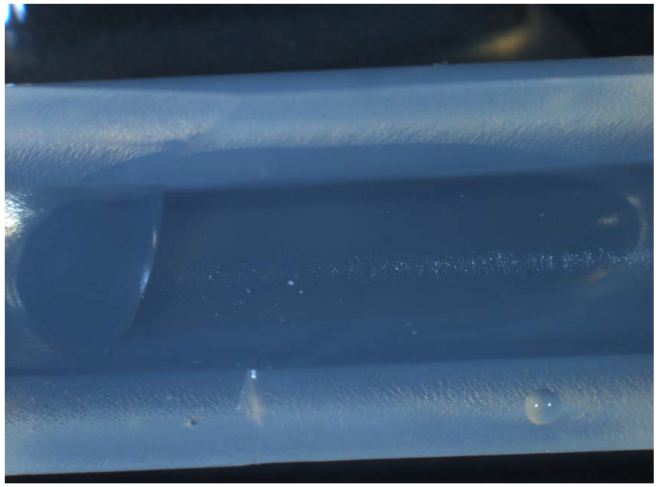

Sphingopyxis macrogoltabida J1 biofilm on silicone tubing at 10x magnification

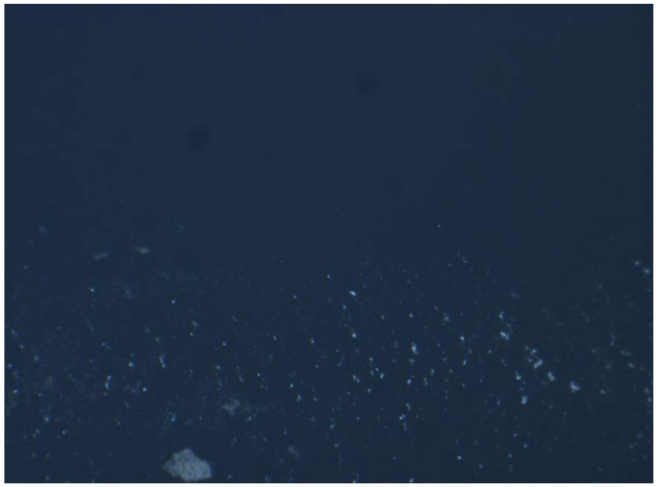

Sphingopyxis macrogoltabida J1 biofilm on silicone tubing at 80x magnification

Observations:

- Tiny white semi-transparent colonies
- Very sparse coverage
- Coverage seems concentrated at the bottom of the tubing section
- Colonies appear similar to those grown on R2A

DISTRIBUTION

External (Electronic Copy)

Angela Adams
U. S. Bureau of Reclamation
Yuma Area Office
7301 Calle Agua Salada
Yuma, AZ 85364
aadams@lc.usbr.gov

Kelli Buckingham-Meyer
Center for Biofilm Engineering
Montana State University
P.O. Box 173980
Bozeman, MT 59717-3980
kellib@erc.montana.edu

Darla Goeres
Center for Biofilm Engineering
Montana State University
P.O. Box 173980
Bozeman, MT 59717-3980
darla_g@erc.montana.edu

Paul Savage
Department of Chemistry and Biochemistry
Brigham Young University
C-100 BNSN
Provo, Utah 84602-5700
paul_savage@byu.edu

Shane Stafslien
Center for Nanoscale Science and Engineering
North Dakota State University
Fargo, ND 58102
Shane.Stafslien@ndsu.edu

William N Varnava
Naval Facilities Engineering Service Center
1100 23rd Ave Code ESC32
Port Hueneme, CA, 93043
william.varnava@navy.mil

John Walp
U. S. Bureau of Reclamation
Brackish Groundwater National
Desalination Research Facility
JWalp@usbr.gov

Internal (Electronic Copy)

1	MS0899	Technical Library, 9536
1	MS0763	LDRD Office, 1911
1	MS0734	A. Martino, 6124
1	MS0735	J. Merson, 6910
1	MS0750	A. Halloran, 6913
1	MS0754	S. Altman, 6915
1	MS0754	M. Kirk, 6915
1	MS0754	C. Marry, 6915
1	MS0754	L. McGrath, 6915
1	MS0754	M. Rigali, 6915
1	MS0754	T. Stewart, 6915
1	MS0888	M. Hibbs, 6124
1	MS0895	H. Jones, 8622
1	MS1413	J.P. Carney, 8622
1	MS9292	S. Branda, 8621
1	MS9291	A. Singh, 8621
1	MS0899	RIM-Reports Management, 9532

Sandia National Laboratories